Analytical mechanics from constraints to invariants

Recover the dynamics of a body from its constraints, symmetries and measured initial conditions. Follow the argument through rotating bodies, resonances, continuum limits and changes of observer.

Contents

1. **Virtual work and the forces hidden by a constraint**
   A bead follows a wire, a pendulum remains the same length, and a rolling wheel obeys a relation between translation and rotation. Their reduced equations describe the motion but can conceal the largest forces in the apparatus. Determine which forces disappear under a virtual displacement, recover their values, and decide when the assumed motion ceases to be physically admissible.
2. **Moving constraints, boundary work and a changing energy**
   A pendulum with a reeled string can gain energy while its support force does no virtual work. A bead on a spinning guide can accelerate without gravity. Follow the work done by the apparatus, derive the relation between a reduced energy and laboratory energy, and identify which quantity a measurement tests.
3. **Noether's theorem, boundary terms and measurable constants**
   A constant of motion can survive when neither laboratory energy nor angular momentum is separately conserved. Construct the conserved quantity from an infinitesimal transformation of the action. Then use boosts, a screw symmetry, and a rotating potential to determine what measured combinations should stay fixed.
4. **Kepler orbits, the eccentricity vector and the loss of apsidal closure**
   An orbit can conserve energy and angular momentum yet gradually rotate its periapsis. The inverse-square problem possesses one more conserved vector that fixes the direction of closest approach. Derive it, turn a single position and velocity measurement into a conic, and measure what a weak perturbation does to the inferred apsidal direction.
5. **Scattering from a central potential and what angular data can recover**
   A detector records angles, whereas the force law refers to separations that were never directly observed. Derive the forward map from incoming impact parameter to angle, distinguish the several trajectories a detector may count in one angular bin, and invert sufficiently complete signed deflection data under stated hypotheses.

6. ## Euler–Poinsot motion, torque-free nutation and the intermediate axis

A freely rotating body has fixed angular momentum in space, yet the components recorded by three body-mounted gyroscopes can vary periodically or linger near an unstable rotation. Solve the nonsymmetric top from its invariants, distinguish its body-component period from its spatial orientation, and extract a stability time scale from a measured inertia tensor.

7. ## The heavy symmetric top, precession branches and the sleeping state

Gravity supplies a torque to a top pivoted away from its centre of mass. Its axis may precess steadily, nutate between two turning angles, or trace loops. Derive all three from the same angular kinetic energy and determine when an upright spinning top can remain stable.

8. ## Symplectic transformations, Poisson brackets and the geometry of measurements

Two phase-space plots can enclose the same volume while predicting different responses to an impulse. Derive the stronger condition that makes a change of variables canonical, test it on measured linear maps and use Poisson brackets to propagate observables without solving separately for every coordinate.

9. ## Action, angle and the slowing clock at a separatrix

A phase portrait contains enough information to extract a period by differentiating an area. Use that fact to build a clock for finite-amplitude pendulum motion, determine precisely where slow-parameter invariance fails, and distinguish a librating trajectory from one that makes complete rotations.

10. ## Canonical perturbations, small denominators and resonant capture

A weak periodic force can produce a bounded ripple on most trajectories and a large change on a narrow band of initial conditions. Derive the averaging transformation away from resonance, construct the slow resonant dynamics where that transformation fails, and estimate the physically observable width and time scale of a resonance.

11. ## Action density, stress waves and the boundary that reflects them

A chain of coupled masses becomes an elastic field when the wavelength is long compared with the spacing. Derive the field equation and its boundary traction from the same variation, follow energy and stress across a junction, and decide whether a measured pulse is limited by material waves or by numerical dispersion.

12. ## Relativistic collisions, centre-of-momentum energy and thresholds

Two particles with the same total laboratory energy can have very different energy available for changing their internal state. Determine the energy and motion of the centre-of-momentum system,

reconstruct two-body elastic scattering, and follow how a detector threshold transforms between frames.

13. Which path is shortest across the surface of a cone?

A point can move along a conical surface while its azimuth and height both change. Unroll the geometry and predict the shortest path between two marked points. The measurable minimum radius distinguishes the geodesic from a line drawn along a horizontal circle.

14. Motion in a medium and momentum carried across a boundary

Two beads can approach exactly the same terminal speed with recognisably different histories. A sand cart can slow down while the total horizontal momentum of sand and cart stays fixed. Both observations begin by specifying which material the equation of motion follows.

15. From a repeating trajectory to a chaotic attractor

A damped pendulum under a periodic drive can settle into the same orbit on each run yet visit a different point on successive drive periods. A return map supplies the right clock for distinguishing a new period from a slowly decaying transient.

16. From differential acceleration to three-dimensional strain and stress

An accelerometer in a falling laboratory can read zero while a pair of falling test masses moves apart. A crystal can support different longitudinal and transverse speeds in the same direction. Both measurements require the spatial variation of a vector field, represented by a tensor.

Analytical mechanics from constraints to invariants · 1. Virtual work and the forces hidden by a constraint

A bead follows a wire, a pendulum remains the same length, and a rolling wheel obeys a relation between translation and rotation. Their reduced equations describe the motion but can conceal the largest forces in the apparatus. Determine which forces disappear under a virtual displacement, recover their values, and decide when the assumed motion ceases to be physically admissible.

Hold the clock fixed when defining a virtual displacement

A system of particles has Cartesian positions $\mathbf{r}_i$ and applied forces $\mathbf{F}_i$. A holonomic constraint is an equation $g_\alpha(\mathbf{r}_1, \dots, \mathbf{r}_N, t) = 0$. At a fixed instant an admissible infinitesimal change of configuration obeys $\sum_i \nabla_i g_\alpha \cdot \delta\mathbf{r}_i = 0$. The physical velocities obey a different relation, $\sum_i \nabla_i g_\alpha \cdot \dot{\mathbf{r}}_i + \partial_t g_\alpha = 0$. A virtual displacement compares geometrically allowed configurations at the same time. It has no prescribed duration and makes no claim that the system's momentum actually points along it.

The distinction becomes measurable for a bead on a moving horizontal table. Every allowed virtual displacement has zero vertical component, so the table's upward normal force gives zero virtual work. An upward-moving table can nevertheless raise the bead and perform positive ordinary work. Ordinary power involves the actual velocity, which includes the table motion. A careless statement that constraint forces do no work confuses two different operations. For a fixed ideal frictionless surface the real velocity is tangent as well, and vanishing virtual work then does imply vanishing ordinary power.

Let $\mathbf{R}_i$ be the reaction forces and use $m_i\ddot{\mathbf{r}}_i = \mathbf{F}_i + \mathbf{R}_i$. Multiply by an admissible $\delta\mathbf{r}_i$ and sum over particles. We call the constraints ideal when $\sum_i \mathbf{R}_i \cdot \delta\mathbf{r}_i = 0$ for every allowed virtual displacement. Eliminating those reactions gives d'Alembert's principle,

$$\sum_i (\mathbf{F}_i - m_i\ddot{\mathbf{r}}_i) \cdot \delta\mathbf{r}_i = 0.$$

This is a dynamical equation expressed through a static-looking virtual-work test. It applies instantaneously along the motion. It does not assert that the total force vanishes or that the acceleration is an independent virtual displacement. One advantage is that the detailed construction of a rigid support need not be known to determine the admissible tangential acceleration; its force can be calculated afterwards when designing the support.

Pass from virtual work to equations for coordinates

Choose independent coordinates q_a with $\mathbf{r}_i = \mathbf{r}_i(q, t)$ and independent virtual increments δq_a. The velocity is $\sum_a \partial_{q_a}\mathbf{r}_i\,\dot{q}_a + \partial_t\mathbf{r}_i$. With kinetic energy $T = \sum_i m_i\dot{\mathbf{r}}_i^2/2$, differentiation at fixed q, t gives

$$\partial_{\dot{q}_a} T = \sum_i m_i\dot{\mathbf{r}}_i \cdot \partial_{q_a}\mathbf{r}_i.$$

Differentiate in time. The product rule produces an acceleration term and a second term involving $d(\partial_{q_a}\mathbf{r}_i)/dt$. The latter equals $\partial_{q_a}\dot{\mathbf{r}}_i$, with the generalised velocities held fixed, and supplies $\partial_{q_a} T$. Hence

$$\frac{d}{dt}\frac{\partial T}{\partial \dot{q}_a} - \frac{\partial T}{\partial q_a} = \sum_i m_i \ddot{\mathbf{r}}_i \cdot \frac{\partial \mathbf{r}_i}{\partial q_a}.$$

The projected applied force is

$$Q_a = \sum_i \mathbf{F}_i \cdot \partial_{q_a} \mathbf{r}_i.$$

Independence of the coordinate variations in d'Alembert's principle gives one equation $d(\partial_{\dot{q}_a} T)/dt - \partial_{q_a} T = Q_a$ per coordinate. When $\mathbf{F}_i$ comes from a potential $V(q,t)$, the conservative contribution is $-\partial_{q_a} V$. Other contributions such as a measured resisting torque remain explicit. A coordinate expressed as an angle has a generalised force in joules per radian; a coordinate expressed as a length has one in newtons. Checking $Q_a\, dq_a$ as work avoids mistaking a generalised force for a Cartesian component.

For a simple pendulum of length l and mass m, choose θ measured from downward vertical. Then $T = ml^2\dot{\theta}^2/2$ and $V = mgl(1-\cos\theta)$. The equation $ml^2\ddot{\theta} = -mgl\sin\theta$ follows at once. The string tension vanished under the angular displacement. It has not been shown to vanish physically. Projecting Newton's equation onto the direction from the bead toward the pivot gives

$$T_{\text{string}} = mg\cos\theta + ml\dot{\theta}^2.$$

This second observable is sensitive to speed even when the reduced angular acceleration depends only on angle.

Recover multipliers before choosing coordinates

Cartesian coordinates keep reaction directions explicit. Put all coordinates into a vector x, let M be the mass matrix and let G contain the rows ∇g_α. The tangent virtual displacements are precisely those satisfying $G\delta x = 0$. A reaction doing zero virtual work must be a linear combination of the normal covectors, $R = G^T\lambda$, when the constraints are independent. Newton's equation becomes

$$M\ddot{x} = F + G^T\lambda.$$

Differentiate the constraints twice along the trajectory: $G\ddot{x} + \gamma = 0$, where γ includes the known velocity, curvature and explicit time terms. Substituting for $\ddot{x}$ determines reactions from a much smaller system,

$$(GM^{-1}G^T)\lambda = -\gamma - GM^{-1}F.$$

For any vector c, $c^T GM^{-1}G^T c = (G^T c)^T M^{-1}(G^T c)$ is positive if G has independent rows and particle masses are positive. Dependent constraint equations make the individual multipliers ambiguous. For instance writing both $g = 0$ and $2g = 0$ declares the same geometrical restriction twice. Only the combined reaction is then determined. The magnitude of a raw multiplier also depends on the units and

normalisation of g. Reporting the force $G^T\lambda$ makes comparisons between alternative constraint descriptions meaningful.

Use $g = (x^2 + y^2 - l^2)/2 = 0$ for a planar pendulum, with y upward, so the gradient is the radius vector $\mathbf{r}$. Newton's equation reads $m\ddot{\mathbf{r}} = -mg\hat{y} + \lambda\mathbf{r}$, where the symbol g in the gravitational term denotes the acceleration magnitude. The acceleration constraint $\mathbf{r}\cdot\ddot{\mathbf{r}} = -v^2$ gives

$$\lambda = (mgy - mv^2)/l^2.$$

The inward tension is $-\lambda l = mv^2/l - mgy/l$. Since $y = -l\cos\theta$, this is the radial-force result already obtained. The multiplier in this convention has units of force per length. Using the radial-distance constraint instead would make its magnitude a force.

Background · What if the support can push but cannot pull?

Replacing a surface by an equality constraint assumes the object stays in contact. A particle sliding along the inside of a smooth vertical circular track illustrates the additional physical test. At the top, gravity and the inward normal reaction together must supply the centripetal acceleration.

$$N = \frac{mv^2}{R} - mg, \qquad N \geq 0.$$

At a top speed below $\sqrt{gR}$ the equality-constrained solution requires negative N. An ordinary track cannot exert that pull. Its normal force then falls to zero and the particle must follow free flight until it meets the track again. A bead threaded on a wire could receive the oppositely directed force and would follow a different trajectory. Both models have the same geometrical path during contact.

Recognise an inequality at a contact

A bead threaded on a stiff loop can experience reaction in either direction, whereas a string can pull only. A surface without adhesion can push only. Derive the constrained motion, calculate its reaction, and compare the required sign with the physical mechanism. When a calculated tension turns negative, replace the constrained trajectory by free flight until a new contact event. Continuing to integrate the pendulum equation would retain a mathematically valid circle and a physically unavailable pushing string.

A mass starts at the bottom of a frictionless vertical loop with speed v_b. Energy conservation gives $v_{\text{top}}^2 = v_b^2 - 4gl$, since the top is $2l$ higher. A string just remaining taut at the top requires $T_{\text{top}} = mv_{\text{top}}^2/l - mg \geq 0$, giving $v_b^2 \geq 5gl$. The energy-only criterion for reaching the elevation is $v_b^2 \geq 4gl$; the interval between these two values illustrates why a trajectory test must include reactions. With $l = 0.80\,\text{m}$, the threshold bottom speed is $6.26\,\text{m/s}$. At this threshold the bottom tension is $6mg$, six times the weight, even though the tension is about to vanish at the top.

Recover the forces on a wedge that is free to slide

Place a wedge of mass M on a smooth horizontal floor and a block of mass m on its smooth upper face. Let the slope descend to the right at angle α. Choose X as the wedge's horizontal position and s as distance down the face. The block's coordinates apart from fixed offsets are $x = X + s\cos\alpha,\ y = -s\sin\alpha$. Its relative velocity points down the slope but its absolute acceleration need not. The kinetic energy contains a mixed term $m\dot{X}\dot{s}\cos\alpha$. Dropping that term is equivalent to holding the wedge stationary while allowing it to recoil, two incompatible mechanical models.

The reduced equations are $(M+m)\ddot{X} + m\ddot{s}\cos\alpha = 0$ and $\ddot{s} + \ddot{X}\cos\alpha = g\sin\alpha$. The first is conservation of total horizontal momentum, since the block–wedge normal force is internal and the floor is frictionless. Elimination gives

$$\ddot{s} = (M+m)g\sin\alpha/(M + m\sin^2\alpha),$$

$$\ddot{X} = -mg\sin\alpha\cos\alpha/(M + m\sin^2\alpha).$$

The acceleration down the moving face exceeds $g\sin\alpha$ because the wedge moves left as the block slides right. Nevertheless the absolute vertical acceleration of the block remains less than or equal to free fall because the upper face pushes upward.

To find the block's normal force, project its absolute acceleration onto the outward unit normal $(\sin\alpha, \cos\alpha)$. The part proportional to $\ddot{s}$ cancels, leaving $\ddot{X}\sin\alpha$. Newton's equation along that direction gives

$$N = m(g\cos\alpha + \ddot{X}\sin\alpha) = mMg\cos\alpha/(M + m\sin^2\alpha).$$

With $M = 3.0\,\mathrm{kg}$, $m = 1.0\,\mathrm{kg}$, $\alpha = 30^\circ$, one finds $\ddot{s} = 6.04\,\mathrm{m/s^2}$,

$$\ddot{X} = -1.31\,\mathrm{m/s^2},$$

$$N = 7.84\,\mathrm{N}.$$

The normal based on a stationary wedge would be $8.50\,\mathrm{N}$. A force sensor under the moving face could distinguish the two models even when a short record of relative slope displacement cannot resolve the difference.

Which reaction does no virtual work here? The normal force on the block has virtual work $N\hat{n}\cdot(\delta X\hat{x} + \delta s\hat{t}) = N\sin\alpha\,\delta X$. The opposite normal force on the wedge gives $-N\sin\alpha\,\delta X$, so the sum cancels. Considering only the block and asserting zero work from the normal for arbitrary δX would be incorrect. At the real velocities the same reaction transfers energy between the bodies even though its net internal power on their pair is zero. The floor's normal reaction balances the vertical momentum change of the whole system. During the slide it is $(M+m)g - m\ddot{s}\sin\alpha$, less than total weight while the block accelerates downwards.

Take the limits as an additional test. At fixed m, α, increasing M to infinity returns the familiar fixed-wedge results. At a nearly horizontal face, downslope acceleration and wedge recoil vanish, restoring the full block weight as normal force. At a vertical face the normal vanishes and the block falls. These limits hold because the contact has no friction and can be maintained with a nonnegative normal. A moving

wedge of independently prescribed acceleration would replace the horizontal momentum equation by a control input, changing both the relative acceleration and the support force.

Distinguish rolling constraints from purely geometric restrictions

A cylinder of radius R, mass m and axial inertia I rolls without slip down a fixed rough incline. Choose coordinate s down the incline and spin angle ϕ in the corresponding sense. The constraint $\dot{s} = R\dot{\phi}$ is integrable in this one-dimensional motion, so it can be inserted as $s - R\phi = \text{constant}$. The resulting kinetic energy is $(m + I/R^2)\dot{s}^2/2$. The reduced equation gives

$$\ddot{s} = g\sin\alpha/[1 + I/(mR^2)].$$

Reconstruct the static friction from translation, $f = gm\sin\alpha - m\ddot{s}$, directed up the slope, and compare it with the available maximum $\mu_s mg\cos\alpha$.

For a homogeneous solid cylinder $I = mR^2/2$, the speed-up is $2g\sin\alpha/3$ and friction magnitude $mg\sin\alpha/3$. A ring of the same mass and radius has $I = mR^2$, half the gravitational downslope acceleration and half the downslope weight component as friction. At 30° the minimum static friction coefficients are respectively $\tan 30^\circ/3 = 0.192$ and $\tan 30^\circ/2 = 0.289$. Two objects on the same surface can therefore diverge qualitatively because the ring slips while the cylinder still rolls. Treating an assumed no-slip relation as exact without testing that inequality can produce an unphysical result despite apparently consistent energy conservation.

The friction on a rigid body rolling without slip on a fixed surface has zero power because its instantaneous point of contact is stationary. The force still changes both linear and angular momentum. On a moving conveyor the contact velocity is no longer zero in the laboratory; friction can supply mechanical energy even while the relative contact velocity vanishes. For a wheel steering on a plane the restrictions $\dot{x} = R\dot{\phi}\cos\psi,\ \dot{y} = R\dot{\phi}\sin\psi$ depend on heading ψ. In general they cannot be integrated into two configuration equations relating x, y, ϕ, ψ globally. d'Alembert's fixed-time allowed variations still project out ideal rolling reactions, but replacing those velocity constraints by invented holonomic coordinates gives the wrong dynamics. The distinction can be seen geometrically by rolling and steering through a closed sequence of steering operations that leaves a net displacement.

Find loads on two supports of a suspended bar

A rigid horizontal bar of mass m and length $2a$ is supported at its ends by two vertical inextensible light cords. At one instant both cords are vertical and the bar is horizontal. An extra downward load of magnitude F is applied at horizontal coordinate s relative to the centre. Ask first for a static experiment. The two vertical reaction forces T_L, T_R obey force balance $T_L + T_R = mg + F$ and moment balance $a(T_R - T_L) = sF$. This gives

$$T_R = (mg + F + sF/a)/2,$$
$$T_L = (mg + F - sF/a)/2.$$

The lever arms encode geometry that the vertical balance alone cannot provide.

The same result can be obtained from virtual variations if the reactions are kept as multipliers until the end. For small vertical translation y of the centre and small tilt θ, the endpoint vertical displacements are $\delta y - a\delta\theta$ on the left and $\delta y + a\delta\theta$ on the right. The load point displacement is $\delta y + s\delta\theta$. Before eliminating the endpoint constraints, project all applied and reaction forces against arbitrary independent $\delta y, \delta\theta$; vanishing of both coefficients gives the preceding balances. After imposing both endpoint constraints directly, these two variations vanish and the reduced model for vertical motion contains no equation from which the support loads can be read. Removing a degree of freedom can remove precisely the observable of interest unless reactions are reconstructed.

For $m = 2.0\,\mathrm{kg}$, $a = 0.40\,\mathrm{m}$, $F = 12\,\mathrm{N}$ and $s = 0.25\,\mathrm{m}$, the total load is $31.62\,\mathrm{N}$ and the load difference $7.50\,\mathrm{N}$. Hence $T_R = 19.56\,\mathrm{N}$, $T_L = 12.06\,\mathrm{N}$. Exchanging the load from right to left reverses the difference while preserving the sum. This symmetry is a calibrating manoeuvre for two load cells with different offsets: subtract readings from mirrored configurations to isolate the lever-arm response, and compare their sum to the known total weight and applied force.

Now imagine three vertical supports at $-a, 0, +a$. Their three tensions enter only two independent balances. Perfectly rigid constraints determine no unique allocation to the centre support. The ambiguity is physical; the stiffnesses, preloads and small height differences of real supports decide the result. With three identical unstrained linear springs and a centred load F, each spring extends equally if the bar stays level, so each carries one third of the total weight. If the middle spring is twice as stiff and all have the same unloaded height, it carries one half and each outer spring one quarter. Both answers satisfy exactly the same force and moment balances. Reporting a unique value from a singular ideal multiplier system would manufacture an unmeasured constitutive assumption.

Test an acceleration constraint against drift of the position itself

Solving $G\ddot{x} + \gamma = 0$ guarantees the correct instantaneous normal acceleration at a state lying on the constraint manifold with tangent velocity. It does not magically repair earlier position or velocity errors in approximate time integration. For a particle constrained to a circle, monitor $g = (r^2 - l^2)/2$, $\dot{g} = \mathbf{r} \cdot \mathbf{v}$, and the computed force. A small tangential displacement can give tiny instantaneous force error while the radius gradually drifts. Integrating an acceleration-level constraint twice without a position or velocity correction can cause substantial mismatch over many revolutions.

A simple projection illustrates what each correction does. Normalise an approximate position vector to length l, then remove the radial component of velocity by $\mathbf{v} \leftarrow \mathbf{v} - \hat{r}(\hat{r} \cdot \mathbf{v})$. The corrected point and tangent satisfy the constraints, but the velocity correction removes kinetic energy $m(\hat{r} \cdot \mathbf{v})^2/2$, and the position change can alter potential energy. Projection is therefore a numerical operation whose physical invariant errors must be measured. A structure-preserving constrained integrator builds the position and momentum conditions into the step and often gives better long-time behaviour. Compare convergence of reaction, constraint residual and energy separately instead of treating a rounded radius as proof of a correct force.

A pendulum on a free cart tests the complete mass matrix

Mount a pendulum pivot on a cart of mass M moving horizontally on a smooth track. The bob has mass m, length l and downward angle θ. Choose the cart position X and use bob coordinates $X + l\sin\theta$, $-l\cos\theta$. The kinetic energy is $(M+m)\dot{X}^2/2 + ml\dot{X}\dot{\theta}\cos\theta + ml^2\dot{\theta}^2/2$. Two different off-diagonal mass terms would contradict its origin as a quadratic form; the same factor $ml\cos\theta$ multiplies the companion acceleration in each equation. This is a useful check on a manually assembled multibody model.

The equations are

$$(M+m)\ddot{X} + ml(\ddot{\theta}\cos\theta - \dot{\theta}^2\sin\theta) = 0,$$

$$l\ddot{\theta} + \ddot{X}\cos\theta + g\sin\theta = 0.$$

In the small-angle regime the horizontal centre of mass moves uniformly. Choosing zero total momentum gives

$$\dot{X} \simeq -ml\dot{\theta}/(M+m).$$

Substitute its derivative into the angular equation to obtain

$$\ddot{\theta} + [(M+m)g/(Ml)]\theta = 0.$$

Releasing the support raises the oscillation frequency because the effective angular inertia falls while the gravitational stiffness stays the same. The result is a statement about the relative pendulum angle, measured from an inertial vertical, with an unforced horizontally moving support.

For $M = 0.60\,\mathrm{kg}$, $m = 0.20\,\mathrm{kg}$ and $l = 0.50\,\mathrm{m}$, the small-angle period is

$$2\pi\sqrt{Ml/[(M+m)g]} = 1.229\,\mathrm{s}.$$

Fixing the cart with a clamp gives $1.419\,\mathrm{s}$ instead. At zero total horizontal momentum the cart displacement from its equilibrium is approximately $-0.125\,\theta$ metres, so a $0.10\,\mathrm{rad}$ angle corresponds to $12.5\,\mathrm{mm}$ of recoil. Simultaneous position measurements on cart and bob should reconstruct a horizontal centre of mass that is stationary to within tracking uncertainty. A missing cart inertia or a wrongly filled cross term can alter both period and recoil; checking just one number may not identify which error occurred.

The reaction on the moving bob can again be recovered. Its radial acceleration along the outward string direction is $\ddot{X}\sin\theta - l\dot{\theta}^2$. Thus the tension is $T = m[g\cos\theta - \ddot{X}\sin\theta + l\dot{\theta}^2]$. The acceleration of the support appears explicitly. Reusing the fixed-pivot formula at all angles would omit a term that vanishes accidentally at the bottom. To test the sign, observe a rightward tilted pendulum whose pivot accelerates right: the support's acceleration has an outward projection along the tilted string, reducing the inward tension needed for the same relative motion. Substituting a directly measured cart acceleration provides an independent load-cell prediction.

Follow a force eliminated by a constraint

Predict when a two-sided circular groove must reverse its normal force. Check the prediction against the exact energy and radial balances.

Open this experiment online

Try the calculation

Bottom speed (m/s) **4**

Loop radius (m) **0.5**

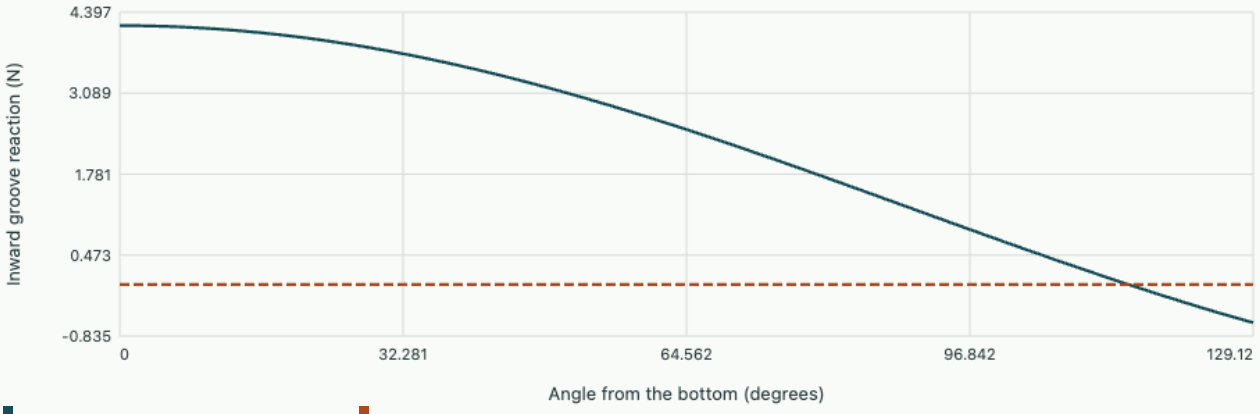

Reachable angle 129.12°. Inward groove reaction there -0.619 N. One-sided loop threshold v_0 = 4.9523 m/s.

Decide which force a sensor actually reports

Reaction forces can be reported as tension along a member, normal traction at a contact, total support load on a floor, or a single Cartesian component read by a load cell. A rigid-body idealisation alone does not specify a sensor's orientation or the weight of its housing. For a fixed pendulum, for example, the string carries tension T, while a vertical force channel at its pivot reads the vertical string contribution $T\cos\theta$. A horizontal channel reads $T\sin\theta$. The force on the pivot is opposite the force exerted on the bob. Selecting the wrong sign or leaving out the fixture's own weight can create a discrepancy even when the dynamical calculation is correct.

Suppose an ideal load cell with its sensitive axis vertical is tared with the fixture installed but the $0.40\,\mathrm{kg}$ bob removed. When the bob is held at 60° by a separate purely tangential actuator and is otherwise stationary, the radial balance gives

$$T = mg\cos 60^\circ = 1.96\,\mathrm{N}.$$

The pivot's vertical reading attributable to the string is $0.981\,\mathrm{N}$. The tangential actuator supplies the remaining vertical support as well as a horizontal component. Once the actuator releases,

instantaneously the same tension and reading hold because radial speed is still zero. At the bottom of the subsequent swing the load jumps to the dynamical value obtained earlier, even though no upper fixture mass has changed.

A student hangs the bob at the same 60° angle using a separate horizontal cord instead of a tangential actuator. Should the pivot cell read the preceding $0.981\,\mathrm{N}$?

▼ **Work through the solution**

The horizontal cord contributes no vertical support. Static balance now requires $T\cos 60^\circ = mg$, giving $T = 7.85\,\mathrm{N}$ and vertical pivot contribution $3.92\,\mathrm{N}$. The horizontal holding force has a nonzero radial projection and changes the radial-force balance. After the horizontal cord is removed the tension immediately changes to $mg\cos 60^\circ$ because no momentum impulse is required for a finite jump in force. A schematic that shows only the bob angle is insufficient to infer the support load without saying how the angle is maintained.

In the free cart experiment bearing drag is weak but measurable. Can an observed frequency shift distinguish it from a wrongly assumed cart mass?

▼ **Work through the solution**

A viscous drag changes the horizontal momentum balance and allows the formerly stationary centre of mass to move as momentum leaks to the track. A mass error in a drag-free model changes the relative period and recoil ratio without supplying an actual external impulse. Track the complete centre of mass using independently weighed masses, compare its momentum change with the integrated bearing force, and measure the decay envelope. The frequency alone is a single scalar and can often be fitted by several combinations of missing mass, spring compliance and drag.

Locate contact loss on a smooth convex surface

A small block starts sliding from near rest just to one side of the top of a smooth fixed sphere of radius R. Measure angle θ from upward vertical. Energy gives $v^2 = 2gR(1-\cos\theta)$ during contact, while the inward radial equation reads $mg\cos\theta - N = mv^2/R$. Thus $N = mg(3\cos\theta - 2)$. Contact first vanishes at $\cos\theta = 2/3$, or 48.2°. For a sphere of radius $0.50\,\mathrm{m}$, this occurs after a vertical drop $R/3 = 0.167\,\mathrm{m}$ and at speed $1.81\,\mathrm{m/s}$. A block balanced exactly at the top at exact rest is an unstable equilibrium in the ideal model; a small initial displacement or speed initiates the measured trajectory.

Once the block leaves, the same spherical coordinates can still be used to describe position, but $r = R$ is no longer an equation of motion. Continue with the measured tangential velocity and free gravitational acceleration. Enforcing the sphere condition beyond release would make the computed normal negative and predict a surface that pulls on the block. The zero normal, the geometric release angle and the subsequent ballistic arc provide three independent observables for the same force reconstruction.

Tutorial on measuring reactions

A $0.40\,\mathrm{kg}$ pendulum of length $0.75\,\mathrm{m}$ is released from rest at 60° from downward vertical. Predict the load-cell reading at the pivot when it passes the bottom. What part does the reduced equation alone omit?

▼ **Work through the solution**

The height change is

$$l(1-\cos 60^\circ) = 0.375\,\mathrm{m}.$$

Energy conservation gives

$$v^2 = 2g(0.375) = 7.36\,\mathrm{m}^2/\mathrm{s}^2.$$

At the bottom the tension is $mg + mv^2/l = 7.85\,\mathrm{N}$, twice the weight. The tangential acceleration there vanishes because gravity points along the string, but the radial acceleration remains nonzero. A sensor measuring the string force sees this centripetal contribution directly.

A bead lies on a smooth moving plane with upwards acceleration a_z. Which acceleration first makes a passive contact impossible if the bead initially shares the plane's motion?

▼ **Work through the solution**

Vertical Newton balance requires $N - mg = ma_z$, or $N = m(g + a_z)$. At $a_z = -g$ the reaction vanishes. A more negative plane acceleration would require the plane to pull the bead down, so contact is lost and the bead follows free fall until the separation closes. For upward acceleration the normal exceeds weight. In all these cases a virtual displacement tangent to the plane produces zero virtual normal work.

Two code implementations use $(x^2 + y^2 - l^2)/2$ and $x^2 + y^2 - l^2$ as constraints for the same state. Their multipliers differ by a factor two. How can the physical result be tested?

▼ **Work through the solution**

The second gradient is twice the first at the same point. Its multiplier must be half the first multiplier for $G^T\lambda$ to coincide. Compare the reaction vector in newtons, its dot product with an independently chosen tangent direction, and the normal acceleration required by the geometry. A comparison of raw multiplier values alone would flag a difference that is entirely due to normalisation.

Compare a constrained trajectory with the motion and force calculations above.

David Tong develops virtual work and constrained coordinates in his classical dynamics course.

Analytical mechanics from constraints to invariants · 2. Moving constraints, boundary work and a changing energy

A pendulum with a reeled string can gain energy while its support force does no virtual work. A bead on a spinning guide can accelerate without gravity. Follow the work done by the apparatus, derive the relation between a reduced energy and laboratory energy, and identify which quantity a measurement tests.

Parameterise the motion of a guide as well as the bead

Let a prescribed moving guide define positions $\mathbf{r}(q,t)$. Its relative velocity along the guide is $\mathbf{r}_q\dot q$ and its imposed local velocity is $\mathbf{r}_t$, where t is differentiated at fixed coordinate. The kinetic energy $T=m|\mathbf{r}_q\dot q+\mathbf{r}_t|^2/2$ includes a quadratic term in $\dot q$, a mixed term linear in $\dot q$, and a term independent of $\dot q$. Dropping the last two merely because the guide motion is prescribed generally changes the bead equation. A term independent of $\dot q$ may still depend on its position q.

For $L=T-V$ define $p=\partial_{\dot q}L$ and $\mathcal{E}=p\dot q-L$. Differentiating along a solution of the Euler–Lagrange equation gives $d\mathcal{E}/dt=-\partial_t L$ in the absence of extra nonconservative generalised forces. This identity involves the partial time derivative at fixed $q,\dot q$. The laboratory energy is

$$E_{\mathrm{lab}}=m|\dot{\mathbf{r}}|^2/2+V.$$

Direct substitution gives $\mathcal{E}=E_{\mathrm{lab}}-m\dot{\mathbf{r}}\cdot\mathbf{r}_t$ for a single particle and ordinary position potential. Thus a time-independent reduced Lagrangian can conserve a quantity different from the laboratory mechanical energy. Which observer supplies a force, and which independent variables are held fixed, determine the energy being tracked.

Work supplied by a steadily rotating straight slot

A smooth horizontal guide turns about its inner end with prescribed angle $\varphi=\Omega t$. Let r be the bead's distance from the pivot. The velocity is $\dot r\hat r+r\Omega\hat\varphi$, and the reduced Lagrangian is $m(\dot r^2+\Omega^2r^2)/2$. Its Euler–Lagrange equation is

$$\ddot r=\Omega^2 r.$$

With $r(0)=r_0,\dot r(0)=0$ the solution is $r_0\cosh\Omega t$ until the bead leaves the slot. In the laboratory no force acts along the radial tangent of the slot, yet radial acceleration in polar coordinates is $\ddot r-r\Omega^2$, precisely zero. The tangential acceleration $2\Omega\dot r$ is provided by the slot wall.

The wall reaction $R_\varphi=2m\Omega\dot r$ exerts a torque rR_φ on the bead. The driving motor balances the opposite reaction on the slot and supplies power $\Omega rR_\varphi=2m\Omega^2r\dot r$. Differentiating $E_{\mathrm{lab}}=m(\dot r^2+\Omega^2r^2)/2$ and using the radial equation gives the same power. The reduced energy $m(\dot r^2-\Omega^2r^2)/2$ is constant. Its difference from E_{lab} equals $-\Omega L_z$, with $L_z=mr^2\Omega$. This is a consequence of uniform imposed rotation, not a negative physical rotational kinetic energy.

For $m=0.10\,\mathrm{kg}$, $r_0=0.050\,\mathrm{m}$ and $\Omega=4.0\,\mathrm{rad/s}$, consider $t=0.25\,\mathrm{s}$. The radial position is $77.2\,\mathrm{mm}$, radial speed $0.235\,\mathrm{m/s}$, and wall reaction $0.188\,\mathrm{N}$. The motor supplies about $0.0580\,\mathrm{W}$ at that instant. Laboratory energy has risen from $0.00200\,\mathrm{J}$ to approximately $0.00752\,\mathrm{J}$. Measuring only the angular

motor speed would miss the incoming mechanical work. The torque on the drive shaft or the changing moment of inertia supplies the other observable required for an energy budget.

A pendulum with prescribed length

Let a point pendulum have length $l(t) > 0$ and angle θ from downward vertical. Using $x = l\sin\theta$, $y = -l\cos\theta$ gives $T = m(\dot{l}^2 + l^2\dot{\theta}^2)/2$ and $V = -mgl\cos\theta$ for a fixed gravitational datum. The angular Euler–Lagrange equation becomes

$$\frac{d}{dt}(ml^2\dot{\theta}) = -mgl\sin\theta,$$

$$\ddot{\theta} + 2\frac{\dot{l}}{l}\dot{\theta} + \frac{g}{l}\sin\theta = 0.$$

The term proportional to $\dot{l}\dot{\theta}$ comes directly from differentiating angular momentum about the pivot. With increasing length the angular speed at fixed angular momentum decreases; reeling in has the opposite effect. It can look like damping or amplification in the angular equation even with no friction. A mechanical energy balance distinguishes the reversible exchange with a reel from energy lost as heat.

The radial Newton equation, taking outward as positive, is $m(\ddot{l} - l\dot{\theta}^2) = mg\cos\theta - T_{\mathrm{string}}$. Hence $T_{\mathrm{string}} = m(g\cos\theta + l\dot{\theta}^2 - \ddot{l})$. The tension power on the bob is $-T_{\mathrm{string}}\dot{l}$. This has the correct sign when a heavy nearly vertical bob is lowered slowly: $\dot{l} > 0$ and the gravitational potential decreases as the string takes energy out. At the bottom of a swing the tension is larger, so a reel shortening the string there does more positive work per unit length than it would at a turning point. Timing a cyclic length change can pump an oscillation while the guide returns to precisely its initial length.

With $m = 0.50\,\mathrm{kg}$, $l = 1.0\,\mathrm{m}$, $\dot{\theta} = 2.0\,\mathrm{rad/s}$, and the bob at the bottom, a short interval of constant-rate shortening at $\dot{l} = -0.030\,\mathrm{m/s}$ has tension $6.91\,\mathrm{N}$ and delivers $0.207\,\mathrm{W}$. When the bob is momentarily at rest at 30°, the tension for the same length and zero radial acceleration is $4.25\,\mathrm{N}$. Reversing the reel rate there would remove only $0.127\,\mathrm{W}$. A complete finite cycle requires integrating the time-varying tensions and checking the acceleration during each reel reversal.

Translate a pivot and separate real forcing from a coordinate choice

For a pivot translating horizontally at prescribed $X(t)$ and constant string length l, write $x = X + l\sin\theta$, $y = -l\cos\theta$. The kinetic energy includes $ml\dot{X}\dot{\theta}\cos\theta$. In the angular Euler–Lagrange equation the terms proportional to $\dot{X}\dot{\theta}\sin\theta$ cancel, leaving $l\ddot{\theta} = -g\sin\theta - \ddot{X}\cos\theta$. A constant pivot velocity therefore does not force the relative angle. Replacing the pivot velocity by its magnitude as a driving force would wrongly violate Galilean invariance. A horizontal pivot acceleration does force the angle; it appears as the opposite inertial acceleration in the translating frame.

For $|\theta| \ll 1$ and $X = X_0\cos\omega t$, the equation becomes

$$\ddot{\theta} + \omega_0^2 \theta = (X_0 \omega^2 / l) \cos \omega t,$$

$$\omega_0^2 = g/l.$$

At drive frequencies well below ω_0,

$$\theta \simeq -\ddot{X}/g.$$

The bob nearly aligns with the effective gravity in the moving frame. Far above ω_0, the particular solution is approximately $-X/l$; then the bob's absolute horizontal coordinate $X + l\theta$ changes little even while the pivot moves. Near resonance the undamped steady particular amplitude is inappropriate, and the initial transient or a physical damping model matters.

Calculate work done by a moving wall in an elastic collision

A particle of mass m moves along a line and collides elastically with a wall whose prescribed laboratory velocity is U during the short contact. In the instantaneous wall frame the incoming relative velocity $v^- - U$ reverses, so

$$v^+ = 2U - v^-.$$

In the laboratory the impulse is $J = m(v^+ - v^-) = 2m(U - v^-)$ and the kinetic energy change is $\Delta K = m[(v^+)^2 - (v^-)^2]/2 = UJ$. The energy gained by the particle equals wall velocity times the impulse delivered by the wall. A perfectly elastic contact still changes laboratory kinetic energy when the wall moves, since elasticity was defined for the relative normal velocity.

Suppose a particle of mass $0.20\,\mathrm{kg}$ moves right at $3.0\,\mathrm{m/s}$ into a right wall moving left at $0.50\,\mathrm{m/s}$. Its final velocity is $-4.0\,\mathrm{m/s}$, and the impulse on the particle is $-1.40\,\mathrm{N\,s}$. The particle's kinetic energy rises from 0.90 to $1.60\,\mathrm{J}$, exactly $UJ = 0.70\,\mathrm{J}$. The actuator keeping the wall on schedule supplies the energy. When the same wall recedes to the right at $0.50\,\mathrm{m/s}$, the outgoing velocity is $-2.0\,\mathrm{m/s}$ and kinetic energy falls by $0.50\,\mathrm{J}$. The difference is not symmetric under reversal of wall speed at fixed incoming particle velocity, because that reversal also changes the relative approach speed.

Now trap a particle between a fixed wall and a length $l(t)$ varying slowly compared with the collision period. To leading order a right-wall collision changes the particle's speed by $-2\dot{l}$, and such collisions occur about once in $2l/v$. Hence $dv/dt \simeq -(v/l)\dot{l}$, so vl is approximately constant. The one-dimensional action around a full bounce cycle is

$$J_{\mathrm{act}} = (2\pi)^{-1}(2mvl) = mvl/\pi.$$

This elementary wall argument explains the adiabatic action without requiring the smooth-force approximation at the instantaneous collision. If the wall speed varies quickly within a round trip, the collision phases matter and the averaged invariant can fail.

Starting with $l_0 = 0.40\,\mathrm{m}$ and speed $4.0\,\mathrm{m/s}$, slow compression to $0.30\,\mathrm{m}$ predicts $v \simeq 5.33\,\mathrm{m/s}$. Its kinetic energy increases by a factor $16/9$, supplied through the moving boundary. A pressure sensor at

the wall measures impulse per time, $2mv$ times the collision frequency $v/(2l)$, giving average force mv^2/l at leading order. Multiplying this force by the inward speed gives the power required by the predicted energy law. An instantaneous compression while the particle is elsewhere would instead change no kinetic energy until a later collision. The final length alone does not determine the energy unless the rate protocol is specified.

Follow a string through a moving boundary in configuration and time

For a vertical moving pivot with height $Y(t)$, coordinates $x = l\sin\theta$, $y = Y - l\cos\theta$ give kinetic energy $m[\dot{Y}^2 + 2l\dot{Y}\dot{\theta}\sin\theta + l^2\dot{\theta}^2]/2$. Derive the angular equation by differentiating $p_\theta = ml^2\dot{\theta} + ml\dot{Y}\sin\theta$. The terms containing $\dot{Y}\dot{\theta}\cos\theta$ cancel as in horizontal translation; the remaining equation is

$$l\ddot{\theta} = -(g + \ddot{Y})\sin\theta.$$

A vertical acceleration changes the restoring coefficient multiplicatively, unlike a horizontal displacement whose small-angle effect is an additive forcing term. The distinction is visible even when the two pivot motions have identical amplitudes and frequencies.

For $Y = A\cos\Omega t$, the effective gravity oscillates as $g - A\Omega^2\cos\Omega t$. The perfectly vertical solution remains an exact solution at any drive amplitude. A small deviation need not remain small, because its linear equation has a periodic coefficient. An observed growth of swing from a tiny initial disturbance near twice the natural frequency is a parametric effect. A camera viewing the pivot and bob together can separate relative angle from large imposed vertical displacement. Estimating angular amplitude from absolute bob height alone introduces a component at the drive frequency unrelated to the swing.

At modest drive $A = 1.0\,\mathrm{mm}$, $\Omega = 20\,\mathrm{rad/s}$, the pivot acceleration amplitude is $0.40\,\mathrm{m/s^2}$, about four percent of gravity. A pendulum of length $0.10\,\mathrm{m}$ has small-angle frequency $9.90\,\mathrm{rad/s}$, putting this drive near twice its natural frequency despite the small displacement. For an exactly stationary vertical bob relative to the pivot, the string tension is $m(g + \ddot{Y})$ as long as that value is positive. A force measurement thus contains a direct drive-frequency signal even before transverse oscillation develops. Combining an angle sensor with a load cell helps distinguish contact loss from growth of parametric oscillation.

A fast vertical drive can also modify the slow stability of the inverted position. A quantitative treatment requires separating a fast small angular ripple from the slow tilt and averaging its feedback, with the support acceleration and frequency satisfying the relevant ordering. The instantaneous sign of $g + \ddot{Y}$ alone is insufficient to establish the stability of the inverted solution. An upright motion that briefly samples a favourable sign each cycle may still drift away over many cycles. Compare initial perturbations at several drive phases and fit the envelope over complete periods before drawing a stability conclusion.

Treat the drive itself as a degree of freedom

A prescribed rotating slot conceals the energy source behind a fixed pattern speed. Replace the motor by a free rotating turntable with moment of inertia I_0, and let its angle φ evolve dynamically. In the horizontal frictionless problem the total kinetic energy is $m\dot{r}^2/2 + (I_0 + mr^2)\dot{\varphi}^2/2$. The angle is cyclic, so the total angular momentum $P = (I_0 + mr^2)\dot{\varphi}$ is constant. As the bead moves out, the turntable slows. The radial equation remains $\ddot{r} = r\dot{\varphi}^2$, but its coefficient now decreases according to the total angular momentum instead of remaining externally fixed.

Eliminate $\dot{\varphi}$ from the total energy to find

$$E = m\dot{r}^2/2 + P^2/[2(I_0 + mr^2)].$$

The reduced radial potential decreases outwards and feeds radial kinetic energy, but the total energy available is finite. Differentiating the potential gives a radial acceleration $P^2 r/(I_0 + mr^2)^2$, consistent with the original radial equation. One should not simply insert $\dot{\varphi} = P/(I_0 + mr^2)$ into the original kinetic Lagrangian before varying r; the correct fixed-momentum Routh reduction subtracts $P\dot{\varphi}$, reversing the sign of the eliminated rotational term. The energy and Lagrangian methods agree once their controlled quantities are distinguished.

With $I_0 = 0.020\,\mathrm{kg\,m^2}$, $m = 0.10\,\mathrm{kg}$, $r_0 = 0.10\,\mathrm{m}$, initial angular speed $4.0\,\mathrm{rad/s}$ and zero radial speed, total momentum is $0.084\,\mathrm{kg\,m^2/s}$ and energy $0.168\,\mathrm{J}$. At $r = 0.30\,\mathrm{m}$ the rotation rate has fallen to $0.084/0.029 = 2.90\,\mathrm{rad/s}$. The remaining radial kinetic energy is $0.168 - 0.084^2/(2 \cdot 0.029) = 0.0463\,\mathrm{J}$, giving radial speed $0.962\,\mathrm{m/s}$. Under a prescribed constant angular speed of four, the radial first integral instead gives $\dot{r} = 4\sqrt{r^2 - r_0^2} = 1.13\,\mathrm{m/s}$ there. The two runs started with identical positions and velocities but have different power connections.

The drive can also be modelled between those limits. Let a servo apply torque $\tau_{\mathrm{drive}} = K_{\mathrm{s}}(\Omega_{\mathrm{command}} - \dot{\varphi})$. Then $d[(I_0 + mr^2)\dot{\varphi}]/dt = \tau_{\mathrm{drive}}$, and the rate of increase of total mechanical energy is $\tau_{\mathrm{drive}}\dot{\varphi}$. A high control gain with finite response time can approximate the prescribed-speed case over part of a trajectory, yet a rapid radial change can cause a measurable speed sag. Recording shaft torque and speed together tests the drive rather than attributing its lag to a fictitious radial friction on the bead.

Infer drive work from a closed loop of length and measured tension

The reel-pendulum experiment produces synchronised records of string force and length. Over a period in which the length returns to its original value, the work on the bob from the reel is $-\oint T\,dl$. A graph of tension against length can enclose a signed area although the string force at each instant is perpendicular to the bob's allowed virtual angular displacement. That loop area measures energy transferred by the imposed control. If the bob returns to its full mechanical state and there are no other energy sources, any net positive reel work must go into losses. If only the string length returns, the bob's energy can increase cycle after cycle.

Suppose the reel shortens by $20\,\mathrm{mm}$ during a high-tension interval averaging $7.0\,\mathrm{N}$, then pays out the same length while the mean tension is $4.5\,\mathrm{N}$. The net mechanical work on the bob is $0.020(7.0-4.5)=0.050\,\mathrm{J}$ for that cycle. A torque sensor on a reel of changing winding radius must convert torque to tension with the actual instantaneous radius. A force signal delayed relative to the length encoder can create a spurious enclosed area, especially when tension changes rapidly near a turning point. Repeating the measurement slowly with a known hanging calibration weight provides a direct check of polarity and timing.

Derive rapid-pivot stabilisation rather than replacing gravity by its mean

The vertical-pivot equation can be written $\ddot{\theta}+[g/l-(A\Omega^2/l)\cos\Omega t]\sin\theta=0$. The time average of the oscillatory coefficient is zero. Nevertheless a high-frequency pivot can alter slow stability because the small fast ripple in θ correlates with the fast acceleration. Let $\theta=\Theta+\xi$, where Θ varies little in a drive period and ξ is small. Keeping the leading rapidly oscillating term gives $\ddot{\xi}\simeq(A\Omega^2/l)\sin\Theta\cos\Omega t$, hence $\xi\simeq-(A/l)\sin\Theta\cos\Omega t$. Its amplitude scales with displacement ratio A/l, so large acceleration and small angular ripple can coexist.

Expand $\sin(\Theta+\xi)\simeq\sin\Theta+\xi\cos\Theta$, insert the fast solution, and average. Terms linear in the cosine average to zero but the product of ripple and imposed acceleration gives a mean cosine square of one half. To leading order the slow equation is

$$\ddot{\Theta}+\frac{g}{l}\sin\Theta+\frac{A^2\Omega^2}{2l^2}\sin\Theta\cos\Theta=0.$$

It derives from an effective potential per angular inertia $U_{\mathrm{eff}}/(ml^2)=-(g/l)\cos\Theta+[A^2\Omega^2/(4l^2)]\sin^2\Theta$, up to a constant. Linearising near $\Theta=\pi+\eta$ gives

$$\ddot{\eta}+[A^2\Omega^2/(2l^2)-g/l]\eta=0.$$

The inverted state is stable within the averaged approximation if $A^2\Omega^2>2gl$. The restoring contribution depends on squared pivot speed amplitude. Replacing effective gravity by its simple time average would miss it entirely.

Choose a rigid pendulum arm with $l=0.20\,\mathrm{m}$, drive amplitude $A=0.0040\,\mathrm{m}$, and $\Omega=600\,\mathrm{s}^{-1}$. The small displacement ratio is 0.020, the pivot speed amplitude is $2.4\,\mathrm{m/s}$, and $A^2\Omega^2=5.76\,\mathrm{m}^2/\mathrm{s}^2$, above $2gl=3.92\,\mathrm{m}^2/\mathrm{s}^2$. The predicted slow angular frequency about the inverted state is $\sqrt{5.76/(2\cdot0.20^2)-9.81/0.20}=4.79\,\mathrm{s}^{-1}$, far below the drive frequency. A slow ripple of tilt $0.10\,\mathrm{rad}$ has a leading drive-frequency micromotion of roughly $0.0020\,\mathrm{rad}$. A camera sampling at an unfortunate phase can hide this micromotion or alias it into apparent slow drift.

The rigid arm in this example is essential. An ordinary string cannot push its bob when an averaged upright configuration requires alternating compression and tension throughout a fast cycle. Check the actual instantaneous radial reaction and the physical actuator's ability to deliver the large acceleration. Also check drive-period, arm elasticity and support resonance before identifying an observed stable

wobble with the averaged rigid-arm prediction. The leading formula assumes small ripple and a clear separation between Ω and all slow angular frequencies; near threshold the slow restoring coefficient is a small difference and higher-order effects or friction become relatively important.

Separate support work from energy in a moving coordinate

Prescribe an accelerating support. Compare the relative response with what a laboratory observer sees and identify how the drive supplies energy.

Open this experiment online

Try the calculation

Support acceleration (m/s²) **1.6**

Spring stiffness (N/m) **8**



The equilibrium is at -0.1 m. The first turning point is -0.2 m at 0.7854 s.

Distinguish two ways of moving an endpoint in Hamilton's principle

When a constraint itself is explicitly time dependent, the identity $\delta g = \nabla g \cdot \delta x = 0$ describes a virtual change at fixed time on the moving surface. A variational problem may instead allow the endpoint time to change. If a terminal point moves along a prescribed spacetime curve $q_b(t)$, the endpoint variation includes $dq_b = \dot{q}_b\, dt$; it is not an arbitrary tangent displacement at fixed laboratory clock. The boundary term in the on-shell action is $p\, dq - H\, dt$. Reading these two terms separately tells which physical terminal conditions a derivation has assumed.

For a free particle of mass m moving in one dimension from the origin at time zero to q at time T, the extremal action is $S = mq^2/(2T)$. Its derivatives are $S_q = mq/T = p$ and $S_T = -mq^2/(2T^2) = -H$. If the terminal marker moves as $q_b(T) = uT$, the action of the connecting extremal is $mu^2T/2$. Its derivative along that endpoint line is $pu - H = mu^2/2$, exactly the direct derivative. Holding the

endpoint position fixed while differentiating instead gives $-mu^2/2$. Both derivative experiments are legitimate, but the different signs demonstrate why one must state what is fixed.

Can a numerical action fit identify momentum and energy from a single sequence of terminal markers all moving at speed u?

▼ **Work through the solution**

Along that one curve it returns the combination $pu - H$. Separating momentum and energy requires independent endpoint variations in position and time, or another dynamical relation. For the free-particle model the known quadratic Hamiltonian supplies such a relation. For an unknown effective system a single endpoint track can leave different combinations indistinguishable. A grid of nearby fixed-time endpoints estimates p, and a separate grid of terminal times at fixed place estimates $-H$. This measurement interpretation is the finite-dimensional counterpart of separating virtual reaction work from actual boundary power.

Infer whether a moving wall may be treated as prescribed

In an actual impact apparatus the wall has finite effective mass M. For a one-dimensional elastic impact with an initially moving wall, conservation of total momentum and reversal of relative velocity give

$$v^+ = [(m - M)v^- + 2MU]/(m + M),$$
$$U^+ = [2mv^- + (M - m)U]/(m + M).$$

Only the limit $M/m \to \infty$, or active feedback able to enforce the schedule on the collision time scale, gives the prescribed-wall expression used earlier. A motor that restores its target speed a second later may still behave as a finite inertia during the collision itself.

Take $m = 0.20\,\mathrm{kg}$, $M = 2.0\,\mathrm{kg}$, $v^- = 3.0\,\mathrm{m/s}$ and $U = -0.50\,\mathrm{m/s}$. The finite wall sends the particle back at approximately $-3.36\,\mathrm{m/s}$ and recoils to $+0.136\,\mathrm{m/s}$, compared with the prescribed-wall prediction of $-4.0\,\mathrm{m/s}$. Check that the initial and final total momenta both equal about $-0.40\,\mathrm{kg\,m/s}$. Measuring wall speed immediately before and after contact separates an imperfectly enforced boundary from an inelastic impact; both can reduce the magnitude of particle rebound relative to an ideal prescribed boundary.

Tutorial on a prescribed moving apparatus

The rotating slot is held at fixed Ω, but the bead is initially given inward speed $-\Omega r_0$. Predict its subsequent motion and whether the motor delivers or receives power.

▼ **Work through the solution**

The general solution is a combination of growing and decaying exponentials. These initial conditions select $r = r_0 e^{-\Omega t}$. The wall reaction $2m\Omega\dot{r}$ is negative, and its power $2m\Omega^2 r\dot{r}$ is also negative. The

motor receives energy from the bead while maintaining its speed. The same geometric constraint can therefore inject or absorb energy depending on the actual trajectory. The origin is approached only asymptotically in the ideal solution.

At $l = 0.80\,\mathrm{m}$ and $\theta = 0$, a bob has zero angular speed and the prescribed reel tries to accelerate the length outward at $12\,\mathrm{m/s^2}$. Can a string enforce this motion?

▼ **Work through the solution**

The radial-force equation gives $T = m(g - 12)$, a negative tension. A string cannot push the bob outward. The reel pays out slack and the bob initially accelerates under gravity, so treating $l(t)$ as its exact radius becomes inadmissible. A rigid telescopic arm capable of compression would impose a different physical constraint and could enforce the same geometrical schedule.

A pivot is displaced sinusoidally by $2.0\,\mathrm{mm}$ at $1.0\,\mathrm{Hz}$ with $l = 0.25\,\mathrm{m}$. Is the low-frequency tilt formula suitable?

▼ **Work through the solution**

The natural angular frequency is $\sqrt{9.81/0.25} = 6.26\,\mathrm{rad/s}$, almost equal to the drive angular frequency $2\pi = 6.28\,\mathrm{rad/s}$. The low-frequency expansion requires a frequency much smaller than the natural one and fails here. Measure damping and initial conditions, or model a finite-time drive. A steady frictionless amplitude calculated from the small difference of squared frequencies is extremely sensitive to uncertainties in the length and drive frequency.

Compare a second rotating constraint and identify what the motor holds fixed.

David Tong's Lagrangian dynamics chapter develops explicitly time-dependent coordinate changes.

Analytical mechanics from constraints to invariants · 3. Noether's theorem, boundary terms and measurable constants

A constant of motion can survive when neither laboratory energy nor angular momentum is separately conserved. Construct the conserved quantity from an infinitesimal transformation of the action. Then use boosts, a screw symmetry, and a rotating potential to determine what measured combinations should stay fixed.

Vary a path and its time labels

Let $q_i(t)$ be a path for $L(q, \dot{q}, t)$. Consider a continuous family of transformations $t' = t + \varepsilon\tau(q, t)$, $q_i'(t') = q_i(t) + \varepsilon\xi_i(q, t)$, to first order in a constant parameter. The transformation at the corresponding new time has displacement ξ_i; at the original time the path perturbation is $\eta_i = \xi_i - \dot{q}_i\tau$. Distinguishing these variations prevents a time translation from being mistaken for a vertical displacement in a configuration-versus-time plot. Differentiating the transformed coordinates gives

$$\delta\dot{q}_i/\varepsilon = \dot{\xi}_i - \dot{q}_i\dot{\tau},$$

with dots on the generator functions meaning derivatives along the path.

The transformed integration element is $dt' = (1 + \varepsilon\dot{\tau})dt$. A variational symmetry need only preserve the action up to an endpoint term. If its first-order change in the Lagrangian times the time element is $\varepsilon\, dF/dt\, dt$, the equations of motion with fixed endpoints are unchanged. Substitute the variations to write

$$\sum_i \left(L_{q_i}\xi_i + p_i\dot{\xi}_i - p_i\dot{q}_i\dot{\tau}\right) + L_t\tau + L\dot{\tau} = \frac{dF}{dt},$$

$$p_i = L_{\dot{q}_i}.$$

On a physical path $L_{q_i} = \dot{p}_i$. Combine the first two terms into $d(\sum p_i\xi_i)/dt$. Define $H = \sum p_i\dot{q}_i - L$; its derivative on a solution is

$$\dot{H} = -L_t.$$

The terms with τ then combine into $-d(H\tau)/dt$. Thus $Q = \sum_i p_i\xi_i - H\tau - F$ is conserved. Reversing the sign of the generator reverses the sign of the charge, which has no bearing on conservation. Scaling the group parameter also rescales the charge, so specifying the transformation matters when reporting its units.

Recover the familiar examples and test broken symmetry

For a common infinitesimal translation along fixed unit vector $\hat{n}$, every particle has $\xi_a = \hat{n}$, $\tau = 0$. A potential depending solely on pair separations is invariant, so $F = 0$. The conserved charge is total momentum along $\hat{n}$. For an infinitesimal rotation about the origin,

$$\xi_a = \hat{n} \times \mathbf{r}_a;$$

the scalar triple product gives $\hat{n} \cdot \sum_a \mathbf{r}_a \times \mathbf{p}_a$, the chosen angular momentum component. For time translation $\tau = 1, \xi = 0$, an explicitly time-independent Lagrangian gives $Q = -H$. In each case the symmetry refers to the system including the prescribed external fields. Internal pair forces may conserve momentum while a fixed trap exerting an external force breaks the translation symmetry of the particles.

The algebra also gives an exact diagnostic for an approximate symmetry. If the variation of $L dt$ differs from the boundary term by $\varepsilon \mathcal{D}\, dt$, the same steps give

$$\dot{Q} = \mathcal{D}.$$

In a weak potential $V(x) = V_0 + \epsilon U(x)$, translation of x gives

$$\dot{p}_x = -\epsilon U'(x).$$

A drifting computed momentum is therefore not automatically a failure of the time integrator. Compare its change with the integrated physical symmetry-breaking force. Reversing the small external bias helps separate the first-order physical drift from a numerical offset that does not reverse.

Derive a boost charge that needs an endpoint term

Consider a free Newtonian particle in one dimension and a small Galilean boost $x' = x + \varepsilon t$. Here $\xi = t$, $\tau = 0$, and $L = m\dot{x}^2/2$ changes to first order by $m\dot{x}\varepsilon = d(mx\varepsilon)/dt$. The Lagrangian is not pointwise invariant, but its change is a total derivative. The charge is $Q = pt - mx$; its constancy is equivalent to $x - (p/m)t$ remaining equal to the initial position. Dropping the endpoint term would give pt, whose derivative is generally the nonzero momentum itself.

For mutually interacting particles with translationally invariant internal forces, summing the argument gives

$$Q = Pt - M R_{\mathrm{cm}}.$$

Constancy of total momentum and boost charge together imply that the centre of mass moves uniformly along a straight line. Take two pucks of masses 0.20 and $0.30\,\mathrm{kg}$ with $x_1(0) = 0$, $x_2(0) = 1.0\,\mathrm{m}$, and velocities 2.0 and $-0.5\,\mathrm{m/s}$. Their total momentum is $0.25\,\mathrm{kg\,m/s}$ and centre of mass starts at $0.60\,\mathrm{m}$. At $t = 0.40\,\mathrm{s}$, including any intervening isolated elastic collision, it must be at $0.80\,\mathrm{m}$. The boost charge $0.25t - 0.50R_{\mathrm{cm}}$ remains $-0.30\,\mathrm{kg\,m}$. Internal impact changes the individual momenta but preserves both total quantities.

Rotate and translate together in a helical landscape

Let a particle move in cylindrical coordinates in a potential $V(r, z - c\varphi)$, with the combination physically interpreted on a helical branch or within a periodic potential compatible with 2π rotation. Rotation

through a small angle ε combined with translation $z \to z + c\varepsilon$ leaves the potential unchanged. The kinetic energy $m(\dot r^2 + r^2\dot\varphi^2 + \dot z^2)/2$ also stays unchanged. The generator has $\xi_\varphi = 1, \xi_z = c$, hence $Q = p_\varphi + c p_z$ is conserved. The constant c has units of length per radian, so both terms have angular-momentum units.

Differentiate directly as a check. Writing $u = z - c\varphi$, Hamilton's equations give

$$\dot p_\varphi = +c\,V_u,$$

$$\dot p_z = -V_u.$$

Each can change, yet the combination has zero derivative. A guided particle receiving a burst of axial momentum can exchange a specific amount of angular momentum with the helical potential. For $c = 0.030\,\mathrm{m}$ and $\Delta p_z = 0.080\,\mathrm{kg\,m/s}$, the relation predicts $\Delta p_\varphi = -0.0024\,\mathrm{kg\,m^2/s}$. A circularly symmetric potential would conserve angular momentum on its own and represents a different field configuration.

Exchange energy and angular momentum in a rotating pattern

A potential $V(r, \varphi - \Omega t)$ with constant pattern speed is unchanged when time increases by ε and the particle coordinates rotate by $\Omega\varepsilon$. Take $\tau = 1, \xi_\varphi = \Omega$. The conserved combination is $H - \Omega p_\varphi$, up to the sign chosen for Q. A torque from the rotating apparatus can change ordinary energy and ordinary angular momentum. Their changes obey $dH = \Omega\, dp_\varphi$ along the trajectory when the Hamiltonian contains only the prescribed rotating potential as explicit time dependence. The external power equals angular speed times the torque acting through that pattern.

Suppose $\Omega = 12\,\mathrm{rad/s}$ and a particle gains $0.015\,\mathrm{kg\,m^2/s}$ in axial angular momentum during a passage past the rotating potential. Its mechanical energy must gain $0.180\,\mathrm{J}$. A numerical run reporting $0.195\,\mathrm{J}$ calls for accounting for other time dependence, sampling uncertainty or integration error. If Ω itself slowly varies, introduce a pattern angle $\alpha(t)$, $\Omega = \dot\alpha$. One still finds $\dot H = \Omega \dot p_\varphi$, but $d(H - \Omega p_\varphi)/dt = -\dot\Omega p_\varphi$. Testing an exact rotating-frame invariant with a ramped motor would therefore diagnose the wrong experiment.

Find the conserved momentum in a magnetic field directly from the action

A charge q of mass m moves in a uniform static field $B\hat z$. Choose vector potential $A_y = Bx$, scalar potential zero. Its Lagrangian in the perpendicular plane is $L = m(\dot x^2 + \dot y^2)/2 + qBx\dot y$. The position y is cyclic, so $p_y = m\dot y + qBx$ is constant. The physical force is also invariant under translations in x, although x appears in this chosen Lagrangian. Under $x \to x + \varepsilon$, its change is $qB\dot y\,\varepsilon = d(qBy\varepsilon)/dt$. The corresponding Noether charge is $p_x - qBy = m\dot x - qBy$. Thus both spatial translation symmetries survive once the endpoint term is included.

Write $\omega_c = qB/m$, which retains the sign of the charge. Rearranging the two constants gives the coordinates of the guiding centre $X_c = x + \dot y/\omega_c$, $Y_c = y - \dot x/\omega_c$. Differentiate using

$m\ddot{x} = qB\dot{y},\ m\ddot{y} = -qB\dot{x}$ to see both are independent of time. A uniform field changes velocity direction but does no work. In a force experiment the centre of the measured circular arc, its radius and its angular orientation can be estimated without measuring any vector potential. The endpoint terms explain why two gauge choices can assign different canonical momenta while predicting the same observed guiding centre.

There is a useful algebraic surprise. Denote the translation charges by $K_x = p_x - qBy$ and $K_y = p_y$ in the chosen gauge. Their canonical bracket is $\{K_x, K_y\} = -qB$. Each is conserved, yet the bracket does not vanish. The result is a constant, so Jacobi's identity is satisfied. The mechanical effect of their infinitesimal flows on positions commutes; a central constant in the charge bracket has zero Hamiltonian vector field. Conservation, commutation of the generated coordinate motions, and zero bracket of the generating functions are related but distinct statements. This example supplies a direct check when applying symmetry counting in phase space.

For an illustrative particle with $q/m = 2.0\,\mathrm{C/kg}$, $B = 0.50\,\mathrm{T}$, initial $(x, y) = (0.20, 0.10)\,\mathrm{m}$ and velocity $(0.30, -0.40)\,\mathrm{m/s}$, the signed cyclotron frequency is $1.0\,\mathrm{s^{-1}}$. The guiding centre is $(-0.20, -0.20)\,\mathrm{m}$, and the radius from that centre is $0.50\,\mathrm{m}$. The speed is $0.50\,\mathrm{m/s}$, consistent with radius $v/|\omega_c|$. Replacing the field by its negative at the same initial state moves the guiding centre to the opposite side of the initial velocity and reverses the sense of rotation. A constant numerical offset in the vector potential should leave both reconstructed centres unchanged.

Use scaling to decide when a formal transformation creates a charge

Many equations of motion have scaling relations. A map taking one solution into another need not preserve the action up to an endpoint term, and therefore need not supply a Noether charge. To test an example, let $L = T - V$ in three dimensions with V homogeneous of degree n, so $V(\lambda \mathbf{r}) = \lambda^n V(\mathbf{r})$. Take $\mathbf{r} \to e^{\varepsilon}\mathbf{r}$, $t \to e^{a\varepsilon}t$. Kinetic energy times dt scales as $e^{(2-a)\varepsilon}$, while potential energy times dt scales as $e^{(n+a)\varepsilon}$. Equating the exponents gives $a = (2 - n)/2$, a map that rescales the entire action by a common factor and preserves stationary paths. Exact invariance of the action additionally requires the common exponent to vanish, giving $a = 2, n = -2$.

For a potential proportional to $1/r^2$, the continuous symmetry has $\xi = \mathbf{r}, \tau = 2t$, $F = 0$, and charge $D = \mathbf{r} \cdot \mathbf{p} - 2tH$. Direct differentiation gives $d(\mathbf{r} \cdot \mathbf{p})/dt = 2T - \mathbf{r} \cdot \nabla V = 2T + 2V = 2H$, verifying conservation. At fixed positive energy this particular scalar product grows linearly in time. This does not require every coordinate to grow linearly; it follows from the scaling structure of the combined kinetic and potential energies. Collision singularities may limit the interval on which a classical solution exists.

For a Newtonian potential $n = -1$, the path scaling gives $a = 3/2$, precisely the scaling of orbital periods with orbital size. The common action exponent is $1/2$, so this scaling does not produce the preceding conserved D. Instead the virial identity $d(\mathbf{r} \cdot \mathbf{p})/dt = 2T + V$ implies $2\langle T \rangle + \langle V \rangle = 0$ on a bounded periodic trajectory after time averaging. This distinction can be checked numerically on one elliptical orbit: the virial combination generally oscillates during a cycle, whereas its integrated full-cycle average vanishes. Mistaking a scaling of solutions for exact invariance of the action would turn that averaged result into a false instantaneous conservation law.

Derive a centre-of-energy statement from a boost charge

For a free relativistic particle in one spatial dimension use $L = -mc^2\sqrt{1-\dot{x}^2/c^2}$. An infinitesimal Lorentz boost, with a parameter carrying velocity units and the sign convention $x' = x + \varepsilon t$, has generators $\xi = t, \tau = x/c^2$. Proper time is invariant, so $L dt$ is invariant and $F = 0$. The Noether charge is $K = pt - Hx/c^2$, where $H = \gamma mc^2$, $p = \gamma m\dot{x}$. Its derivative vanishes because $p = H\dot{x}/c^2$. At low speed H/c^2 approaches m, and the Newtonian boost charge reappears up to relativistic corrections.

For an isolated set of freely propagating particles away from local collisions, sum the charges to obtain

$$K = Pt - (E_{\mathrm{tot}}/c^2)X_E,$$

where $X_E = \sum E_i x_i / E_{\mathrm{tot}}$ is the centre of energy. If collisions conserve total energy and momentum and occur at the same spacetime point for their participants, the summed charge passes continuously across them. Its constancy implies

$$dX_E/dt = c^2 P / E_{\mathrm{tot}}.$$

In an interacting field problem energy stored between particles also belongs in the weighted centre; assigning every bit of energy to particle positions can violate the balance. A field-carrying interaction illustrates why the Newtonian centre of mass alone is insufficient in a relativistic energy accounting.

Imagine equal positive rest masses at $x = 0$ and $x = 2.0\,\mathrm{m}$. At the observation instant their energies are $2mc^2$ and mc^2, with the more energetic particle moving to the right and the second at rest. Their ordinary mass centre is $1.0\,\mathrm{m}$, while their energy centre is $2/3\,\mathrm{m}$. The total momentum is $\sqrt{3}\,mc$, the total energy $3mc^2$, so the centre of energy moves at $c/\sqrt{3}$. The numerical difference is not a correction to the measured coordinates but a change in the physical quantity whose motion follows a boost symmetry. A centre-of-momentum frame for the pair moves at the same speed.

Diagnose symmetry from noisy finite-time balances

In an experiment one rarely has symbolic access to every component of the Lagrangian. A practical symmetry test measures the candidate charge at two times and independently integrates the physical source expected to change it. For the rotating potential, use $R = \Delta H - \int_{t_1}^{t_2} \Omega(t)\, dL_z$. If Ω is measured on the same clock as the trajectory, the integral can be estimated by summing the mean Ω across each angular-momentum increment. This avoids taking a second time derivative of position merely to reconstruct the torque. An equivalent form obtained by parts is $\Delta(H - \Omega L_z) + \int L_z\, d\Omega$. Both versions should agree if endpoint times and signs are consistent.

Take a short programmed ramp in which Ω increases linearly from 10 to $12\,\mathrm{s^{-1}}$ and L_z from 0.030 to $0.050\,\mathrm{kg\,m^2/s}$ over the same time. If the rotating pattern is the only external work source, the energy change is mean speed times angular-momentum change,

$$11(0.020) = 0.220\,\mathrm{J}.$$

The product ΩL_z changes by $0.600 - 0.300 = 0.300\,\mathrm{J}$, so $H - \Omega L_z$ falls by $0.080\,\mathrm{J}$. The missing amount equals

$$-\int L_z \, d\Omega = -0.040(2) = -0.080\,\mathrm{J}.$$

These two balances provide a nontrivial sign test when the drive speed is varied deliberately.

When measurements are noisy, an observed discrepancy must be compared with the uncertainties of both charge and physical source. An erroneous angular zero in a central problem can affect the torque reconstruction while leaving a scalar speed unchanged; a simple time shift between the motor encoder and position camera can mimic an extra source of work. Change the drive direction, repeat with constant speed, and estimate the effect of clock offsets using resampled records. These experiments test the specific symmetry under investigation. A plot that appears almost flat on an arbitrary vertical scale supplies neither a physical tolerance nor a discrimination among competing error sources.

Derive a conservation law for an elastic field

Noether's argument also applies when the coordinates form a continuous field $u(x,t)$. Consider a uniform string or rod with density per length ρ_l, displacement field u and stiffness coefficient C, so $\mathcal{L} = \rho_l u_t^2/2 - C u_x^2/2$. A constant shift $u \to u + \varepsilon$ changes no strain and leaves the density invariant. The Euler–Lagrange equation becomes $\partial_t(\rho_l u_t) + \partial_x(-C u_x) = 0$, a local conservation law. For an axial rod the density $\rho_l u_t$ is ordinary longitudinal momentum per unit length, and the boundary term is axial traction with its outward sign. A uniform displacement symmetry survives a free translation of the whole rod but is broken if an end displacement is imposed relative to a clamp.

Integrate from $x = 0$ to L. The total physical momentum changes as $dP/dt = C u_x(L) - C u_x(0)$. A fixed end can exert a nonzero reaction and spoil conservation of the rod's momentum even when it does no power because its actual velocity vanishes. The distinction between a momentum source and an energy source is experimental: a rigid wall reflecting a pulse can accept net impulse while taking no mechanical energy. Including the support in the system restores the corresponding balance. Checking only the field density's invariance in the interior neglects boundary conditions, which are part of a physical symmetry.

The uniformity of material parameters also gives an invariance under translations of the material coordinate x in an infinite or periodic homogeneous domain. The associated density is proportional to $-\rho_l u_t u_x$, often called wave pseudomomentum under this convention. Derive its local balance by multiplying $\rho_l u_{tt} = C u_{xx}$ by $-u_x$ and applying the product rule. One obtains

$$\partial_t(-\rho_l u_t u_x) + \partial_x[C u_x^2/2 + \rho_l u_t^2/2] = 0.$$

This conserved quantity differs from the ordinary momentum found from shifting u itself. A small-amplitude sinusoidal travelling wave can have zero mean material velocity over one period yet positive mean transport of this wave quantity.

For $u = A\cos(kx - \omega t)$,

$$u_t = \omega A \sin(kx - \omega t),$$
$$u_x = -kA \sin(kx - \omega t).$$

The cycle-averaged wave density is $\rho_l \omega k A^2/2$ while ordinary momentum density averages to zero. With $\rho_l = 0.20\,\mathrm{kg/m}$, $A = 1.0\,\mathrm{mm}$, $k = 5.0\,\mathrm{m^{-1}}$, and $\omega = 100\,\mathrm{s^{-1}}$, the average wave density is $5.0 \times 10^{-5}\,\mathrm{kg/s}$. Its units are momentum per unit length, but equal dimensions do not make the two conserved charges interchangeable. To identify the charge, specify whether the symmetry shifts every displacement equally or shifts the material-coordinate pattern.

Test the evolution of a phase-space patch

Follow a family of initial conditions in a Hamiltonian flow. Compare changes in its shape with the conservation of its phase-space area.

Open this experiment online

Try the calculation

Time after release (s) **4**

Drag rate γ (1/s) **0.2**

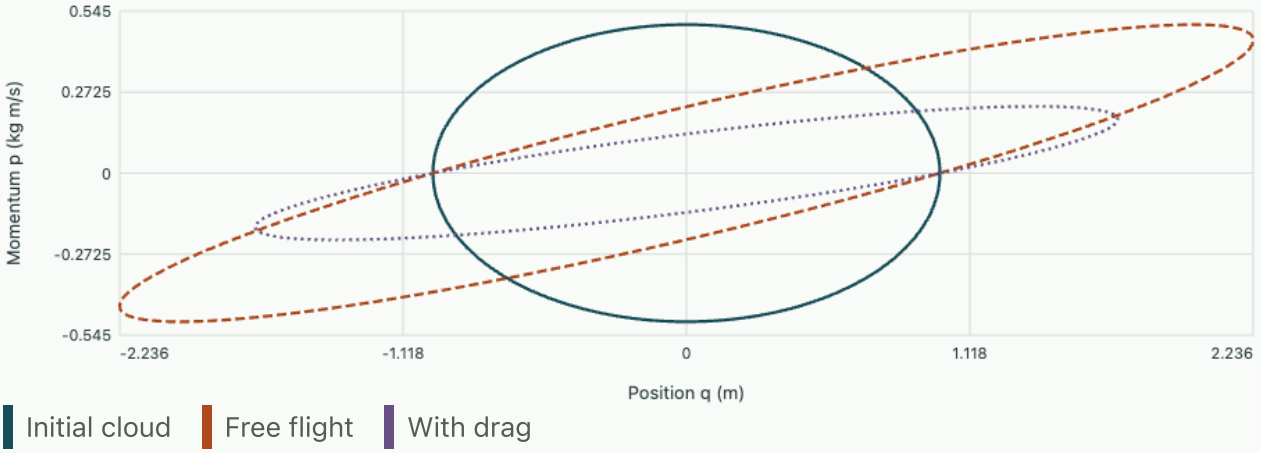

Free position spread 2.236 m. The damped ellipse retains 44.93% of its initial area and has position spread 1.702 m.

Derive an identity without assuming the equations of motion

The usual on-shell proof substitutes the Euler–Lagrange equations just before a total derivative appears. Retaining the difference gives an equally useful off-shell identity. Define the residual $R_i = dp_i/dt - \partial L/\partial q_i$. For a true variational symmetry and any differentiable trial path, repeat the calculation with $\eta_i = \xi_i - \dot{q}_i \tau$. The result is

$$dQ/dt = \sum_i R_i \eta_i.$$

Thus the drift of a Noether charge evaluated on an approximate path is a particular projection of its dynamical residual. A path can have zero drift of one charge while violating equations in directions to which that charge is insensitive.

For a free particle in two dimensions, perfect conservation of p_x enforces zero residual acceleration in the x direction but says nothing about a spurious force in y. Conversely tracking two independent translational charges checks both components. Energy conservation tests a different projection, $dH/dt = \dot{\mathbf{q}} \cdot \mathbf{R}$ for a time-independent Lagrangian. An error force always perpendicular to velocity can leave the speed and energy unchanged while bending an originally straight trajectory. That is one reason an invariant energy graph cannot replace a force residual or a comparison of trajectories.

A numerical planar free particle follows a circle of constant speed even though the programmed potential vanishes. Its energy is conserved exactly. Which Noether quantities expose the problem most directly?

▼ **Work through the solution**

The two laboratory translation momenta should each be constant. On the reported circle their vector changes direction continuously, so their residuals immediately reveal the missing transverse equation. A check of only the magnitude of momentum would also pass because that magnitude is fixed by energy. The angular momentum about the circle centre can remain constant too. Testing a set of charges selected for the actual symmetry and measured geometry identifies information lost by each scalar test on its own.

If the Lagrangian acquires a small explicitly time-dependent conservative potential $V_1(t)q^2$, what quantity should replace a flat-energy test?

▼ **Work through the solution**

The energy change on a physical path is $\Delta H = \int \dot{V}_1(t) q(t)^2 \, dt$. Positive or negative changes are allowed according to how the externally imposed stiffness is varied during the motion. Compare the measured change with this integral while keeping the time dependence inside the Hamiltonian itself. A flat-energy requirement would incorrectly penalise physical work by the control, whereas a residual after the input integral tests the dynamics.

Separate a discrete symmetry from a continuous one

A potential $V(q) = a(q^2 - b^2)^2$ is invariant under the discrete reflection $q \mapsto -q$. Reflecting both position and velocity maps any solution into another solution with equal energy. There is no continuously tunable parameter that takes the identity smoothly to this isolated reflection while preserving the same one-dimensional potential at every intermediate step. No infinitesimal translation generator follows from this symmetry, and the momentum generally changes along either path. A pair of measured trajectories

launched from mirrored initial data should match after reflection, but neither trajectory is required to have zero or constant momentum.

For $a = 1$ and $b = 1$ in consistent scaled units, release particles from $q = 0.50$ and -0.50 at rest. The force is $-4q(q^2 - 1)$, giving initial accelerations $+1.50/m$ and $-1.50/m$. The two accelerations are mirror images, not individually zero. A numerical method that accidentally introduces a constant bias force breaks the reflection comparison and shifts the two turning times in opposite senses. Energy can remain nearly conserved with respect to a slightly tilted effective potential, so trajectory pairing is a complementary diagnostic. Reflection symmetry imposes a relationship between solutions even when Noether's continuous-symmetry construction supplies no new conserved scalar.

Tutorial on identifying symmetries

A Lagrangian is replaced by $L' = L + dG(q, t)/dt$. Does the numerical value of an appropriately derived Noether charge have to change?

▼ Work through the solution

The new momentum is $p_i' = p_i + G_{q_i}$, and $H' = H - G_t$. Under the given symmetry the new boundary term is $F' = F + \sum_i G_{q_i}\xi_i + G_t\tau$. Substitution into $p'\xi - H'\tau - F'$ cancels the extra terms exactly. Charges can still be shifted by a physically irrelevant additive constant through the choice of boundary term. Comparing raw canonical momentum in two such conventions without also transforming F, H confuses intermediate variables with observations.

A central potential is changed into an axisymmetric potential $V(r, \theta)$. Which angular-momentum tests remain exact?

▼ Work through the solution

Rotation about the symmetry axis remains a continuous symmetry, so its angular-momentum component is conserved. Tilt rotations generally change the potential, so the transverse components need not stay constant. The torque may cause the angular momentum direction or magnitude to evolve while maintaining its axial component. A code test that requires all components to remain fixed would reject many legitimate axisymmetric trajectories.

A table exerts an unmodelled approximately constant horizontal drag $0.010\,\mathrm{N}$ opposite the motion of the two pucks for $0.40\,\mathrm{s}$. Estimate how the translation and boost checks change.

▼ Work through the solution

Total momentum changes by $-0.0040\,\mathrm{kg\,m/s}$. The derivative of $Pt - MR_{\mathrm{cm}}$ is $t\dot{P}$, since $P = M\dot{R}_{\mathrm{cm}}$. Its change is therefore $-0.010(0.40)^2/2 = -0.00080\,\mathrm{kg\,m}$ under constant drag. The differing time dependence gives an additional way to distinguish a sustained external force from an initial position calibration error.

Follow the action of an infinitesimal generator on phase space.

David Tong treats continuous symmetries and Noether's theorem in Lagrangian dynamics.

Analytical mechanics from constraints to invariants · 4. Kepler orbits, the eccentricity vector and the loss of apsidal closure

An orbit can conserve energy and angular momentum yet gradually rotate its periapsis. The inverse-square problem possesses one more conserved vector that fixes the direction of closest approach. Derive it, turn a single position and velocity measurement into a conic, and measure what a weak perturbation does to the inferred apsidal direction.

Reduce the two-body system without freezing either mass

Two bodies of masses m_1, m_2 have positions $\mathbf{r}_1, \mathbf{r}_2$. Define total mass $M = m_1 + m_2$, centre $\mathbf{R} = (m_1\mathbf{r}_1 + m_2\mathbf{r}_2)/M$, relative coordinate $\mathbf{r} = \mathbf{r}_1 - \mathbf{r}_2$, and reduced mass $\mu = m_1 m_2 / M$. Substitution into the kinetic energy cancels the cross terms, giving $M\dot{\mathbf{R}}^2/2 + \mu\dot{\mathbf{r}}^2/2$. Newtonian gravitational potential is $-\kappa/r$ with $\kappa = G m_1 m_2$. The centre moves uniformly when isolated, while the relative motion obeys $\mu\ddot{\mathbf{r}} = -\kappa\hat{r}/r^2$. Dividing by the reduced mass gives the acceleration parameter $k = \kappa/\mu = GM$; replacing it by Gm_1 is the test-particle approximation.

Use specific energy $\epsilon = v^2/2 - k/r$ and specific angular momentum $\mathbf{h} = \mathbf{r} \times \mathbf{v}$, both per unit reduced mass. A central force makes $\dot{\mathbf{h}} = 0$, fixing the plane of nonradial motion. The area of the triangle swept in time dt is $r^2 d\varphi/2 = h\,dt/2$, yielding the constant areal rate. The radial energy is $\dot{r}^2/2 + h^2/(2r^2) - k/r$. Its turning points determine the accessible radii, but energy and h alone cannot specify where the major axis lies in the chosen inertial plane.

Construct a vector whose derivative vanishes

The derivative of $\mathbf{v} \times \mathbf{h}$ is $(-k\hat{r}/r^2) \times \mathbf{h}$. Use $\mathbf{h} = r^2\dot{\varphi}\,\hat{z}$ with an oriented plane in which motion is positive. Since $\hat{r} \times \hat{z} = -\hat{\varphi}$, the derivative becomes

$$k\dot{\varphi}\hat{\varphi} = k\,d\hat{r}/dt.$$

Consequently the eccentricity vector

$$\mathbf{e} = \frac{\mathbf{v} \times \mathbf{h}}{k} - \hat{r}$$

is constant. The dimensional Runge–Lenz vector is proportional to this choice: for relative momentum $\mathbf{p} = \mu\mathbf{v}$,

$$\mathbf{A} = \mathbf{p} \times \mathbf{L} - \mu\kappa\hat{r} = \mu\kappa\mathbf{e}.$$

Every term in the specific expression is dimensionless. The step equating the derivative to $k\,d\hat{r}/dt$ uses exactly the inverse-square radial force. General central forces retain areal velocity but lose this cancellation.

Dot $\mathbf{e}$ with $\hat{r}$. The triple product $(\mathbf{v} \times \mathbf{h}) \cdot \hat{r} = h^2/r$ gives

$$e\cos(\varphi-\varpi)=h^2/(kr)-1,$$

where ϖ is the fixed direction of $\mathbf{e}$. Thus $r=p/[1+e\cos(\varphi-\varpi)]$, $p=h^2/k$, the conic in focus-centred polar coordinates. Squaring $\mathbf{e}$ and eliminating v^2 with the energy gives

$$e^2=1+2\epsilon h^2/k^2.$$

Bound ellipses have $\epsilon<0, e<1$, parabolic escape has $\epsilon=0, e=1$, and positive energy gives hyperbolas for nonzero angular momentum. Radial trajectories require separate care because their orbital plane and apsidal angle are degenerate.

Recover the orbit from a single state vector

In units chosen so $k=1$, a measured relative position is $(2,0,0)$ and velocity is $(0.2,0.6,0)$. Compute $h_z=1.2$, $\epsilon=(0.04+0.36)/2-1/2=-0.30$, and $p=1.44$. The cross product $\mathbf{v}\times\mathbf{h}=(0.72,-0.24,0)$ gives $\mathbf{e}=(-0.28,-0.24,0)$, with $e=\sqrt{0.136}\approx 0.369$. The direction of periapsis is about 220.6° from the positive x axis. At the measured point $\dot r>0$, so the body is travelling from periapsis toward apoapsis. Dropping the radial component of velocity would rotate the eccentricity vector and change the inferred shape.

The semimajor axis is

$$a=-k/(2\epsilon)=1.667.$$

Periapsis and apoapsis radii $a(1-e)$ and $a(1+e)$ are approximately 1.05 and 2.28, consistent with the observed radius of two. The orbital period is $2\pi\sqrt{a^3/k}=13.52$ time units. Derive this last result by dividing ellipse area πab by the areal speed $h/2$. Using $b=a\sqrt{1-e^2}$ and $h^2=ka(1-e^2)$ cancels eccentricity exactly. This shows why changing the initial radial velocity can change shape and orientation while the period depends only on binding energy.

Determine time along an ellipse and check limiting cases

Introduce the eccentric anomaly E by $x=a(\cos E-e)$, $y=a\sqrt{1-e^2}\sin E$ in axes centred on the focus, with x pointing toward periapsis. Then $r=a(1-e\cos E)$. Compute $x\,dy-y\,dx=ab(1-e\cos E)\,dE$ and equate it to $h\,dt$. Integrating from periapsis gives

$$n(t-t_p)=E-e\sin E,$$

where $n=\sqrt{k/a^3}$. This relation turns orbital geometry into an observation clock. The true anomaly is generally different from the linearly advancing mean anomaly because the body sweeps angle faster at small radius.

For $e = 0.6$ and the time $t - t_p = T/4$, the mean anomaly is $\pi/2$. Newton iteration for $F(E) = E - 0.6 \sin E - \pi/2$ uses denominator $1 - 0.6 \cos E$, which stays positive. Starting near $E = 2.0$ yields $E \simeq 2.091$ radians and $r \simeq 1.30a$. The orbit has already moved beyond its semimajor radius at a quarter period. At $e = 0$, E equals the mean and true anomalies up to an arbitrary origin, and $\mathbf{e} = 0$ has no definable periapsis direction. Estimating a periapsis angle for a nearly circular noisy orbit is therefore poorly conditioned even when the radius and period are well measured.

Perturb the force and measure apsidal precession

For any central acceleration $f(r)\hat{r}$, put $u = 1/r$. Since $\dot{\varphi} = hu^2$, radial velocity is $-h\,du/d\varphi$. Substituting into the radial acceleration gives Binet's equation $u'' + u = -f(1/u)/(h^2u^2)$, where primes denote angular derivatives. Choose $f(r) = -k/r^2 - \alpha/r^3$. Then $u'' + (1 - \alpha/h^2)u = k/h^2$. If $0 < \alpha < h^2$, a radial oscillation requires angular advance $2\pi/\sqrt{1 - \alpha/h^2}$, greater than one full turn. Successive periapses advance by that value minus 2π, approximately $\pi\alpha/h^2$ for a weak perturbation.

With $\alpha/h^2 = 0.010$, the exact precession per radial cycle is approximately $0.03165\,\mathrm{rad} = 1.81^\circ$. Ordinary energy and angular momentum remain constant in this conservative central potential. The Kepler eccentricity vector evaluated from instantaneous position and velocity now changes. Track periapses using zeros of the radial velocity with positive radial acceleration, then compare their inertial angles. A numerical Kepler integrator can precess even for $\alpha = 0$; refine the time step and repeat the unperturbed control before assigning a small precession to the physical perturbation.

Infer an orbit using quantities that remain well conditioned

Suppose positions and velocities are measured with finite precision. A circular orbit has exact eccentricity vector zero, so even tiny perpendicular perturbations can swing the direction of that vector through large angles. Keep its Cartesian components when computing a fit near circularity. For an initially transverse circular state at radius r and speed $v_c = \sqrt{k/r}$, perturb the velocity by radial δv_r and tangential δv_t. In the local $(\hat{r}, \hat{\varphi})$ basis the eccentricity components are $rv_t^2/k - 1$ and $-rv_rv_t/k$. At first order they become $2\delta v_t/v_c$ and $-\delta v_r/v_c$. This linear response is well behaved even though taking an inverse tangent to quote periapsis longitude can become meaningless.

For a circular speed of $10.0\,\mathrm{m/s}$, radial and tangential measurement errors each of $0.010\,\mathrm{m/s}$ correspond to component uncertainties about 0.0010 and 0.0020. A reported eccentricity of 0.0012 is not accompanied by a precise preferred direction under those uncertainties. Repeated orbital samples reduce independent noise but do not remove a persistent tangential velocity bias. Measuring the radius and period independently supplies an additional constraint on k and the orbital energy. A model that regards the primary as fixed also introduces a systematic mass error when the secondary has non-negligible mass.

At the opposite extreme, a near-parabolic orbit can have a well-defined eccentricity direction but a badly conditioned energy estimate. Its energy is the small difference of $v^2/2$ and k/r. Since $a = -k/(2\epsilon)$, a small energy uncertainty produces a very large uncertainty in semimajor axis and period. Report the measured state vector, eccentricity vector and energy uncertainty before interpreting an enormous best-

fit period. If the energy uncertainty straddles zero, bounded and unbounded conics are both consistent with the measured data. Integrating a single best-fit ellipse for many revolutions does not resolve that ambiguity.

Calculate the velocity impulse to transfer between circular radii

The same two-body invariants reconstruct a transfer between circular trajectories without requiring a time-stepped simulation. Set a lower radius r_1 and an upper radius $r_2 > r_1$. An ellipse tangent to both has periapsis r_1, apoapsis r_2, semimajor axis $a_t = (r_1 + r_2)/2$, and eccentricity $(r_2 - r_1)/(r_2 + r_1)$. At either apsis its speed follows from energy:

$$v_t(r) = \sqrt{k(2/r - 1/a_t)}.$$

A first instantaneous tangential velocity change moves the particle from its lower circular trajectory to the transfer ellipse. A second tangential change at the opposite apsis matches the upper circular speed. These formulas describe impulses idealised as short compared with the orbital period.

Choose normalised $k = r_1 = 1$, $r_2 = 2$. Initial speed is one, transfer semimajor axis 1.5, and periapsis speed $\sqrt{4/3} = 1.1547$. The first change is 0.1547. At the upper radius the transfer speed is $\sqrt{1/3} = 0.57735$, while the circular speed there is

$$1/\sqrt{2} = 0.70711.$$

The second change must also be forward, by 0.12976. The flight time between the two impulses is $\pi\sqrt{1.5^3} = 5.77$ time units, half the transfer period. Simply increasing the initial speed until the path reaches radius two does not make it circular upon arrival. Matching position and angular momentum at the final boundary requires the second change.

Verify the energy increment from an impulse independently. A change $\Delta\mathbf{v}$ at fixed position gives

$$\Delta\epsilon = \mathbf{v}\cdot\Delta\mathbf{v} + |\Delta\mathbf{v}|^2/2.$$

At the lower radius our impulse raises ϵ from -0.5 to $-1/3$, an increase of $1/6$. Substitution of the rounded 0.1547 gives the same value. The same velocity increment generally changes energy more when applied where the initial speed is larger and aligned with the impulse. This is a statement about mechanical work at different initial states, not an exception to conservation between impulses.

A laboratory analogue uses a central potential engineered over a limited radius range. A small finite-duration tangential push changes radius as well as speed during the push. To check the impulse approximation compute the change in angular momentum as $\int \mathbf{r}\times\mathbf{a}_{\text{applied}}\,dt$ and energy as $\int \mathbf{v}\cdot\mathbf{a}_{\text{applied}}\,dt$. Compare these with the instantaneous predictions and shorten the pulse while holding its integrated velocity change fixed. If the return radius still drifts, map the force against radius to distinguish a finite-pulse error from an actual deviation from inverse-square attraction.

Continue the time law across the escape boundary

A hyperbolic Kepler orbit can be described without calling a divergent ellipse period a clock. Define a positive hyperbolic length $a_h = k/(2\epsilon)$ for $\epsilon > 0$, and let $e > 1$. With periapsis on the positive x axis use $x = a_h(e - \cosh H)$,

$$y = a_h\sqrt{e^2 - 1}\sinh H.$$

Then $r = a_h(e\cosh H - 1)$, and the swept-area relation gives

$$t - t_p = \sqrt{a_h^3/k}(e\sinh H - H).$$

The hyperbolic anomaly H increases monotonically from negative to positive along the passage. At large positive H the ratio dr/dt approaches $\sqrt{k/a_h} = \sqrt{2\epsilon}$, the asymptotic speed predicted by the conserved energy.

At the parabolic boundary $e = 1, \epsilon = 0$, put $D = \tan(\varphi/2)$ with φ measured from periapsis. If q_p is the periapsis distance, the semilatus rectum is $p = 2q_p$ and $r = q_p(1 + D^2)$. Since $dt = r^2 d\varphi/h$, $d\varphi = 2dD/(1 + D^2)$ and $h = \sqrt{2kq_p}$, integration gives Barker's relation $t - t_p = \sqrt{2q_p^3/k}(D + D^3/3)$. This expression is finite on either side of the periapsis for finite radius, even as the time to reach infinity diverges. A parabolic passage therefore has an entirely useful local time-of-flight law despite having no period.

For $k = 1$, $q_p = 1$ in scaled units, a parabolic trajectory reaches $\varphi = 90^\circ$ at $D = 1,\ r = 2$. Its elapsed time is

$$4\sqrt{2}/3 = 1.886.$$

Using the instantaneous angular speed at periapsis for the entire quarter turn would predict $(\pi/2)/\sqrt{2} = 1.111$, much too short. The areal speed stays constant, but angular speed decreases by a factor of four by the time radius has doubled. Integrating $r^2 d\varphi/h$ along the conic captures that slowdown directly.

Near zero energy, formulas involving a semimajor axis of enormous magnitude can lose numerical accuracy through cancellation. For example $r = a(1 - e\cos E)$ involves subtracting two near-equal terms near periapsis in a high-eccentricity ellipse. Expressions in $q_p = a(1 - e)$ and half-angle quantities, such as $r = q_p + 2ae\sin^2(E/2)$, avoid one damaging subtraction. A state-based numerical propagation should preserve angular momentum, compare the periapsis passage time with a quadrature, and test both small positive and small negative energies. Agreement only in the well-bound ellipse regime is a weak test of an algorithm used for near-escape trajectories.

Relate the Runge–Lenz direction to a velocity-space circle

The spatial Kepler conic has a simpler partner in velocity space. In the orbital plane,

$$d\mathbf{v}/d\varphi = \mathbf{a}/\dot{\varphi} = (-k\hat{r}/r^2)/(h/r^2) = -(k/h)\hat{r}.$$

Since $d\hat{\varphi}/d\varphi = -\hat{r}$, integration gives

$$\mathbf{v} = (k/h)\hat{\varphi} + \mathbf{v}_c,$$

where $\mathbf{v}_c$ is a constant vector. Thus the velocity vector traces a circle of radius k/h, or part of that circle on an unbound orbit. At periapsis a prograde orbit has speed $(k/h)(1+e)$, so the circle centre is shifted in the prograde tangential direction by ke/h. The offset direction is perpendicular to the eccentricity vector.

One can recover k/h and e from a set of calibrated velocity samples by fitting a circle in the orbital plane and comparing its radius with the offset of its centre from zero velocity. This method still needs the correct inertial frame: adding a constant observer velocity translates every velocity-space point, moving the fitted centre while preserving the circle radius. A time sequence of relative velocities between the two masses removes a common boost. If the force departs from inverse square, the derivative $d\mathbf{v}/d\varphi$ acquires radius dependence and the velocity circle generally distorts. Simultaneously checking the spatial conic and the velocity circle makes a more discriminating test than plotting either shape alone.

Derive which central orbits remain nearly closed

A circular orbit at radius r_c in a smooth potential per mass $U(r)$ has $h^2 = r_c^3 U'(r_c)$. Its angular frequency obeys $\Omega^2 = U'(r_c)/r_c$. Small radial deviations at fixed h see the effective potential $U + h^2/(2r^2)$, so their squared epicyclic frequency is

$$\kappa_r^2 = U''(r_c) + 3U'(r_c)/r_c.$$

During one radial oscillation the orbital angle advances roughly $2\pi\Omega/\kappa_r$. If the two frequencies differ, the apsidal orientation generally rotates, even though energy and angular momentum remain constants. This local result distinguishes near-circular closure from the much stronger claim that all bounded orbits close for a given force law.

For an attractive radial acceleration $-kr^{-s}$, $U' = kr^{-s}$ and $\kappa_r^2 = (3-s)\Omega^2$. A stable circular orbit requires $s < 3$. For inverse square, $s = 2$, radial and angular frequencies agree, so the apsis returns to its starting orientation each revolution. For an isotropic harmonic potential the force is proportional to r, so $s = -1$ and $\kappa_r = 2\Omega$. There are two radial minima per full turn; its closed ellipse is centred on the force centre rather than focused there. A rational near-circular ratio at one energy or radius does not by itself prove global closure for all eccentricities. The Runge–Lenz derivation supplied much stronger information for the inverse-square case.

Suppose a weak field calibration drift changes the local logarithmic force slope from $s = 2$ to $s = 1.98$, approximately constant over a narrow radial range. The near-circular radial frequency is 1.00995Ω. Consecutive closest approaches are separated by $2\pi/\sqrt{1.02} \approx 6.221\,\mathrm{rad}$, giving a retrograde change about $0.062\,\mathrm{rad}$ per radial period. The sign is opposite the advance induced by the additional attractive inverse-cube contribution considered before. Estimating the radial oscillation frequency and orbital

frequency independently can therefore diagnose deviations that an energy test would miss. At larger eccentricity the sampled force covers a broader radial interval and the local-power approximation must be replaced by the full turning-point integral.

Reconstruct a Kepler ellipse from one state

Vary initial radial and tangential velocity separately. Infer the direction of the eccentricity vector and compare both turning radii with the energy equation.

Open this experiment online

Try the calculation

Initial radial velocity **0.1**

Initial tangential velocity **0.9**

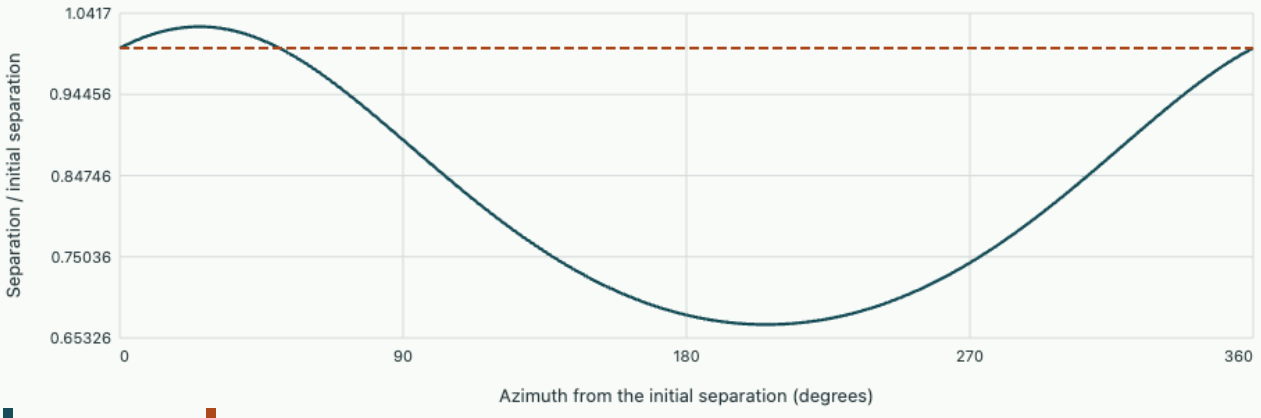

Eccentricity 0.21024. Closest approach 0.66929; largest separation 1.0256.

Use conservation of the eccentricity vector to test an orbital integrator

A code integrating $\ddot{\mathbf{r}} = -k\mathbf{r}/r^3$ can be tested on a moderate ellipse where both apses are well resolved. Choose $k = 1$, semimajor axis $a = 1$, eccentricity $e = 0.6$, and start at periapsis $\mathbf{r} = (0.4, 0)$, $\mathbf{v} = (0, 2.0)$. Then $h = 0.8$, $\epsilon = -0.5$, and the eccentricity vector is exactly $(0.6, 0)$. The apoapsis must lie at $(-1.6, 0)$ with speed 0.5, and the return time is 2π. This one initial condition tests two-dimensional direction, speed, position and clock against independent invariant predictions.

A kick–drift method for a central force can preserve angular momentum exactly at each substep. A radial kick changes velocity along position and gives zero torque; a free drift changes position along velocity and likewise preserves the cross product. Such a method can nevertheless rotate the eccentricity vector slowly or distort the time of periapsis. A symmetric velocity-Verlet step often produces bounded energy errors but still a systematic numerical periapsis shift. Record the eccentricity vector just after each

interpolated periapsis crossing over a fixed number of physical periods and compare its direction as the step is halved. Do not locate a closest approach merely by selecting the nearest stored time sample if that timing error is comparable to the shift under study.

A high-eccentricity orbit requires a smaller near-periapsis time step than its full period alone suggests. At the example periapsis, a local bend time is $r_p/v_p = 0.20$ in the scaled units, about one thirtieth of the period. For $e = 0.95$ at the same semimajor axis it becomes $0.05/\sqrt{39} \approx 0.0080$, almost eight hundred times smaller than the period. A time step that produces a smooth-looking wide ellipse at $e = 0.6$ may skip much of the rapid turning near $e = 0.95$. Refine according to the fastest relevant local dynamics as well as the final integration length.

How could a simulation distinguish a real apsidal advance from an error in fitting the coordinate origin?

▼ **Work through the solution**

Translate the calculated orbit to a candidate force centre and evaluate both the radial force law and the eccentricity vector at many positions. A constant wrong origin changes the measured radius and radial direction in a phase-correlated way even within a single orbit. A physical perturbation about the true centre can preserve zero torque and produce a gradual cycle-to-cycle change. Check angular momentum about the candidate centre, the direction of the measured acceleration, and convergence under grid or time-step refinement. Several diagnostics are needed because a short arc alone may admit many fitted centres and apsidal directions.

Determine the total mass from a visual binary

If the two bodies can both be resolved, measure their relative semimajor axis a and period T. Kepler's area relation gives $M = 4\pi^2 a^3/(GT^2)$, the sum of masses. Motion about the common centre divides the same relative semimajor axis in inverse proportion to the masses: $a_1/a_2 = m_2/m_1$. For a visual orbit with $a_1/a_2 = 0.50$ and a dynamically inferred total of three mass units, the bodies have masses two and one in those units. An orbit of only one luminous body around an unobserved centre normally supplies fewer independent constraints.

A projected semimajor axis and a measured angular period require additional geometric information before applying the mass law. The apparent ellipse on the sky can be shortened by inclination and the focus of the spatial ellipse does not in general map to a focus of the apparent ellipse. Distances converting an angular semimajor axis to metres enter cubed: an independent distance bias of two percent produces approximately a six-percent mass bias at fixed angular scale and period. This makes the gravitational invariant a sensitive quantitative measurement rather than simply a qualitative statement that the relative trajectory looks elliptical.

Tutorial on orbital inference

A body passes periapsis of an ellipse at r_p with purely transverse speed v_p. Express its eccentricity in terms of these measurements. Which ambiguity occurs if the apsis has not been identified?

▼ **Work through the solution**

At an apsis the eccentricity vector is $(rv^2/k - 1)\hat{r}$. At periapsis it points outward along $\hat{r}$, giving $e = r_p v_p^2/k - 1$. At apoapsis the coefficient is negative and its magnitude is the eccentricity. A purely transverse velocity identifies a turning point of radius but does not by itself distinguish which apsis without comparing v with the circular value $\sqrt{k/r}$ or measuring radial acceleration.

At fixed orbital radius the speed is increased tangentially from circular speed to exactly $\sqrt{2}$ times circular speed. What has changed in a, e and the apsidal interpretation?

▼ **Work through the solution**

The specific kinetic energy now equals k/r, giving total energy zero. The resulting orbit is parabolic with $e = 1$ and no finite semimajor axis or orbital period. The launch point is periapsis since radial speed is initially zero and the transverse speed exceeds the circular value. Taking the ellipse period formula with a very large fitted a near this energy boundary makes tiny measurement errors produce enormous period uncertainties.

Two solutions report nearly identical energy histories but their eccentricity vectors rotate in opposite directions as time advances. What can a controlled comparison establish?

▼ **Work through the solution**

Compute angular momentum and eccentricity vector from positions and velocities using one common force parameter and frame. Run both at decreasing time steps over a fixed physical number of orbits, with the same periapsis event interpolation. If the rotation vanishes under refinement in the inverse-square problem, the original precession was a discretisation effect. If a prescribed conservative non-Kepler term remains present, a finite shift can survive with energy conserved. Energy conservation is one scalar condition and cannot determine the apsidal direction.

Test a state vector and compare the predicted turning radii.

Torsten Fließbach's mechanics course includes dynamics in central potentials.

Analytical mechanics from constraints to invariants · 5. Scattering from a central potential and what angular data can recover

A detector records angles, whereas the force law refers to separations that were never directly observed. Derive the forward map from incoming impact parameter to angle, distinguish the several trajectories a detector may count in one angular bin, and invert sufficiently complete signed deflection data under stated hypotheses.

Build the deflection integral from a radial turning point

Use relative mass μ, asymptotic relative speed v_∞, incoming energy $E = \mu v_\infty^2/2 > 0$ and impact parameter $b \geq 0$. With a central interaction that tends to zero at infinity, angular momentum is $\ell = \mu v_\infty b$. For a single repulsive encounter let r_0 be the closest approach. Energy gives

$$\dot{r}^2 = v_\infty^2[1 - U(r)/E - b^2/r^2];$$

r_0 is the outer turning root reached from infinity. Dividing $\dot{\varphi} = \ell/(\mu r^2)$ by the radial speed and integrating over the outgoing half trajectory gives

$$\Phi(b) = \int_{r_0}^{\infty} \frac{b\,dr}{r^2\sqrt{1 - U(r)/E - b^2/r^2}},$$

$$\chi(b) = \pi - 2\Phi(b).$$

The straight, free trajectory sweeps $\Phi = \pi/2$ between closest approach and infinity and gives zero deflection. For repulsive bend away from the centre this sign convention gives positive χ. A weak attraction can give negative signed deflection even though a detector reporting the angle between incoming and outgoing velocities may supply only its magnitude. If the path winds by more than a complete turn, angular data modulo 2π also lose winding information. The square-root singularity in the integral for an ordinary turning point is integrable. A substitution $r = r_0 + s^2$ makes the near-endpoint quadrature regular. A double turning point requires separate analysis because it can make the angular advance diverge.

Incoming trajectories with parameters between b and $b + db$ represent annular area $2\pi b\,db$ for an axially symmetric beam. At a detected polar angle θ the solid angle of a ring is $2\pi \sin\theta\,d\theta$. Conservation of incoming counts gives

$$\frac{d\sigma}{d\Omega} = \sum_j \frac{b_j}{\sin\theta}\left|\frac{db_j}{d\theta}\right|.$$

The sum includes all incoming impact parameters reaching that angular bin. Correcting measured counts requires incident flux, target number, angular acceptance and efficiency. The formula is a density in solid angle. Its apparent divergence at an isolated angle need not imply an infinite number in a finite acceptance bin. Integrate the density against the actual bin solid angle or use the preimage areas of the bin directly.

Solve a hard sphere and an inverse-square repulsion

A hard sphere of effective exclusion radius a specularly reverses the incoming normal velocity at the impact surface. The angle between incoming and outgoing directions is $\theta = 2\arccos(b/a)$ for $b < a$. Therefore $b = a\cos(\theta/2)$,

$$|db/d\theta| = (a/2)\sin(\theta/2).$$

The factors cancel to give $d\sigma/d\Omega = a^2/4$, independent of polar angle, and total cross section πa^2. Equal polar angular bins do not give equal counts: their solid angles differ by $\sin\theta$. This geometric distinction often accounts for a measured histogram that does not look uniform even for a constant differential cross section.

For $U(r) = K/r$ with $K > 0$, the orbit is a repulsive hyperbola. The analytic relation is

$$\tan(\theta/2) = K/(2Eb).$$

It can be derived from the energy and the angle through the deflection integral: put $u = b/r$ so that $\Phi = \int_0^{u_0} du/\sqrt{1 - (K/Eb)u - u^2}$. Complete the square and evaluate the arcsine at the root to get

$$\Phi = \pi/2 - \arctan[K/(2Eb)].$$

Define $d = K/(2E)$; then $b = d\cot(\theta/2)$,

$$d\sigma/d\Omega = d^2/[4\sin^4(\theta/2)].$$

High precision near the forward direction is physically limited by finite beam size, detector acceptance and any screening of the long-range interaction.

For $d = 2.0\,\mathrm{mm}$ in an abstract mechanical analogue, a deflection of 60° corresponds to $b = 3.46\,\mathrm{mm}$, and the differential cross section is $16\,\mathrm{mm}^2/\mathrm{sr}$. The cross section for deflections greater than 60° is the area $\pi b^2 = 37.7\,\mathrm{mm}^2$. The differential value and integrated area answer different laboratory questions. Doubling energy at fixed interaction halves d, quarters the cross section into a fixed angular interval and reduces the deflection at a fixed incoming b. Measuring only a total count without specifying angular threshold is inadequate for a long-range interaction.

Recover impact parameter from angular counting under monotonicity

Suppose the deflection decreases continuously from π at $b = 0$ to zero at large b. Integrating counts for all angles at least θ then gives precisely the incident disk $\pi b(\theta)^2$. The recovered map satisfies

$$b(\theta)^2 = 2\int_\theta^\pi (d\sigma/d\Omega)(\theta')\sin\theta'\,d\theta'.$$

Applying this formula to constant hard-sphere intensity gives $b^2 = a^2(1+\cos\theta)/2$, the geometrical result. It also exposes the information needed from a detector: a finite upper cutoff can leave the reconstruction with an unknown disk-area offset.

Failing monotonicity, the same cumulative counts give the total area of all incoming regions producing deflections above threshold, which can be a collection of annuli. No unique $b(\theta)$ follows from that one number. Near a smooth extremum $\theta(b) = \theta_r + c(b-b_r)^2/2 + \cdots$, two branches contribute inverse square-root factors proportional to $1/\sqrt{|\theta-\theta_r|}$. A finite bin contains finite counts because integrating that singularity gives a square root. Tagging the incoming impact parameter in a controlled beam or measuring trajectory time delay can separate branches invisible in a final-angle histogram.

Invert a signed deflection function at one energy

Assume smooth $U(r)$ with $\rho(r) = r\sqrt{1-U(r)/E}$ strictly increasing on the radial interval sampled by the trajectories. The turning condition is

$$\rho(r_0) = b.$$

Write $W(\rho) = \ln[r(\rho)/\rho]$ and transform the deflection integral to $\Phi = b\int_b^\infty [d\ln r/d\rho]\, d\rho/\sqrt{\rho^2-b^2}$. The term from $d\ln\rho/d\rho$ gives the free angle $\pi/2$; the remainder has $\chi = -2b\int_b^\infty W'(\rho)\, d\rho/\sqrt{\rho^2-b^2}$. This is an Abel-type map. Multiply by $1/\sqrt{b^2-s^2}$ and integrate from $b=s$ to infinity. Interchanging the integrals produces the inner integral

$$\int_s^\rho \frac{b\,db}{\sqrt{b^2-s^2}\sqrt{\rho^2-b^2}} = \frac{\pi}{2}.$$

Substitute $b^2 = s^2 + (\rho^2-s^2)\sin^2\alpha$ to check the identity. With $W(\infty)=0$ the inversion is $W(s) = \pi^{-1}\int_s^\infty \chi(b)\, db/\sqrt{b^2-s^2}$. Recover $r = se^{W(s)}$ and finally $U(r) = E[1-(s/r)^2]$ parametrically. This derivation explains the restrictions. A trajectory only samples radii outside its turning point, the signed angle must retain branch information, and the map to ρ must be single valued. Unknown large-b tails influence the integral even when only comparatively small radii are of interest.

Derive the weak-deflection formula from a straight incoming trajectory

When the deflection is small one can calculate the transverse impulse along the undeflected line before evaluating a nonlinear radial integral. Put the incoming velocity along x and the impact point at $y = b > 0$, so the unperturbed trajectory is $x = v_\infty t$, $r = \sqrt{x^2+b^2}$. The transverse force is $-U'(r)b/r$. Dividing its time integral by the incoming momentum μv_∞ gives the signed leading deflection

$$\chi(b) \simeq -\frac{b}{E}\int_b^\infty \frac{U'(r)\, dr}{\sqrt{r^2-b^2}}.$$

The factor follows from replacing dt by dx/v_∞, using symmetry between positive and negative x, and the identity $dx = r\,dr/\sqrt{r^2 - b^2}$. A decreasing positive potential gives a positive angle, consistent with repulsive scattering in the chapter's convention. The approximation neglects longitudinal momentum change at leading order; a finite speed change far from the interaction would also be inconsistent with elastic energy conservation. Near a turning barrier or for a large angle the original deflection integral must replace this straight path.

An analytically tractable finite-range model is $U(r) = U_0 \exp[-r^2/(2a^2)]$. Along the incoming straight line the transverse force is $(U_0 b/a^2)\exp[-(x^2 + b^2)/(2a^2)]$. The Gaussian x integral gives

$$\chi(b) \simeq \sqrt{\pi/2}(U_0/E)(b/a)\exp[-b^2/(2a^2)].$$

A central hit has zero transverse force by symmetry if the particle crosses through the weak smooth potential rather than being reflected. Distant particles see little interaction, so the deflection must peak at an intermediate impact parameter. Differentiation places the maximum at $b = a$, with height $\sqrt{\pi/(2e)}U_0/E$.

For $U_0/E = 0.10$ the peak is about $0.0760\,\mathrm{rad} = 4.36^\circ$, comfortably small for this leading calculation. Two impact-parameter families can contribute to one smaller nonzero angle. For example $b = 0.50a$ gives $0.0553\,\mathrm{rad}$; a trajectory with b between $1.5a$ and $1.7a$ produces a similar deflection on the declining branch. A detector counting more events near four degrees may be recording the merging of these branches, rather than a particularly large local force at the turning separation. Reconstructing $b(\theta)$ from monotonically accumulated disk areas would be invalid for this smooth repulsive bump even though every encounter is elastic.

Measure the energy dependence to distinguish the weak limit. For fixed b/a the leading angle scales as $1/E$. Doubling energy halves the predicted peak angle. A finite spread of incident energies therefore broadens the observed rainbow before detector angular resolution is considered. A position-tagged incident beam can furnish $\chi(b)$ point by point; a detector measuring final angles alone mixes weakly and more strongly penetrating paths. Adding incoming-position information changes what inverse problem is identifiable, without improving the detector's angular precision.

Limit a scattering inference using finite range and measurement bandwidth

The Abel reconstruction requires data to arbitrarily large b. A finite experiment measures up to $b_{\max}$, and the unmeasured tail contributes an integral to $W(s)$. For the example of a known asymptotic $\chi = C/b$, the tail from $b_{\max}$ to infinity evaluates to $C\,\arcsin(s/b_{\max})/(\pi s)$ for $s < b_{\max}$. Substitute $b = s/\cos\alpha$ to obtain this result. For $s \ll b_{\max}$, it approaches $C/(\pi b_{\max})$. Setting the tail to zero therefore introduces an offset across the reconstructed log-radius even at small s. Bounded angular noise and uncertainty in the tail model should be propagated separately.

As a numerical illustration take $C = 5.0\,\mathrm{mm}$,

$$b_{\max} = 100\,\mathrm{mm},$$
$$s = 20\,\mathrm{mm}.$$

The missing contribution is about 0.0160, corresponding to roughly a 1.6% multiplicative error in reconstructed radius if other terms were exact. At that same s, the leading whole weak-tail value $C/(2s) = 0.125$ would be biased appreciably by this omission. A model with a short exponential tail would give a quite different correction. Adding a physically motivated tail with an uncertainty range is more informative than extending a noisy measured curve by an unrestricted polynomial.

The lower integration endpoint has a square-root weight. Uniform samples in b can be wasteful near a selected reconstruction radius and coarse interpolation there can dominate the result. Substitute $b = s\cosh u$ to obtain

$$db/\sqrt{b^2 - s^2} = du.$$

The Abel integral becomes a straightforward integral of $\chi(s\cosh u)$ over u, with a finite upper limit if the data stop at $b_{\max}$. This substitution removes a numerical singularity but adds no information about missing impact parameters. Validate a reconstruction by inserting its inferred potential back into the original forward integral and predicting angular measurements withheld from the fit. Agreement with the very data used in the inversion alone can conceal an incorrect tail or a misassigned branch.

Convert centre-of-momentum angles into laboratory angles

An ordinary collision experiment often launches a particle of mass m_1 into a stationary particle of mass m_2. In Newtonian elastic scattering the centre-of-mass speed is $V = m_1 v_{\mathrm{in}}/(m_1 + m_2)$, while the projectile's speed in that frame is $u_1 = m_2 v_{\mathrm{in}}/(m_1 + m_2)$. Rotate that velocity by the centre-of-mass angle χ in the scattering plane, then add the centre velocity back. The outgoing laboratory velocity components are $V + u_1\cos\chi$ longitudinally and $u_1\sin\chi$ transversely. Consequently $\theta_{\mathrm{lab}} = \operatorname{atan2}(\sin\chi, m_1/m_2 + \cos\chi)$. The centre-of-mass solid-angle density derived from the impact parameter does not transfer unchanged to a lab angular histogram.

If $m_1 = m_2$, the identity $1 + \cos\chi = 2\cos^2(\chi/2)$ gives $\theta_{\mathrm{lab}} = \chi/2$ except when the projectile stops and loses a well-defined direction. A heavy projectile can be restricted to a narrow forward cone. Let $r = m_1/m_2 > 1$. Differentiating the laboratory angle gives

$$d\theta_{\mathrm{lab}}/d\chi = (1 + r\cos\chi)/(1 + 2r\cos\chi + r^2).$$

It vanishes at $\cos\chi = -1/r$. At that angle $\sin\theta_{\max} = 1/r$; hence $r = 2$ limits the projectile to $\theta_{\max} = 30^\circ$. Two centre-of-mass angles can generate the same nonzero laboratory angle below this maximum. This laboratory-frame fold may appear even for a monotone centre-of-mass repulsive potential.

Energy helps separate the branches. The outgoing laboratory projectile energy divided by its incident energy is $[m_1^2 + m_2^2 + 2m_1m_2\cos\chi]/(m_1 + m_2)^2$. For $m_1 = 2m_2$, head-on reversal in the momentum frame gives energy fraction $1/9$, while forward scattering gives one. Both can land near the laboratory

beam direction. A detector reporting angle only cannot distinguish a barely deflected fast projectile from a strongly deflected slow one emerging along almost the same line. Recording time of flight to a downstream detector or measuring the recoil supplies the missing information. Instrumental and kinematic multiplicity should therefore be addressed before attributing a two-branch angular signal to an exotic force law.

Ask what a flight-time measurement adds to angle data

At a given impact parameter choose a large comparison sphere of radius R enclosing a short-range potential. The transit time from its incoming boundary to the outgoing boundary is $t_U(R,b) = 2v_\infty^{-1}\int_{r_0}^{R} dr/\sqrt{1-U/E-b^2/r^2}$. The free reference at the same b is $t_0 = 2\sqrt{R^2-b^2}/v_\infty$. Their difference is a classical time delay under a precisely specified pair of surfaces. It combines a different path length with the altered speed along the path. A repulsive barrier can cause either a shorter geometrical penetration or longer dwell near a turning point, so the sign cannot be inferred merely from the word repulsive.

For an impenetrable sphere of radius $a > b$, the particle moves at free speed on each straight segment. The radial turning point is replaced by specular contact at a, so $t_{\mathrm{hard}} = 2[\sqrt{R^2-b^2} - \sqrt{a^2-b^2}]/v_\infty$. The delay is $-2\sqrt{a^2-b^2}/v_\infty$. Using $a = 3.0\,\mathrm{mm}$, $b = 1.8\,\mathrm{mm}$, and $v_\infty = 2.0\,\mathrm{m/s}$, one finds $-2.4\,\mathrm{ms}$. The hard sphere takes less transit time between the two points where the respective trajectories cross the large sphere. Those points differ from the endpoints of the free line, so this negative delay implies no acceleration above the fixed free speed.

For a potential with a true long-range $1/r$ tail the simple free-reference difference can acquire a logarithmic dependence on the comparison radius. A reported time delay then needs its reference geometry and tail model, just as a measured forward angle needs its angular acceptance. In the inverse problem, combining deflection and delay can help separate long dwell near a nearly unstable circular orbit from a large geometrical bend at an ordinary turning point. A large angle alone contains insufficient information to assign the time spent close to the scattering centre.

Reconstruct a finite-depth potential well from two deflections

A circularly symmetric square well provides a forward problem in which the trajectory is straight in each region and changes direction at the potential boundary. Let $U(r) = -U_0 < 0$ for $r < a$ and zero outside. A particle with $b < a$ enters with speed v_∞ and travels inside at $v_{\mathrm{in}} = v_\infty\sqrt{1+U_0/E} \equiv n v_\infty$. Angular momentum conservation across the radial impulse gives

$$v_\infty \sin i = v_{\mathrm{in}} \sin r_i,$$

where i and r_i are angles of the velocity to the normal outside and inside. Thus $\sin i = b/a,\ \sin r_i = b/(na)$. At each crossing the direction bends toward the centre. The magnitude of net deflection is $2(i - r_i)$, with negative signed deflection in the convention used for attraction here.

Take $n = 1.25,\ b = 0.60a$. Then $i = 36.87^\circ$, $r_i = 28.69^\circ$, and the total deflection has magnitude 16.35°. As b approaches a from below, the magnitude approaches $2[\pi/2 - \arcsin(1/n)]$, about 73.7°.

For $b > a$ the trajectory does not touch the ideal sharp boundary and is undeflected. A smooth finite-width transition removes the ideal discontinuity at grazing incidence and can generate trajectories that linger near the outer part of the well. Examining a well with measured edge width is therefore different from trying to fit all grazing events with a perfectly sharp step.

If a is known, an incoming position tag and a measured deflection at one b determine $n = \sin i / \sin(i - |\chi|/2)$, hence $U_0/E = n^2 - 1$. The preceding numbers give

$$U_0/E = 0.5625.$$

For an independently known E this determines the well depth. If a is unknown too, one angle supplies only one equation for two parameters. Multiple impact parameters, an independent threshold for entering the well, or a measured time of flight can supply the additional scale. Near $b = 0$ the deflection is approximately $2(b/a)(1 - 1/n)$, so a series of very small impact parameters measures mainly that one combination; broad coverage is needed to resolve a and n individually.

The time inside the well is $2a \cos r_i/(nv_\infty)$, because the interior chord has offset b/n and speed nv_∞. At the same b, the time between intersections of the free path with the circle is $2a \cos i/v_\infty$. For $n = 1.25, b = 0.6a$, their ratio is $\cos 28.69^\circ/[1.25 \cos 36.87^\circ] \approx 0.877$. The faster interior motion crosses a longer chord in less time. For grazing free paths the reference chord becomes very short and the comparison can reverse. Reporting which part of the trajectory the timing equipment resolves is therefore as important as measuring the dwell accurately.

Recover incoming annuli from scattering angles

Bin the exactly solvable hard-sphere reflection in polar angle and compare the integrated cross-section with the incoming geometric area.

Open this experiment online

Try the calculation

Polar detector bins 8

Effective radius (cm) 1

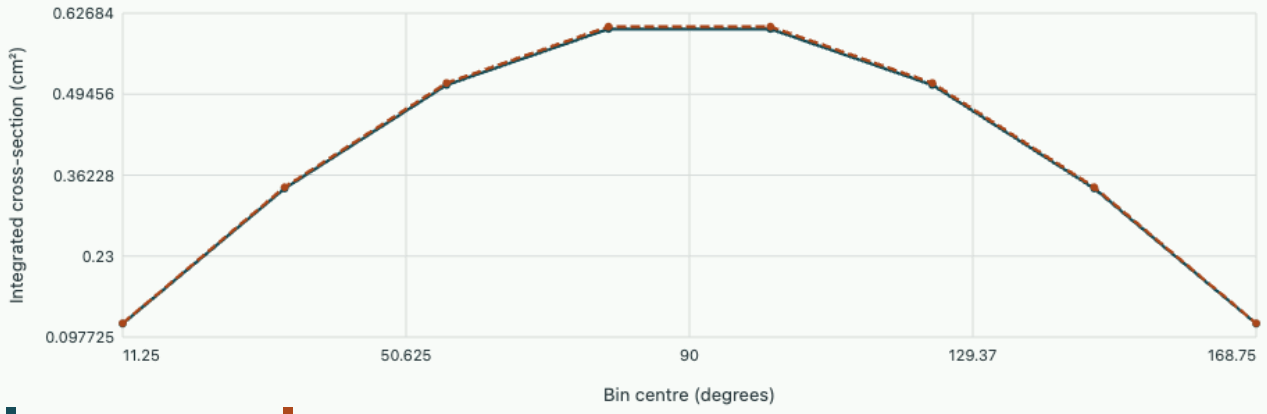

Incoming annulus Midpoint solid angle

Exact sum 3.1416 cm². Midpoint sum 3.1619 cm². Differential cross-section 0.25 cm²/sr.

Propagate uncertainties from a detector ring to an inferred force

Suppose N counts are recorded in an angular ring and the product of incident fluence, target count and calibrated efficiency is C. The estimate of bin-averaged cross section is $N/(C\Delta\Omega)$, with $\Delta\Omega = 2\pi[\cos\theta_{\mathrm{low}} - \cos\theta_{\mathrm{high}}]$ for full azimuth. Approximately independent counting events have fractional standard error $1/\sqrt{N}$, but the fluence and efficiency create correlated scale errors across angular bins. When integrating bins to reconstruct $b^2(\theta)$, a shared five-percent normalisation uncertainty does not shrink just because the number of angular bins grows. It propagates into an approximately 2.5% scale uncertainty in the recovered impact parameter.

For an ideal hard sphere, let an experiment integrate the area feeding angles greater than 90° and find $14.1 \pm 0.7\,\mathrm{mm}^2$. Since this is $\pi b(90^\circ)^2 = \pi a^2/2$, the inferred radius is $\sqrt{2(14.1)/\pi} = 3.00\,\mathrm{mm}$ with uncertainty approximately $0.075\,\mathrm{mm}$ for small errors. If the unobserved backward final ten degrees are simply omitted, an extra solid angle $\Delta\Omega = 2\pi[1 - \cos 10^\circ]$ is missed. Its small size for a smooth hard-sphere law can be estimated, but a general inverse analysis cannot assume that backward intensity is smooth without testing it.

Is multiplying each measured bin centre by the angular density there sufficient for a steep forward-scattering law?

▼ **Work through the solution**

A finite bin measures an integral against solid angle, not the value at its centre. For a rapidly varying $\sin^{-4}(\theta/2)$ density near zero, the lower-angle part of the bin can dominate its count. Use the exact preimage annulus $\pi[b(\theta_{\mathrm{low}})^2 - b(\theta_{\mathrm{high}})^2]$ or integrate the model numerically over the detector's angle-dependent efficiency. Repeat with narrower bins as a check. If the lower acceptance overlaps the direct

beam, separate the unscattered population and account for its instrumental angular spread before assigning a cross section to small deflections.

Work directly in counts for a finite annular detector

For the repulsive inverse-square example take $d = 2.0\,\mathrm{mm}$ and a full-azimuth ring that accepts polar angles from 55° to 65°. The expected incident area is $\pi d^2[\cot^2(27.5^\circ) - \cot^2(32.5^\circ)]$, about $15.4\,\mathrm{mm}^2$. Multiplying by an incident fluence of 100 particles per square millimetre and efficiency 0.80 predicts about 1230 counts. A Poisson fluctuation scale is then roughly 35 counts. The exact integral supplies a meaningful reference even when the plotting software reports a differential value at the centre of the bin.

Moving both angular boundaries one degree outward decreases the count because the repulsion sends fewer particles through larger angles. The change can be calculated by reevaluating the two cotangents, keeping the fluence and efficiency fixed. This sensitivity allows a calibration uncertainty in the angular zero to be propagated into a count prediction without treating it as a force uncertainty. If fluence is independently measured the dependence on d^2 can then estimate the interaction scale. If fluence is itself unknown, a single count measures only their product; independent calibration or measurements across energies are needed to separate them.

Tutorial on inverse scattering

An incoming uniform beam scatters from a hard disk in three-dimensional impact geometry with effective radius $3.0\,\mathrm{mm}$. What area feeds the polar bin from 60° to 90°?

▼ **Work through the solution**

The accepted impact parameters run from $a\cos 45^\circ$ to $a\cos 30^\circ$. The difference of their squared radii is $9(0.75 - 0.50) = 2.25\,\mathrm{mm}^2$, giving area $2.25\pi = 7.07\,\mathrm{mm}^2$. Alternatively the bin has solid angle $2\pi(\cos 60^\circ - \cos 90^\circ) = \pi$ steradians and differential cross section $a^2/4 = 2.25\,\mathrm{mm}^2/\mathrm{sr}$. The agreement checks both the Jacobian and the angular convention.

At large impact parameter a weak repulsion gives $\chi(b) \simeq C/b$ with C a length. Use the inversion to identify the leading tail of the potential.

▼ **Work through the solution**

Substitute $b = s/\cos\alpha$ into the Abel integral. One obtains

$$W(s) \simeq C/(2s).$$

Thus $r \simeq s + C/2$ and $U/E = 1 - e^{-2W} \simeq C/s \simeq C/r$. The potential tail is EC/r. For the exact repulsive Coulomb result $C = K/E$, matching the original K/r. This check uses the weak-tail expansion at large radii only; continuing it to small radii would discard higher deflection terms.

A measured angular bin near a rainbow doubles in width towards its allowed side. By what approximate factor do its counts change if background is negligible?

▼ **Work through the solution**

At a simple fold the angular density grows as the inverse square root of distance from the extremal angle. For a bin of width $\Delta\theta$ starting at the fold, the integral scales as $\sqrt{\Delta\theta}$ provided $\sin\theta_r$ is nonzero and other weights are locally smooth. Doubling the width gives a factor $\sqrt{2}$, unlike the factor two from a smooth background. Finite angular resolution rounds off the divergence and can obscure this scaling in very narrow bins.

Compare angular bins and conserved incoming area.

Fließbach's mechanics text treats trajectories in central fields.

Analytical mechanics from constraints to invariants · 6. Euler–Poinsot motion, torque-free nutation and the intermediate axis

A freely rotating body has fixed angular momentum in space, yet the components recorded by three body-mounted gyroscopes can vary periodically or linger near an unstable rotation. Solve the nonsymmetric top from its invariants, distinguish its body-component period from its spatial orientation, and extract a stability time scale from a measured inertia tensor.

Derive the body equations from a spatial conservation law

Choose principal axes fixed in a rigid body and label its moments $I_1 < I_2 < I_3$. In the co-rotating basis the angular-momentum components are

$$L_i = I_i \omega_i.$$

For any vector expressed in that basis, its inertial derivative is its component derivative plus $\boldsymbol{\omega} \times \mathbf{L}$. With no external torque the inertial derivative is zero. Taking components gives

$$I_1 \dot{\omega}_1 = (I_2 - I_3)\omega_2 \omega_3,$$
$$I_2 \dot{\omega}_2 = (I_3 - I_1)\omega_3 \omega_1,$$
$$I_3 \dot{\omega}_3 = (I_1 - I_2)\omega_1 \omega_2.$$

Multiply these equations by the corresponding ω_i and sum: the coefficients of $\omega_1\omega_2\omega_3$ cancel, giving constant $E = \sum I_i \omega_i^2/2$. Multiplying instead by $I_i\omega_i$ gives constant $L^2 = \sum I_i^2 \omega_i^2$. In body angular-momentum space the motion lies on the intersection of a sphere and an energy ellipsoid. At fixed L, the possible energies range from $L^2/(2I_3)$ to $L^2/(2I_1)$. The intermediate value $L^2/(2I_2)$ divides two families of closed curves and contains the unstable principal-axis orientations.

In Poinsot's construction the inertia ellipsoid in angular-velocity space rolls on an invariable plane normal to the fixed spatial angular momentum. The ellipsoid corresponding to a given energy is

$$\sum I_i \omega_i^2 = 2E.$$

Its normal at the instantaneous angular velocity is proportional to $\mathbf{L}$; the tangent plane obeys $\mathbf{L} \cdot \mathbf{x} = 2E$. In space that plane therefore has fixed distance $2E/L$ from the origin. Its instantaneous point in the body along $\boldsymbol{\omega}$ has zero instantaneous rotational velocity because the vector cross product of angular velocity with itself is zero. These facts underlie the rolling construction. A photographed body axis traces a different curve from the moving contact point or from a body-frame gyro trace.

Test all three principal rotations locally

For rotation $(0, 0, \Omega)$, linearise the first two Euler equations in transverse perturbations. Eliminating one component gives

$$\ddot{\omega}_1 = -\Omega^2[(I_3 - I_2)(I_3 - I_1)/(I_1 I_2)]\omega_1.$$

Small transverse deviations oscillate. Performing the analogous process about I_1 also gives a restoring sign. About $(0, \Omega, 0)$ the sign reverses and the growing exponent is $\lambda = |\Omega|\sqrt{(I_2 - I_1)(I_3 - I_2)/(I_1 I_3)}$. The unstable rotation is still an exact solution when both perturbations vanish identically. Instability describes the evolution of arbitrarily small disturbances, not a spontaneous violation of the torque-free equations.

For moments proportional to $1, 2, 3$ and intermediate-axis rotation $\Omega = 6.0\,\mathrm{rad/s}$, $\lambda = 3.46\,\mathrm{s}^{-1}$ and the linear e-folding time is $0.289\,\mathrm{s}$. A perturbation with a growing-mode component 10^{-3} of the spin reaches roughly 10^{-1} in $\ln(100)/\lambda = 1.33\,\mathrm{s}$. Its nonlinear fate remains bounded by the momentum sphere and energy ellipsoid. An exponential growth fit carried past the first large reorientation would therefore misrepresent the global motion. Initial perturbations projected entirely on the decaying linear eigenvector can delay the first visible flip.

Solve the low-energy family with elliptic functions

For $L^2/(2I_3) < E < L^2/(2I_2)$ the trajectory surrounds the largest-inertia axis. Start at a crossing with $\omega_2 = 0, \omega_1 = A > 0, \omega_3 = C > 0$. Solving the two invariants gives

$$A^2 = (2EI_3 - L^2)/[I_1(I_3 - I_1)],$$
$$C^2 = (L^2 - 2EI_1)/[I_3(I_3 - I_1)].$$

When ω_1 reaches zero the other transverse component has maximum $B^2 = (2EI_3 - L^2)/[I_2(I_3 - I_2)]$. Use $s = \omega_2/B$. Eliminating the other squares with the invariants gives

$$\omega_1^2 = A^2(1 - s^2),$$
$$\omega_3^2 = C^2(1 - k_e^2 s^2).$$

Euler's second equation now reduces to

$$\dot{s}^2 = \nu^2(1 - s^2)(1 - k_e^2 s^2),$$
$$\nu^2 = \frac{(I_3 - I_2)(L^2 - 2EI_1)}{I_1 I_2 I_3},$$
$$k_e^2 = \frac{(I_2 - I_1)(2EI_3 - L^2)}{(I_3 - I_2)(L^2 - 2EI_1)}.$$

Separating variables defines $u = \nu t = \int_0^s dw/\sqrt{(1 - w^2)(1 - k_e^2 w^2)}$. Its inverse is Jacobi's $\mathrm{sn}(u, k_e)$. The continuously signed square roots are cn and dn, giving $(\omega_1, \omega_2, \omega_3) = (A\,\mathrm{cn}, B\,\mathrm{sn}, C\,\mathrm{dn})$. This construction defines the special functions from the mechanical quadrature instead of assuming them as a table of answers. At $k_e = 0$ the inverse is a sine and the stabilising motion is harmonic. As $k_e \to 1$, the integral to $s = 1$ diverges logarithmically and the period grows without bound.

The body-frame period is

$$T_b = 4K(k_e)/\nu,$$

with K the same integral evaluated at one. Some software defines elliptic functions in terms of parameter $m = k_e^2$ rather than modulus k_e. Supplying one to an implementation expecting the other produces a plausible curve with the wrong period. Check the derivative at the zero crossing $\dot{\omega}_2(0) = B\nu$ and the time of its first maximum K/ν before fitting a long trace. The third component dn repeats after half the full period, so a single principal-axis gyro can report a dominant frequency twice that of the full body vector.

Reconstruct the observed nutation angle

Orient the inertial vertical along $\mathbf{L}$. The angle between body axis three and this fixed direction obeys $\cos\theta = L_3/L = I_3\omega_3/L$. For $I_1, I_2, I_3 = (1, 2, 3)\,\mathrm{kg\,m^2}$ and initial $\boldsymbol{\omega} = (0.50, 0, 1.00)\,\mathrm{rad/s}$, the invariants give $L^2 = 9.25$, $2E = 3.25$ in SI, $A = B = 0.50\,\mathrm{rad/s}$, $C = 1.00\,\mathrm{rad/s}$, $\nu = 1.00\,\mathrm{s^{-1}}$, and $k_e^2 = 1/12$. Thus the nutation angle changes from $\arccos(3/\sqrt{9.25}) \approx 9.46^\circ$ to $\arccos[3\sqrt{11/12}/\sqrt{9.25}] \approx 19.2^\circ$. A torque is unnecessary for this change in the angle of a body axis relative to fixed $\mathbf{L}$.

The principal-axis components alone determine body orientation only when supplemented with an initial attitude and the kinematic equation. For the Euler-angle convention with polar axis $\mathbf{L}$, the azimuthal rate of body axis three is $\dot{\phi} = L(L_1^2/I_1 + L_2^2/I_2)/(L_1^2 + L_2^2)$ away from the polar singularity. It follows by differentiating the body-axis unit vector in space and projecting onto its azimuthal direction. A complete period of the body components therefore leaves a finite spatial rotation about fixed $\mathbf{L}$. Return of the three gyro readings does not imply that a painted mark has returned to its starting position in the laboratory.

Solve the high-energy family and join both sides at the separatrix

For $L^2/(2I_2) < E < L^2/(2I_1)$ the closed curves on the angular-momentum sphere surround axis one. The component ω_1 now keeps its sign while ω_3 changes sign through a cycle. As in the first family, choose a phase with $\omega_2 = 0$ and both other components positive. The two invariants give the same initial $A^2 = (2EI_3 - L^2)/[I_1(I_3 - I_1)]$ and $C^2 = (L^2 - 2EI_1)/[I_3(I_3 - I_1)]$. Now the maximum of ω_2 occurs when $\omega_3 = 0$, so

$$B^2 = (L^2 - 2EI_1)/[I_2(I_2 - I_1)].$$

Which component reaches zero is the physical branch choice that determines the arrangement of elliptic functions.

Let $s = \omega_2/B$. The invariant equations give

$$\omega_3^2 = C^2(1 - s^2),$$

$$\omega_1^2 = A^2(1 - k_h^2 s^2).$$

Substitution in the second Euler equation yields the same elliptic quadrature but with $\nu_h^2 = (I_2 - I_1)(2EI_3 - L^2)/(I_1 I_2 I_3)$ and $k_h^2 = (I_3 - I_2)(L^2 - 2EI_1)/[(I_2 - I_1)(2EI_3 - L^2)]$. All components are given by $(A\,\mathrm{dn}, B\,\mathrm{sn}, C\,\mathrm{cn})(\nu_h t, k_h)$, where the notation means each function is

evaluated at the same time and modulus. On this energy side $0 < k_h < 1$. The low-energy modulus formula evaluated here would exceed one, signalling that the original choice of component scaling and physical extrema must be changed.

For the same inertias $1, 2, 3$, choose initial $(1, 0, 0.20)\,\mathrm{rad/s}$. Then $L^2 = 1.36,\ 2E = 1.12$, and the high-energy inequality holds since $2E > L^2/I_2 = 0.68$. The formulas give

$$A = 1,\ B = \sqrt{0.12} = 0.3464,\ C = 0.20,\ \nu_h = \sqrt{1/3} = 0.5774\,\mathrm{s^{-1}},\ k_h^2 = 0.12.$$

The minimum ω_1 is $A\sqrt{1 - k_h^2} = 0.9381\,\mathrm{rad/s}$, so that principal gyro never reverses even though the third one does. A body-marking aligned with axis three can undergo a conspicuous reversal while the dominant axis-one spin changes only modestly. These component predictions are more specific than an energy or angular-speed trace.

At $2E = L^2/I_2$, both moduli approach one. The definitions give

$$\mathrm{sn}(u, 1) = \tanh u,$$
$$\mathrm{cn}(u, 1) = \mathrm{dn}(u, 1) = \mathrm{sech}\, u.$$

One separatrix solution therefore has $\omega_2 = B\tanh(\nu t)$ with $\omega_1 = A\,\mathrm{sech}(\nu t)$ and $\omega_3 = C\,\mathrm{sech}(\nu t)$, up to signs and time shifts consistent with Euler's equations. It connects opposite steady orientations along axis two as t goes from negative to positive infinity. Its asymptotic approach is exponential, with ν equal to the small-disturbance growth exponent at the intermediate-axis equilibrium after inserting $B = L/I_2$. A nearby periodic orbit spends much of its time near the unstable spin and flips more rapidly between those intervals.

Reconstruct spatial attitude without a singular azimuth

Let $R(t)$ map body components into a laboratory basis. For body angular velocity $\boldsymbol{\omega}_b$, its kinematic equation is

$$\dot{R} = R[\boldsymbol{\omega}_b]_\times,$$

where the skew matrix acts by a cross product. Starting from measured $R(0)$, propagate by multiplying by the rotation appropriate to each short time interval. Exponentiating the skew matrix for an interval with constant estimated body angular velocity preserves orthogonality and determinant exactly. Applying a naive forward-Euler matrix addition $R + hR[\omega]_\times$ generally stretches the basis, even if the angular velocity components came from an exact elliptic solution.

For a constant rotation about axis three at one radian per second, a single Euler step of duration $0.10\,\mathrm{s}$ takes a transverse unit vector to one of length $\sqrt{1 + 0.10^2} = 1.00499$. After one hundred such steps the transverse length would grow by $(1.01)^{50} \approx 1.64$. A quaternion or matrix exponential avoids that artificial stretch. Normalising each axis separately is insufficient if the axes lose orthogonality; check $R^T R$ against identity and $\det R$ against one. Also compute $R(I_1\omega_1, I_2\omega_2, I_3\omega_3)^T$ at every time. It should give the same spatial vector in a torque-free run.

A measured attitude time series allows a different inference from fitting Euler angles separately. Use relative rotations between successive images to estimate angular velocity in the correct body or spatial frame. A camera can momentarily lose sensitivity to yaw when a marked axis points towards it; simultaneous orthogonal views or multiple non-collinear marks avoid that degeneracy. The gyro and attitude measurements together distinguish a true physical precession from an Euler-angle wrap by 2π. Synchronise their clocks before comparing the phase of a nutation extremum, since even a small time delay produces a plausible-looking mismatch near a fast flip.

Infer inertia ratios from a free-rotation record

A calibrated triad records $\omega_i(t)$ in axes thought to be principal. Euler's equations predict that $\dot{\omega}_1/(\omega_2\omega_3)$ is the constant $(I_2 - I_3)/I_1$ wherever the denominator is appreciable, and similarly for cyclic indices. Instead of dividing noisy derivatives near zeros, integrate each component over a time interval. For example $\omega_1(t_2) - \omega_1(t_1) = a_1 \int_{t_1}^{t_2} \omega_2\omega_3 \, dt$. Fit a_1 over several intervals and repeat for a_2, a_3. Select intervals with different angular configurations so that products do not all average nearly to zero. The ratios depend on inertia shape; multiplying every moment by a common constant leaves a torque-free angular-velocity record unchanged.

For a record giving $a_1 = -1.0$, $a_2 = 1.0$ and $a_3 = -1/3$, solve the homogeneous equations $I_2 - I_3 = -I_1$, $I_3 - I_1 = I_2$, $I_1 - I_2 = -I_3/3$. They give $I_1 : I_2 : I_3 = 1 : 2 : 3$. An independent angular-momentum or torque calibration is needed to set the absolute scale. A known short applied torque impulse that changes one principal angular velocity by a measured amount can do this, provided the other gyroscopic contributions over that impulse are small or accounted for. A fit that estimates all absolute inertias from angular velocity alone can have an apparently excellent residual and still be structurally underdetermined.

If the sensors are not along principal axes the inertia matrix contains off-diagonal entries. The coordinate-free body equation is

$$I\dot{\boldsymbol{\omega}} + \boldsymbol{\omega} \times (I\boldsymbol{\omega}) = 0.$$

Each measured time sample gives equations linear in the constant entries of the symmetric inertia tensor. With sufficiently rich motion one may estimate these entries up to scale, then diagonalise the fitted tensor to recover principal directions. Pure rotation along one axis gives insufficient excitation to reveal three distinct directions. Comparing a family of initial spins with a single tensor provides a stronger validity test than fitting a different set of effective principal inertias to each record.

Relate a body-frame period to a measured geometric phase

After a closed polhode in body angular-momentum space the laboratory orientation differs by a rotation about the fixed spatial momentum. That phase can be separated into a term accumulated at a dynamical rate and a term depending on the oriented solid angle of the body momentum path. For a fixed L, the angular-velocity component along the momentum is $\boldsymbol{\omega} \cdot \hat{L} = 2E/L$, since $\mathbf{L} \cdot \boldsymbol{\omega} = 2E$. Over one body period it contributes $2ET_b/L$. Parallel transport of a transverse reference direction along the unit

momentum curve contributes minus the oriented solid angle enclosed, up to whole turns and the chosen orientation of the sphere. The resulting net attitude phase is $2ET_b/L - \Omega_{\text{solid}} \pmod{2\pi}$.

The geometric part can be visualised by carrying a local tangent basis along the closed curve. Its two basis vectors are constrained to stay perpendicular to the moving unit momentum and are transported with no imposed twist around that direction. A return to the initial unit momentum need not return that basis to its starting orientation. For a latitude circle on the unit sphere the enclosed cap area is $2\pi(1-\cos\theta)$; shrinking the path to a point makes the geometric phase vanish modulo 2π. This is why comparing a painted mark after a nutation only to an integrated scalar spin speed can give a discrepancy even with exact torque-free motion.

In practice the total phase can be measured without choosing a cap convention. Fit the attitude at two times separated by the full gyro period, form $R(t+T_b)R(t)^T$, and extract the relative rotation around the known fixed spatial momentum. Independently integrate $2E/L$ over that interval and compare the difference modulo 2π with the signed spherical area traced by normalised body momentum. A factor-of-two error in the identified period, common if only ω_3 is recorded in the low-energy family, generally leaves the relative attitude rotation axis different from $\mathbf{L}$. The axis check can reveal the error before assigning a numerical geometric phase.

Identify which inertias can exist in an actual rigid body

Three positive principal moments inserted into Euler's equations define a mathematical top, but the moments of a physical nonnegative mass distribution also satisfy triangle inequalities. In principal coordinates $I_1 = \int (y^2 + z^2)\, dm$,

$$I_2 = \int (z^2 + x^2)\, dm,$$

$$I_3 = \int (x^2 + y^2)\, dm.$$

Therefore $I_1 + I_2 - I_3 = 2\int z^2\, dm \geq 0$, and likewise by cyclic permutation. Equality means all mass is confined to the corresponding coordinate plane. The convenient example $1, 2, 3$ lies on that boundary and can be realised by an ideal planar lamina. A fitted ratio $1, 2, 3.5$ would imply negative mean squared distance along one direction and should prompt a calibration or modelling check.

A uniform thin rectangular plate of mass M and side lengths b along body axis one and a along body axis two has $I_1 = Ma^2/12,\ I_2 = Mb^2/12,\ I_3 = M(a^2+b^2)/12$. Choosing $b = \sqrt{2}\,a$ gives exactly $1:2:3$. For $M = 0.60\,\mathrm{kg}$, $a = 0.20\,\mathrm{m}$, $b = 0.283\,\mathrm{m}$, the moments are approximately $0.0020, 0.0040, 0.0060\,\mathrm{kg\,m^2}$. The component equations for these moments give the same time histories as the scaled numerical example for identical initial angular velocities, while the actual angular momentum and energy are smaller by a factor 500. This gives a physical specimen for checking principal-axis stability without requiring a massive rotor.

Adding a small mass at a known location changes both inertia and possibly the centre of mass. If a symmetric pair of equal small masses is attached at $\pm d\hat{e}_3$, their combined mass m_a adds $m_a d^2$ to I_1 and I_2, nothing to I_3, and leaves the centre fixed. For the plate above and $m_a = 0.10\,\mathrm{kg}, d = 0.10\,\mathrm{m}$,

the new moments are $0.0030, 0.0050, 0.0060\,\mathrm{kg\,m^2}$. The intermediate-axis growth exponent at fixed Ω changes from $|\Omega|/\sqrt{3}$ to $|\Omega|\sqrt{(0.005-0.003)(0.006-0.005)/(0.003\cdot 0.006)} = |\Omega|/3$. A reversible mass-placement experiment tests the inertia dependence of instability, not merely the existence of a visually dramatic flip.

Test intermediate-axis stability with the full body equations

Change the initial tilt and spin. Compare the linear perturbation and the complete torque-free motion while monitoring energy and angular momentum in the OneSimulation output.

Open this experiment online

Try the calculation

Nominal middle-axis speed (rad/s) **12**

Initial transverse speed (rad/s) **0.1**

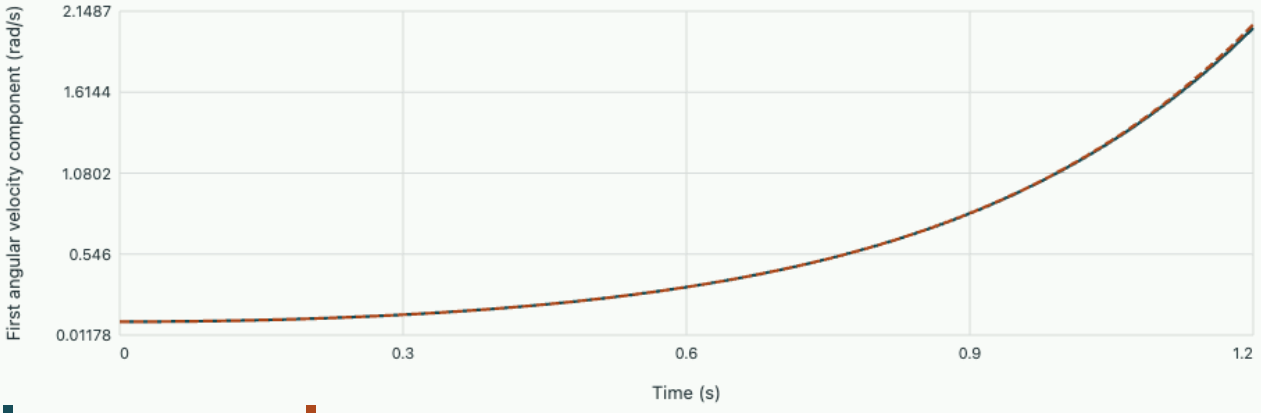

Initial linear growth rate 3.0984 s⁻¹. With zero initial transverse slope the predicted first doubling time is 0.42505 s.

Download the OneSimulation model

In your OneSimulation environment, run the model with these inputs.

```
python spectra-and-orbits.py rotor --spin 12 --seed 0.1
```

Estimate distance from a separatrix using dwell time

Near the intermediate-axis energy, elliptic modulus approaches one on either side. Writing $d = 1 - k_e^2$ on the low-energy family gives $K \sim \ln(4/\sqrt{d})$. Thus $T_b \sim 4\ln(4/\sqrt{d})/\nu$ for a slowly varying scale ν. Changing d by a factor of one hundred increases the expected body period by approximately $4\ln 10/\nu$. A tiny difference in the initial inertia-weighted energy can produce a readily observed increase in the time

between reorientation events while the maximum angular speed scarcely changes. The logarithm follows from passages near a hyperbolic equilibrium, where the signed unstable perturbation grows exponentially.

If $\nu = 3.0\,\mathrm{s}^{-1}$ and $d = 10^{-4}$, the leading estimate is

$$T_b = (4/3)\ln 400 \approx 7.99\,\mathrm{s}.$$

Reducing d to 10^{-6} gives $T_b \approx 11.06\,\mathrm{s}$. Inverting this relation makes estimates of d exponentially sensitive to a period offset. An uncertain start or stop event of a few tenths of a second, or a weak external torque during a long dwell, can affect an inferred separatrix energy considerably. Report the uncertainty of $E - L^2/(2I_2)$ as well as the fitted period when claiming close approach to the unstable family.

One experimental check is to use both the crossing speed of $\omega_2 = 0$ and the time between successive such crossings. At a low-energy upward crossing the slope has magnitude $B\nu$; it remains finite near the separatrix even while the period diverges. A simple global slowdown from increased bearing drag tends to modify the crossing speed as well as the dwell. A correctly prepared near-separatrix torque-free motion has relatively rapid crossings separated by long intervals close to intermediate-axis rotation. The distinction is visible in the time domain and does not depend on estimating a derivative at the slowest, noisiest part of the record.

A fit places a nominally torque-free experiment slightly above the separatrix when E, L are computed from gyros, but below it when inferred from the oscillating component pattern. What should be checked first?

▼ Work through the solution

Recalculate both invariants from the same time stamps, calibrated orientation and inertia axes. The energy classification subtracts comparable quantities and can be sensitive to cross-axis bias. The low-energy family keeps its third component's sign, whereas the high-energy family keeps its first component's sign with the stated ordering. Verify that a full body period was actually recorded and that sign changes were resolvable. Persistent disagreement after uncertainty and sampling checks can indicate a slow torque, changing mass distribution or a misspecified principal-axis alignment.

Quantify a small external torque before fitting a free-top period

Suppose the laboratory angular momentum has magnitude $3.0\,\mathrm{kg\,m^2/s}$ and an approximately constant transverse torque $0.010\,\mathrm{N\,m}$ acts for a $6.0\,\mathrm{s}$ body period. The accumulated transverse impulse is $0.060\,\mathrm{kg\,m^2/s}$, enough to tilt the spatial angular-momentum direction by roughly $0.020\,\mathrm{rad}$, or 1.15°. Its magnitude changes only to second order if the torque remains perpendicular to the initial momentum. A check using only L^2 could therefore show a small relative error while the invariable plane has moved perceptibly.

Use two marked inertial reference directions to track the spatial momentum vector and plot its Cartesian increments against the integrated measured torque. When gravity acts about a support whose line

passes through the mass centre, its torque vanishes ideally, but a small offset can supply just such a transverse disturbance. Reversing the initial spin while retaining the support geometry helps distinguish a fixed parasitic torque from gyro bias. If the spatial direction changes appreciably during one long near-separatrix dwell, fitting a torque-free elliptic period to the complete signal becomes inaccurate even if the early, fast gyro crossings agree with the free model.

Tutorial on a torque-free body's time scales

What period should be measured for the transverse gyro in the worked example? Use the small-parameter expansion $K = (\pi/2)[1 + m/4 + 9m^2/64 + \cdots]$ with $m = k_e^2$.

▼ **Work through the solution**

Substitution of $m = 1/12$ gives $K \approx 1.605$ and $T_b \approx 6.42\,\mathrm{s}$. The third-axis component repeats after about $3.21\,\mathrm{s}$, while the second component first reaches its positive maximum at $1.61\,\mathrm{s}$. Checking all three features tests the phase relation among the gyros and helps identify a sensor axis swap.

For a body with $I_1 = I_2 < I_3$, how do Euler's equations simplify and which feature of the asymmetric example disappears?

▼ **Work through the solution**

The third body component remains exactly constant, and the first two rotate sinusoidally at body-frame frequency $(I_3 - I_1)|\omega_3|/I_1$. The polar angle to fixed angular momentum is constant. A body axis can still precess in space, but the varying torque-free polar nutation caused by distinct transverse inertias disappears. Taking this limit in the low-energy solution gives $k_e \to 0$ consistently.

A gyro experiment reports slow amplitude decay along with fixed spatial angular momentum. Can that arise in a strictly rigid, torque-free model conserving kinetic energy?

▼ **Work through the solution**

The two rigid-body invariants fix the allowed intersection curve, so a persistent drift between such curves requires an effect beyond that ideal model or a changing calibration. Internal dissipation in a deformable body can decrease kinetic energy while conserving total spatial angular momentum, favouring rotation about the largest-inertia axis. An external torque could instead change angular momentum. Measuring both invariants helps distinguish the two explanations.

Compare principal-axis stability before fitting an asymmetric-top gyro trace.

David Tong derives the Euler equations, Euler angles and free-top motion.

Analytical mechanics from constraints to invariants · 7. The heavy symmetric top, precession branches and the sleeping state

Gravity supplies a torque to a top pivoted away from its centre of mass. Its axis may precess steadily, nutate between two turning angles, or trace loops. Derive all three from the same angular kinetic energy and determine when an upright spinning top can remain stable.

Project gravity onto a body with one fixed point

Let $I_1 = I_2 = I$ and I_3 be moments about the pivot, with the centre of mass a distance l along the symmetry axis. Use Euler angles θ, ϕ, ψ, where θ measures the tilt from upward laboratory vertical, ϕ measures the azimuth of the symmetry axis, and ψ spins the body about that axis relative to the nodal line. The centre-of-mass height is $l\cos\theta$, so gravity contributes $V = Mgl\cos\theta$. In the body the spin component of angular velocity is $\omega_3 = \dot\psi + \dot\phi\cos\theta$. The squared transverse component is $\dot\theta^2 + \dot\phi^2\sin^2\theta$. Consequently

$$L = \tfrac{1}{2}I(\dot\theta^2 + \dot\phi^2\sin^2\theta) + \tfrac{1}{2}I_3(\dot\psi + \dot\phi\cos\theta)^2 - Mgl\cos\theta.$$

The angles ϕ and ψ are absent themselves. Their momenta $L_z = I\dot\phi\sin^2\theta + L_3\cos\theta$ and $L_3 = I_3\omega_3$ are constants. Gravity torque about the pivot is perpendicular to the vertical and to the body symmetry axis, consistent with these two conservation laws. The entire vector $\mathbf{L}$ need not be constant. Distinguish the axial spin ω_3 measured by a body gyro from the Euler rate $\dot\psi$. A precessing top can have appreciable $\dot\phi\cos\theta$; using the painted-mark rate in a spin estimate without specifying the reference can bias a precession prediction.

Eliminate cyclic velocities to find the nutation potential

Solve $\dot\phi = (L_z - L_3\cos\theta)/(I\sin^2\theta)$ and $\dot\psi = L_3/I_3 - \dot\phi\cos\theta$. The energy can now be written $E = L_3^2/(2I_3) + I\dot\theta^2/2 + V_{\mathrm{eff}}(\theta)$, with

$$V_{\mathrm{eff}}(\theta) = Mgl\cos\theta + \frac{(L_z - L_3\cos\theta)^2}{2I\sin^2\theta}.$$

The second term is not an additional gravitational interaction. It is the transverse rotational energy required by the two fixed angular momenta at each tilt. A root of $E - L_3^2/(2I_3) - V_{\mathrm{eff}} = 0$ is a polar turning angle; a simple root is generally reached and reversed in finite time. A minimum gives stable regular precession under sufficiently small nutations at fixed conserved momenta. The apparent divergence at a pole disappears if the numerator vanishes in the same limit. The possibility of the upright sleeping state therefore requires

$$L_z = L_3.$$

Putting $u = \cos\theta$ gives a polynomial first integral. With $E' = E - L_3^2/(2I_3)$, one obtains

$$I^2\dot{u}^2 = 2I(E' - Mglu)(1-u^2) - (L_z - L_3 u)^2 = P_3(u).$$

The accessible range lies within $[-1, 1]$ where $P_3 \geq 0$. The physical turning points can be found without assigning an Euler azimuth at a pole. A nutation period is $2I\int_{u_{\min}}^{u_{\max}} du/\sqrt{P_3(u)}$. Computing the azimuthal advance over the same cycle requires averaging $\dot{\phi}(u)$ with the same time weight. An arithmetic average of the two turning-point precession rates misses the longer dwell times near the endpoints.

Find slow and fast regular precession

For constant tilt and constant $\dot{\phi} = \Omega$, the θ equation at a nonzero tilt gives

$$I\Omega^2 \cos\theta - L_3\Omega + Mgl = 0.$$

This relation follows directly by differentiating the Lagrangian with respect to θ, using $\partial_\theta[\dot{\psi} + \dot{\phi}\cos\theta] = -\dot{\phi}\sin\theta$. It is quadratic in precession speed, so the often-used $\Omega \simeq Mgl/L_3$ is only one limit. For a top above the horizontal plane and $L_3 > 0$, two positive precession branches exist if $L_3^2 \geq 4IMgl\cos\theta$. Their sum is $L_3/(I\cos\theta)$, and their product is $Mgl/(I\cos\theta)$.

Take $I = 0.020\,\mathrm{kg\,m^2}$, $I_3 = 0.010\,\mathrm{kg\,m^2}$, $Mgl = 0.200\,\mathrm{N\,m}$,

$$L_3 = 0.200\,\mathrm{kg\,m^2/s},$$
$$\theta = 60^\circ.$$

The quadratic is $0.010\Omega^2 - 0.200\Omega + 0.200 = 0$, with roots 1.056 and $18.94\,\mathrm{rad/s}$. Both have the same material spin $\omega_3 = 20\,\mathrm{rad/s}$, but their vertical angular momenta are different. The slow branch has $L_z = 0.020(1.056)(0.75) + 0.200(0.5) = 0.1158\,\mathrm{kg\,m^2/s}$; the fast branch has about $0.384\,\mathrm{kg\,m^2/s}$. Preparing a tilt and a spin alone therefore does not select a unique regular precession. The initial angular velocity of the tilted axis also matters.

Distinguish looping, cusped and monotone azimuth traces

During nutation the sign of $\dot{\phi}$ is the sign of $L_z - L_3 u$. If $u_* = L_z/L_3$ lies strictly between the turning points, the azimuth reverses along each nutation and the axis can trace loops on the unit sphere. If u_* equals a turning point, both $\dot{\theta}$ and $\dot{\phi}$ can vanish together there, producing a cusp in the ideal trace. If the numerator keeps one sign the azimuth advances monotonically even as tilt oscillates. Seeing an apparent loop in a two-dimensional camera projection is insufficient by itself; recover the three-dimensional orientation or check the signed azimuthal rate.

One classic release starts with a tilted axis that initially has no angular velocity except spin about its own direction. Then $L_z = L_3\cos\theta_0$, $\dot{\phi} = 0$, $\dot{\theta} = 0$. The gravitational torque starts tilting the axis down; on returning to that initial turning point the projected angular speed again momentarily vanishes. By contrast, giving the top the correct nonzero precession velocity at release puts it on a regular precession

branch with no initial nutation. Identical tilt and spin measurements can thus yield dramatically different trajectories if the release mechanism imparts a different transverse angular velocity.

Derive the upright stability threshold

At $L_z = L_3$, reduce the ratio $(1-\cos\theta)^2/\sin^2\theta$ to $(1-\cos\theta)/(1+\cos\theta)$. Near zero tilt the effective potential is $Mgl + [L_3^2/(8I) - Mgl/2]\theta^2 + O(\theta^4)$. A positive coefficient gives an energy minimum and requires $L_3^2 > 4IMgl$. For the preceding I, Mgl this critical angular momentum is $0.1265\,\mathrm{kg\,m^2/s}$, or an axial spin speed $12.65\,\mathrm{rad/s}$ for the chosen I_3. A high spin stabilises the upper position by coupling tilt to conservation of angular momentum. The purely gravitational potential by itself has a maximum there.

The fixed-$L_z = L_3$ quadratic energy curvature describes a polar disturbance within that momentum class. Near the axis ϕ, ψ individually become coordinate singularities. To analyse arbitrary small perturbations, use horizontal components of the unit axis and linearise their coupled gyroscopic equations. The two circular precession frequencies at the pole solve $I\Omega^2 - L_3\Omega + Mgl = 0$, giving the same discriminant. Exactly at threshold the linear frequencies coalesce, and nonlinear terms or dissipation can dominate a finite disturbance. Distinguishing a stable ideal top from an experimentally long-lived slowly slowing top requires monitoring spin over the entire observation interval.

Measure the nutation frequency of a regular precession branch

Take any regular precession tilted away from the poles, with prescribed constants L_z, L_3. A small perturbation of the polar angle gives $I\ddot{\eta} + V_{\mathrm{eff}}''(\theta_0)\eta = 0$, so the nutation frequency at fixed momenta follows from the second derivative of the effective potential. Differentiating while holding the instantaneous $\dot{\phi}$ fixed would give a different result, because a displaced top with the same momenta must change its precession rate. This distinction matters when preparing a perturbation: a small tap that adds a transverse angular impulse can change the constants as well as the tilt.

A convenient explicit formula follows by writing $F(\theta) = L_z - L_3\cos\theta$,

$$w(\theta) = F/(I\sin^2\theta).$$

Then $V_{\mathrm{eff}}' = \sin\theta[-Mgl + L_3 w - Iw^2\cos\theta]$. At a regular solution the bracket vanishes. Differentiate w as $w' = (L_3/I - 2w\cos\theta)/\sin\theta$, substitute into the derivative of the bracket, and obtain

$$\omega_{\mathrm{nut}}^2 = \frac{V_{\mathrm{eff}}''(\theta_0)}{I} = \left(\frac{L_3}{I} - 2\Omega\cos\theta_0\right)^2 + \Omega^2\sin^2\theta_0.$$

For the 60° example,

$$L_3/I = 10.0\,\mathrm{s^{-1}}.$$

On the slow branch $\Omega = 1.056\,\mathrm{s}^{-1}$, this gives $\omega_{\mathrm{nut}} \approx 8.99\,\mathrm{s}^{-1}$, or a nutation period of $0.699\,\mathrm{s}$. On the fast branch $\Omega = 18.94\,\mathrm{s}^{-1}$, it gives approximately $18.7\,\mathrm{s}^{-1}$, or $0.336\,\mathrm{s}$. Both tilted regular solutions have positive fixed-momentum curvature in this example. Comparing just the precession rates would miss the different small oscillations around their two reduced equilibria.

Suppose a small angular displacement conserves L_z, L_3 on the slow branch. The correlated rate shift is $w'\delta\theta$. At the example point $w' = (10 - 1.056)/\sin 60^\circ = 10.33\,\mathrm{s}^{-1}/\mathrm{rad}$. A nutation of $0.020\,\mathrm{rad}$ therefore modulates the precession rate by about $0.207\,\mathrm{rad/s}$, a substantial fraction of its slow steady value. A low-resolution video that measures azimuth per frame can show a conspicuous modulation even when the nutation angle itself is visually small. Filtering only one angle and fitting it with constant angular speed would hide this dynamical correlation.

Recover a nutation trajectory from energy and two turn angles

Suppose a measured top has $I = 0.020\,\mathrm{kg\,m^2}$, $Mgl = 0.20\,\mathrm{J}$, $L_3 = 0.20\,\mathrm{kg\,m^2/s}$, and is released without precession or nutation at $\cos\theta_0 = 0.50$. Its constants are $L_z = 0.10\,\mathrm{kg\,m^2/s}$ and $E' = 0.10\,\mathrm{J}$. The polar polynomial becomes

$$P_3(u) = 0.04(0.10 - 0.20u)(1 - u^2) - (0.10 - 0.20u)^2.$$

Factoring out $0.10 - 0.20u$ leaves $0.04(1 - u^2) - (0.10 - 0.20u)$. The other roots satisfy $0.04u^2 - 0.20u + 0.06 = 0$, giving $u \simeq 0.3206$ and $u \simeq 4.68$. Only the first lies within the physical interval. Thus the tilt runs from 60° to about 71.3°, and the unphysical cubic root must be discarded.

At the initial $u = 0.50$, the azimuthal numerator vanishes and the top momentarily has no precession. At the lower turning $u \simeq 0.3206$, the precession rate is $(0.10 - 0.20u)/[0.020(1 - u^2)] \approx 2.0\,\mathrm{rad/s}$. These two measurements together discriminate the cusped release from regular slow precession. A detector reporting only a mean precession rate near one radian per second could confuse them. Timing the first turning angle after release offers an independent check of Mgl/I, while a direct gyro constrains L_3/I_3.

To evaluate the nutation quadrature numerically without endpoint difficulties, substitute $u = u_{\min} + (u_{\max} - u_{\min})\sin^2\alpha$. As α approaches either endpoint, du cancels the simple square-root singularity from P_3. Integrate once with numerator one for time and once with the extra factor $\dot\phi(u)$ for azimuth. Repeat after halving the quadrature spacing. An exactly repeated root signals a limiting regular solution or a separatrix; the simple-turning substitution alone cannot regularise an actual logarithmically divergent period. In the cusped trajectory above the angular trace is continuous at the polar turning, even though the tangent to that trace can vanish.

Use horizontal tilt coordinates at the sleeping pole

Near the upright orientation the separate Euler angles ϕ, ψ are ill conditioned. Instead let the symmetry-axis unit vector be $\mathbf{n} = (x, y, 1) + O(x^2 + y^2)$ in an inertial frame with z upward. Here x, y are small dimensionless tilts, not translations. The instantaneous transverse angular velocity is $\mathbf{n} \times \dot{\mathbf{n}} \approx (-\dot y, \dot x, 0)$

, because $(\mathbf{n}\times\dot{\mathbf{n}})\times\mathbf{n}=\dot{\mathbf{n}}$. The laboratory angular momentum to first order is $I\mathbf{n}\times\dot{\mathbf{n}}+L_3\mathbf{n}$. Its derivative equals the gravitational torque $Mgl\,\hat{z}\times\mathbf{n}$. Equating the two horizontal components yields

$$I\ddot{x}+L_3\dot{y}-Mgl\,x=0,$$

$$I\ddot{y}-L_3\dot{x}-Mgl\,y=0.$$

Let $w=x+iy$. These combine into $I\ddot{w}-iL_3\dot{w}-Mgl\,w=0$. Substituting $w\propto e^{i\Omega t}$ returns $I\Omega^2-L_3\Omega+Mgl=0$ without ever assigning azimuth to the exact pole. For spin strictly above threshold, a general small tilt is a superposition of two circular motions of the two real frequencies. Their vector sum traces a wobble. For spin below threshold, the two frequencies form a complex conjugate pair and one mode grows exponentially. A perfectly vertical initial state can remain exactly vertical in an ideal simulation on either side, so stability requires a nonzero test perturbation.

Take a below-threshold spin $L_3=0.100\,\mathrm{kg\,m^2/s}$ with the earlier $I=0.020$ and $Mgl=0.200$. The real precession rate is $L_3/(2I)=2.50\,\mathrm{s^{-1}}$ and the exponential growth rate is

$$\sqrt{4IMgl-L_3^2}/(2I)=1.94\,\mathrm{s^{-1}}.$$

If the growing-mode component starts at $1\,\mathrm{mrad}$, a $20\,\mathrm{mrad}$ excursion takes about $\ln 20/1.94=1.55\,\mathrm{s}$ within the linear model. Below threshold the top need not collapse immediately after release. A short video can show several degrees of apparently orderly precession before growing tilt becomes unmistakable.

Just above threshold the mode frequencies are nearly degenerate. Decomposing noisy initial conditions into two circular amplitudes then involves division by their small frequency separation. A finite tilt impulse can produce a large beat envelope even though both ideal modes remain bounded. At exactly the repeated root the general linear solution contains $te^{i\Omega t}$ as well as $e^{i\Omega t}$; neutral-looking roots alone do not ensure boundedness. This distinction matters when inferring a critical spin from finite observation windows. Report the initial perturbation and the tilt threshold used to define loss of stability.

Infer the centre-of-mass offset from controlled precession

If regular precession can be prepared at a known tilt, the quadratic balance gives

$$Mgl=L_3\Omega-I\Omega^2\cos\theta.$$

Neglecting the second term is customary only on a sufficiently slow branch. With the slow 60° case the neglected term is about $0.0112\,\mathrm{N\,m}$, or 5.6% of the true gravitational torque scale. Inferring the centre-of-mass offset by using $l=L_3\Omega/(Mg)$ would overestimate l by this fraction. On the fast branch the two terms nearly cancel and a small error in I or Ω can be magnified substantially in the inferred Mgl.

For a top of measured mass $0.50\,\mathrm{kg}$ and $Mgl=0.200\,\mathrm{N\,m}$, the offset is $0.0408\,\mathrm{m}$. An uncertainty of $0.002\,\mathrm{N\,m}$ in gravitational torque corresponds to about $0.41\,\mathrm{mm}$ before mass and local gravity uncertainty. Repeat at several known tilts while measuring body spin and laboratory precession individually. A consistent l across slow and fast branches checks the kinetic-energy model, whereas a

gradual decrease of apparent L_3 during a single run suggests pivot drag or aerodynamic torque. A static suspension measurement of the centre of mass is a useful independent reference when estimating inertias from dynamic data.

Verify the torque law with a horizontal gyroscope

An instructive limiting experiment supports one end of a spinning wheel axle at a pivot, leaving its symmetry axis nearly horizontal. Choose the centre of mass along the free end of the axle and define the wheel's axial angular momentum by the right-hand rule. The gravitational torque is $\boldsymbol{\tau} = Mgl\,\hat{z} \times \mathbf{n}$. If $\mathbf{L}$ is approximately $L_3\mathbf{n}$, a regular precession at laboratory angular speed Ω gives

$$\dot{\mathbf{L}} \approx L_3 \Omega\, \hat{z} \times \mathbf{n}.$$

Equating the torque gives

$$\Omega = Mgl / L_3.$$

At exactly horizontal tilt this agrees with the finite root of the full quadratic; slightly away from horizontal the small transverse angular momentum affects the quantitative result.

For a wheel with $I_3 = 0.012\,\mathrm{kg\,m^2}$, axial spin $40\,\mathrm{rad/s}$, mass $0.40\,\mathrm{kg}$ and pivot offset $0.060\,\mathrm{m}$,

$$L_3 = 0.480\,\mathrm{kg\,m^2/s},$$

$$Mgl = 0.235\,\mathrm{N\,m}.$$

Horizontal precession is $0.490\,\mathrm{rad/s}$, one revolution in $12.8\,\mathrm{s}$. Reversing the spin reverses the precession direction. Moving the pivot to the other side of the centre also reverses the gravitational torque for a fixed axis convention. Testing each reversal separately helps distinguish the true gyroscopic response from a static torque due to a tilted support or a twisting suspension lead.

The phrase that gravity causes the wheel to stay up hides a vertical support force and a changing horizontal angular momentum. The pivot supplies most or all of the vertical force required to support the wheel's weight. With steady horizontal precession, the centre of mass also accelerates horizontally toward the precession axis with magnitude $l\Omega^2$. Thus the pivot must supply a horizontal radial reaction $Ml\Omega^2$. For the numerical wheel this is only $0.0058\,\mathrm{N}$, much smaller than the $3.92\,\mathrm{N}$ vertical support. A torque signal can be easy to see through slow precession while the corresponding horizontal reaction is weak. A load cell measuring only vertical force would not directly measure the gravitational torque acting about the pivot.

Spin friction alters the interpretation of a long run. Suppose the measured axial spin falls from 40 to $35\,\mathrm{rad/s}$ over one minute and the axis remains close to horizontal regular precession. The predicted precession speed rises from 0.490 to $0.561\,\mathrm{rad/s}$, even though mechanical energy is being dissipated. This is not negative damping. Less axial angular momentum must change direction under essentially the same gravitational torque, so its direction turns more rapidly. If the spin-down time becomes comparable with a nutation period, an instantaneous regular-precession approximation is no longer sufficient; include dissipative torques in the full equations and measure both tilt and angular momentum.

Identify the precession branches

Change the angular momentum of a supported top before identifying its steady rotation rates. Check which approximation singles out the slower branch.

Open this experiment online

Try the calculation

Tilt from vertical (°) **60**

Moment arm (mm) **60**

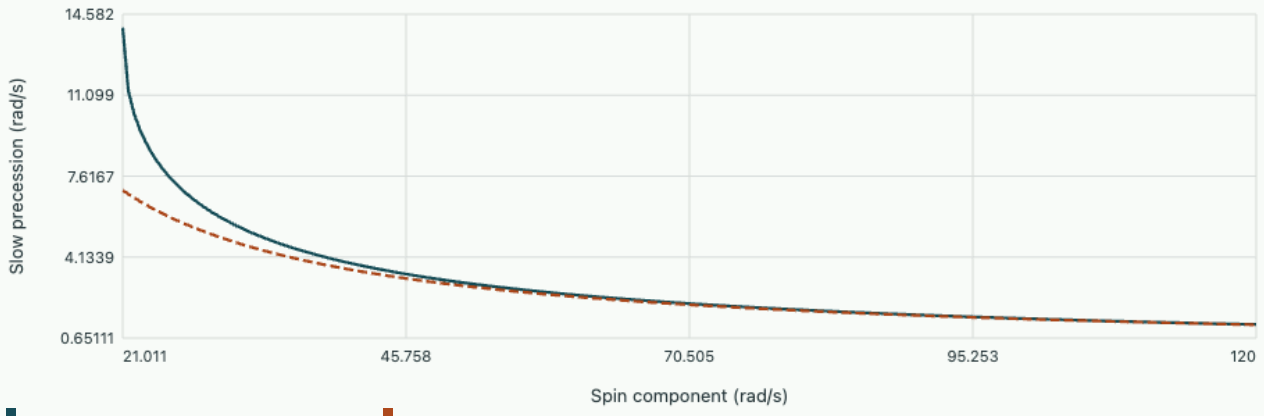

For this tilt the two regular-precession branches first exist at spin 21.0 rad/s. At 100 rad/s the exact slow rate is 1.488 rad/s.

Extract polar turning points from uncertain orientation data

A camera supplies a unit direction $\mathbf{n}(t)$, while body and pivot calibrations supply I, I_3, Mgl. To infer L_3, either measure the gyro component along $\mathbf{n}$ or combine two independent orientation marks so that spin about the axis is observable. A single unmarked axis direction cannot reveal that spin. Vertical angular momentum follows from $L_z = I(\mathbf{n} \times \dot{\mathbf{n}})_z + L_3 n_z$. This expression remains regular at a vertical pose and avoids differentiating an azimuth divided by a small $\sin\theta$. Estimating $\dot{\mathbf{n}}$ still requires timing and finite-difference checks, especially near a fast turn.

The transverse kinetic energy is $I|\dot{\mathbf{n}}|^2/2$, so $E' = I|\dot{\mathbf{n}}|^2/2 + Mgl\,n_z$. These vector formulas allow each time sample to supply independent estimates of the invariants. Compute their median or uncertainty-weighted values over a torque-free-about-vertical segment, then locate the physical roots of $P_3(u)$. Reject roots outside $[-1, 1]$ before converting to angles, and propagate measured parameter ranges into intervals for the roots. Near a repeated root a small coefficient error can split the pair substantially or apparently remove it. A nearly steady precession should therefore be assessed using the dynamic measurement uncertainty, not classified solely by the discriminant of a fitted cubic.

A direction-only camera sees apparently steady 60° precession at $1.0\,\mathrm{rad/s}$. Can it infer the axial spin without measuring a second body mark?

▼ **Work through the solution**

In a precisely known ideal regular state the torque balance gives $L_3 = (I\Omega^2\cos\theta + Mgl)/\Omega$, so one can infer spin from a dynamical model and calibrated inertias. Using $I = 0.020$, $Mgl = 0.200$ gives

$$L_3 = 0.210\,\mathrm{kg\,m^2/s}.$$

That is an indirect inference, sensitive to gravity calibration, pivot torque, and the assumption of exactly regular precession. The orientation of one axis alone supplies no purely kinematic measurement of rotation about itself. A second mark or gyro offers an independent check rather than fitting the same torque law twice.

A numerical implementation rescales $\mathbf{n}$ to unit length at every step and observes bounded plotted angles. Does this establish correct top dynamics?

▼ **Work through the solution**

Unit length is only the configuration constraint. Reconstruct L_z, L_3, E', compare polar turning points with the cubic, and repeat at smaller time step. The vector can stay exactly on the sphere while its azimuth and nutation phase drift, or while a spurious torque transfers axial angular momentum. A support torque and gravitational work budget, with a clear reference for the potential, test complementary aspects that normalisation alone cannot enforce.

Check the fixed-pivot inertia before drawing an instability boundary

A laboratory data sheet may quote the transverse inertia about the centre of mass, whereas the Lagrangian here needs the inertia about the pivot. With a pivot on the symmetry axis a distance l from the centre, the parallel-axis relation gives $I = I_{\mathrm{cm}} + Ml^2$ for each transverse direction, while I_3 remains unchanged. For $M = 0.50\,\mathrm{kg}$, $l = 0.080\,\mathrm{m}$, and $I_{\mathrm{cm}} = 0.010\,\mathrm{kg\,m^2}$, the correct value is $0.0132\,\mathrm{kg\,m^2}$. Neglecting the shift underpredicts the critical spin by a factor $\sqrt{0.010/0.0132} = 0.870$.

Moving the pivot changes both the gravitational torque scale Mgl and the transverse inertia. Doubling l does not merely multiply the stability threshold by $\sqrt{2}$ if Ml^2 is appreciable. Compute the new I and then the product that enters $L_{3,\mathrm{crit}}^2 = 4IMgl$. A two-pivot experiment with one unchanged rotor provides a direct test of the parallel-axis correction and checks why a table of freely rotating principal moments cannot be inserted unaltered into a supported top calculation.

Tutorial on a heavy top

With the same constants, impose a tilt of 90°. Does the regular precession formula become singular when $\cos\theta = 0$?

▼ **Work through the solution**

The unsimplified quadratic becomes $-L_3\Omega + Mgl = 0$, so the finite regular precession is

$$\Omega = Mgl/L_3 = 1.0\,\mathrm{rad/s}.$$

A quadratic formula written with $2I\cos\theta$ in the denominator masks this regular solution. The other branch becomes unbounded as the horizontal configuration is approached from the side with positive cosine at fixed spin. Keep the original equation when taking a degenerate limit.

A top undergoes nutation with u between 0.30 and 0.70, with $L_z = 0.11$ and $L_3 = 0.20$ in consistent angular-momentum units. Does the azimuth reverse?

▼ **Work through the solution**

The numerator of $\dot\phi$ vanishes at $u = 0.55$, inside the allowed interval. For $u < 0.55$ precession is positive in this convention; for $u > 0.55$ it is negative. A camera recording the full axis should therefore find an azimuthal reversal twice per nutation period. The polar velocity need not vanish at those two reversals, so these instants are distinct from the polar turning points.

A frictionless rigid-top simulation reports exact E, L_z, L_3 but returns a nutation frequency differing by ten percent from an independent measurement. Name two checks that use more than the conserved values.

▼ **Work through the solution**

Compute the turning points from the cubic and compare the measured times between them against its quadrature, then reconstruct the azimuthal phase over the same cycle. Check whether the measured spin was ω_3 or a painted-mark Euler rate and whether the inertias include the parallel-axis contribution about the pivot. A numerical method can conserve constants while producing a phase error, and an inconsistent initial state can preserve different constants perfectly.

Compare a free principal-axis rotation with a pivoted top subject to gravity.

David Tong's rigid-body chapter includes the heavy symmetric top.

Analytical mechanics from constraints to invariants · 8. Symplectic transformations, Poisson brackets and the geometry of measurements

Two phase-space plots can enclose the same volume while predicting different responses to an impulse. Derive the stronger condition that makes a change of variables canonical, test it on measured linear maps and use Poisson brackets to propagate observables without solving separately for every coordinate.

Derive the matrix condition from Hamilton's equations

Collect n canonical positions and momenta into $z = (q_1, \dots, q_n, p_1, \dots, p_n)^T$. Write Hamilton's equations as $\dot{z} = J\nabla_z H$, where J has zero diagonal blocks, identity upper right and minus identity lower left. For a time-independent change $Z = f(z)$ with Jacobian $S = \partial Z/\partial z$, the chain rule gives

$$\dot{Z} = SJS^T \nabla_Z H.$$

To preserve the canonical form for every differentiable Hamiltonian require

$$SJS^T = J.$$

For an invertible square matrix this is equivalent to $S^T J S = J$. In geometric terms the bilinear antisymmetric form $\omega(u, v) = u^T J v$ has the same value on any transported pair of tangent vectors.

Taking determinants gives $(\det S)^2 = 1$, and symplectic maps have positive determinant equal to one. One way to see the sign is to take the top exterior power of the preserved two-form: ω^n fixes an oriented volume. In one canonical pair the identity $S^T J S = (\det S) J$ makes determinant one sufficient. In two or more pairs a single volume condition cannot enforce every entry of the matrix condition. For example in ordering (q_1, q_2, p_1, p_2), scaling by diagonal entries $(2, 1, 1, 1/2)$ preserves four-dimensional volume. But $\{Q_1, P_1\} = 2$ and $\{Q_2, P_2\} = 1/2$, so neither conjugate pair has the required bracket. A volume-preserving histogram test alone would miss this failure.

Identify brackets of observables and what they measure

Define $\{A, B\} = (\nabla A)^T J \nabla B = \sum_i (A_{q_i} B_{p_i} - A_{p_i} B_{q_i})$. For any explicitly time-dependent observable $A(z, t)$, differentiation along Hamiltonian trajectories gives

$$\dot{A} = \{A, H\} + \partial_t A.$$

The bracket is antisymmetric and obeys the product rule. Computing it with the chain rule in the new variables proves that canonical transformations preserve brackets, even between nonlinear observables. Conversely the fundamental brackets $\{Q_i, P_j\} = \delta_{ij}$, $\{Q_i, Q_j\} = \{P_i, P_j\} = 0$ are precisely the entries of $SJS^T = J$.

For a particle set $L_z = x p_y - y p_x$. Its Hamiltonian flow as a generator sends x to $x - \varepsilon y$, y to $y + \varepsilon x$ and rotates momenta by the same infinitesimal angle. The angular momentum components satisfy $\{L_x, L_y\} = L_z$ with cyclic permutations. Derive one entry directly for $L_x = y p_z - z p_y$ and

$L_y = zp_x - xp_z$. The z, p_z pair contributes $xp_y - yp_x$, with the other terms zero. Rotations about two different axes generally fail to commute. The resulting commutator has the form of a rotation about the third axis even though each underlying infinitesimal motion preserves every canonical bracket.

Jacobi's identity $\{A, \{B, C\}\} + \{B, \{C, A\}\} + \{C, \{A, B\}\} = 0$ implies that the bracket of two time-independent conserved quantities is conserved under the same Hamiltonian. If the Hamiltonian is invariant under rotations about x and y, its invariance about z follows from this relation and $\{L_x, L_y\} = L_z$. Conservation alone need not make two observables commute. A central force can conserve all three angular momentum components, but their mutual brackets remain nonzero. For independent commuting integrals in an integrability argument one must check the involution condition explicitly.

Construct a canonical map for any smooth point transformation

Suppose new coordinates depend only on old coordinates, $Q = f(q)$. Preserve the canonical one-form exactly,

$$p^T dq = P^T dQ = P^T Df\, dq.$$

Thus $p = (Df)^T P$ and $P = (Df)^{-T} p$. Applying the same coordinate matrix to momenta works only for a restricted case such as an orthogonal change of coordinates. An extension of position must be accompanied by a reciprocal rescaling of its conjugate momentum. For $Q = q^2$ on $q > 0$, for example, $P = p/(2q)$. The free Hamiltonian becomes $2QP^2/m$; even a physically free particle can acquire a coordinate-dependent expression for its kinetic energy.

Polar coordinates demonstrate why a momentum variable need not equal a measured tangential component. In the plane $x = r\cos\varphi, y = r\sin\varphi$. Substituting into $p_x dx + p_y dy$ gives

$$p_r = \mathbf{p} \cdot \hat{r},$$

$$p_\varphi = r\,\mathbf{p} \cdot \hat{\varphi} = L_z.$$

The physical tangential momentum is p_φ / r. At radius $0.40\,\mathrm{m}$ and transverse momentum $0.60\,\mathrm{kg\,m/s}$, the canonical angular momentum is $0.24\,\mathrm{kg\,m^2/s}$. Treating the transverse component itself as conjugate to angle would make $\{\varphi, p_\varphi^{\mathrm{wrong}}\} = 1/r$. The coordinate singularity at $r = 0$ also prevents these canonical polar variables from covering the entire original phase space with one chart.

Generate shears and test a numerical map

A type-two generating function $F_2(q, P, t)$ defines $p = \partial_q F_2$, $Q = \partial_P F_2$, and $K = H + \partial_t F_2$ where the transformation can be locally inverted. The differential $d(F_2 - QP)$ equals $p\,dq - P\,dQ + (K - H)\,dt$. Thus the actions differ only by an endpoint term; taking another exterior derivative at fixed time gives the symplectic form condition. For $F_2 = qP + sP^2/(2m)$, the map is $p = P, Q = q + sp/m$, free drift over time s. For $F_2 = qP + sV(q)$, the map is

$P = p - sV'(q), Q = q$, a potential kick. Their composition is canonical for any step size even though an alternating drift and kick need not give the exact trajectory.

Take a unit-mass, unit-frequency oscillator with $h = 0.5$. A kick followed by drift gives $P = p - hq$, $Q = q + hP = (1 - h^2)q + hp$. Its amplification matrix has determinant one and trace $2 - h^2 = 1.75$, so its eigenvalues form a unit-modulus conjugate pair. The numerical phase per step is $\arccos(1 - h^2/2) = 0.50536$, slightly ahead of the exact phase 0.50000. Starting at $q = 1, p = 0$, the first step gives $Q = 0.75, P = -0.50$, and physical energy becomes 0.40625 instead of 0.5. Exact bracket preservation does not imply exact conservation of the original energy at every point. If $h > 2$ the same matrix remains symplectic but has a real expanding and contracting eigenvalue; geometric preservation is compatible with numerical instability.

For a numerical implementation with analytic equations unavailable, approximate the Jacobian of a one-step map at selected states by perturbing one canonical component at a time. Compute $S^T J S - J$ after nondimensionalising coordinates and momenta in conjugate pairs. Repeat with smaller perturbations and at different integration tolerances. A determinant close to one in four dimensions is insufficient. Testing the transported brackets of one position–momentum pair and one cross-pair can reveal a swapped column or misplaced mass factor before a long simulation exhibits visible energy drift.

Track canonical area for a transported experimental ensemble

A narrow group of trajectories lets an experimenter estimate a tangent map without applying a separate perturbation to each coordinate at the same time. Prepare a small covariance ellipse in one canonical pair $z = (q, p)$, propagate each member through a known linear Hamiltonian device, and compute $\Sigma_{\mathrm{out}} = S \Sigma_{\mathrm{in}} S^T$. The ellipse area is proportional to $\sqrt{\det \Sigma}$, and a symplectic map in one pair preserves that area. Its projections can grow or contract individually: a focusing device can reduce position spread while increasing momentum spread or correlation. Measuring only the two marginal widths ignores their covariance and can falsely suggest area growth.

For a free unit-mass drift of duration two in scaled units,

$$S = \begin{pmatrix} 1 & 2 \\ 0 & 1 \end{pmatrix}.$$

Start with $\Sigma = \mathrm{diag}(1, 1)$. The outgoing covariance has entries $\Sigma_{qq} = 5, \Sigma_{pp} = 1, \Sigma_{qp} = 2$. The apparent rectangle of marginal standard deviations grows by $\sqrt{5}$, yet the determinant remains $5 - 4 = 1$. A plot that suppresses the correlation has discarded exactly the information needed for the area test. Noise in the two channels also contributes to observed covariance, so calibrate sensor variances independently before attributing a small apparent growth to physical dissipation or numerical smoothing.

For two pairs it is possible for a perfectly canonical coupling to exchange projected emittances. Take a uniform rotation of the two positions and the same rotation of their conjugate momenta. It is canonical by construction. If the two incoming pairs have different covariance areas, a ninety-degree rotation swaps them completely; at forty-five degrees each outgoing projected pair contains a mixture. The full four-dimensional symplectic structure remains intact. An experimentally available two-dimensional marginal

then tests only part of the dynamics. Counting phase-space points in a volume and measuring cross-pair brackets answer different questions about a strongly coupled system.

The eigenvalues of $J\Sigma$ are invariant under the linear canonical covariance transport. Indeed $JS = S^{-T}J$ for symplectic S, so $J\Sigma_{\mathrm{out}} = S^{-T}(J\Sigma_{\mathrm{in}})S^{T}$, a similarity transformation. For a positive covariance these eigenvalues occur as conjugate imaginary pairs, and their positive magnitudes give symplectic covariance scales. This algebraic test can distinguish loss of correlations in a fitted transfer matrix from actual exchange between pairs. It assumes linear propagation of the ensemble. A nonlinear canonical map can stretch a finite ellipse into a curved shape whose covariance determinant changes while its exact enclosed area remains preserved.

Use generating functions to find a moving normal-mode basis

Consider a two-dimensional isotropic oscillator and rotate its coordinate axes by a prescribed time-dependent angle $\alpha(t)$. Let $Q = R(\alpha)^{T} q$, $P = R(\alpha)^{T} p$ for a proper planar rotation. At any fixed time the map is orthogonal and symplectic. To derive the Hamiltonian in these moving variables, use $F_2(q, P, t) = q^{T} R(\alpha) P$. Its time derivative at fixed old q and new P is $-\dot{\alpha}(Q_x P_y - Q_y P_x)$, with the sign corresponding to axes rotating counterclockwise in the laboratory. The transformed Hamiltonian is therefore

$$K = H_0(Q, P) - \dot{\alpha} L_z.$$

For constant rotation rate and an isotropic potential the new Hamiltonian has no explicit time dependence. Its value is the combination energy minus rotation rate times angular momentum encountered in the Noether argument. Hamilton's equations now include $-\dot{\alpha}\,\hat{z} \times Q$ in $\dot{Q}$ relative to the rotated physical velocity. Thus the transformed canonical momentum P equals the rotated laboratory momentum rather than $m\dot{Q}$. Confusing the two yields incorrect initial conditions for a rotating-frame simulation even if the transformation matrix at the starting instant is the identity.

Take $m = 1.0\,\mathrm{kg}$, a laboratory point initially at $q = (0.20, 0)\,\mathrm{m}$ with $p = (0, 0.30)\,\mathrm{kg\,m/s}$, and axes initially aligned but rotating at $2.0\,\mathrm{rad/s}$. The canonical P_y is $0.30\,\mathrm{kg\,m/s}$. The derivative of the rotating-frame coordinate is

$$0.30 - 2.0(0.20) = -0.10\,\mathrm{m/s}.$$

It moves in the negative rotating-frame y direction while its laboratory velocity points positive y. The angular momentum is $0.060\,\mathrm{kg\,m^2/s}$, so K lies $0.120\,\mathrm{J}$ below the laboratory Hamiltonian. Both position–momentum transformations preserve brackets; the extra term derives from the moving basis, not a failure of canonical geometry.

An oscillator with two nearly equal natural frequencies provides another reason to track the generating function. If one diagonalises a slowly changing stiffness matrix at each time and keeps only the instantaneous diagonal frequencies, the omitted rotation of the eigenvectors couples the nominal modes through a term of this type. When the eigendirections turn rapidly near a degeneracy, the coupling can be appreciable even if both eigenvalues change little. Measuring the orientation as well as the

eigenfrequencies allows the size of this effect to be estimated before fitting amplitude transfer to a spurious dissipation term.

Compare exact phase transport with a dissipative fit

A damped oscillator with $m\ddot{q} + c\dot{q} + kq = 0$ has equations $\dot{q} = p/m$, $\dot{p} = -kq - cp/m$. In the physical (q, p) plane their divergence is $-c/m$. A small material phase-space area therefore contracts as $A(t) = A(0)e^{-ct/m}$. No time-independent canonical coordinate change on the same two-dimensional isolated phase space can turn that physical contraction into a Hamiltonian flow preserving area. This conclusion concerns the reduced dissipative description. An expanded system including the degrees of freedom that absorb energy can still be Hamiltonian.

For $c/m = 0.40\,\mathrm{s}^{-1}$, a pair of independent initial perturbations spanning area one in calibrated coordinates spans only 0.449 after two seconds. A numerical step of $0.10\,\mathrm{s}$ fitted to that exact map should have determinant $e^{-0.04} = 0.9608$. Forcing its determinant to one during system identification would remove a real dissipative measurement. Conversely a conservative oscillator propagated by forward Euler at matched units and $h = 0.10$ has amplification determinant $1 + h^2 = 1.01$, corresponding to a spurious area growth. A geometric diagnostic is interpretable only after deciding what physical system and coordinate pair were actually observed.

The pair q, v differs from canonical q, p by a constant mass scaling for an ordinary single particle. In one pair with constant mass that scaling does not change a measured same-coordinate before-and-after determinant. For a position-dependent mass, constrained coordinates with a varying metric, or explicit time-dependent changes of measurement scale, volume in raw position–velocity coordinates need not equal canonical volume. For example a free particle expressed in $Q = q^2$ has canonical momentum $P = m\dot{Q}/(4Q)$. A detector estimating phase area in $(Q, \dot{Q})$ without the Q-dependent factor can infer contraction or expansion even when canonical phase area is exactly conserved.

Compute a bracket of mechanical momenta and recover the Lorentz force

For a charge e in a prescribed vector potential write mechanical momentum $\boldsymbol{\pi} = \mathbf{p} - e\mathbf{A}(\mathbf{q}, t)$. The canonical brackets are $\{q_i, p_j\} = \delta_{ij}$, but the measured mechanical components satisfy

$$\{\pi_i, \pi_j\} = e(\partial_i A_j - \partial_j A_i) = e\epsilon_{ijk}B_k.$$

At nonzero magnetic field they are not simultaneously canonical momenta conjugate to the Cartesian positions. This result is gauge invariant because it involves only the curl of the vector potential. It offers a physical example where replacing canonical by measured momenta in a software interface changes the matrix of fundamental brackets.

With $H = \pi^2/(2m) + e\phi$, the time derivative is

$$\dot{\pi}_i = \{\pi_i, H\} + \partial_t \pi_i.$$

The kinetic-energy bracket contributes $(e/m)(\boldsymbol{\pi}\times\mathbf{B})_i$; the scalar potential contributes $-e\partial_i\phi$; and the explicit derivative supplies $-e\partial_t A_i$. Their sum is $e[\mathbf{E}+(\boldsymbol{\pi}/m)\times\mathbf{B}]_i$. Dropping the last term would make time-dependent electric acceleration depend on gauge. In a static uniform B_z, the transverse mechanical momenta rotate although their energy is constant. Canonical bracket structure therefore contains observable information about the force even before integrating a trajectory.

A useful finite-difference test sets $A_y = Bx$ and samples the map from canonical to mechanical variables around one state. The measured bracket $\{\pi_x,\pi_y\} = eB$ should be constant in space. A code that insists on zero will attribute the entire magnetic response to an erroneous Hamiltonian gradient. A code using mechanical variables legitimately can instead use their noncanonical bracket matrix; its equations must then preserve the correct transformed structure, not the original constant J. Testing the resulting acceleration at zero velocity and at a transverse velocity distinguishes electric and magnetic terms and catches sign errors in the antisymmetric entries.

Derive a reversible drift–kick–drift scheme and its measured phase

For $H = p^2/(2m) + V(q)$, exact kinetic flow for a duration t is $D_t : (q,p) \mapsto (q + tp/m, p)$. Exact potential flow is $K_t : (q,p) \mapsto (q, p - tV'(q))$. Each is canonical. Compose $D_{h/2}K_hD_{h/2}$ in chronological order. Applying the same construction with $-h$ undoes each substep in reverse order, so the full map is time reversible. Symmetry eliminates the even local-error powers in the effective generator, giving a second-order method for smooth V. The individual Hamiltonian pieces need not commute; if they did, the split map would be exact at any step.

For a unit oscillator, carrying out the algebra gives

$$Q = (1 - h^2/2)q + h(1 - h^2/4)p,$$

$$P = -hq + (1 - h^2/2)p.$$

Verify directly that the determinant is one. The trace gives the same step angle $2\arcsin(h/2)$ as the first-order kick–drift matrix in its stable range, but the new off-diagonal coefficients make the amplitude errors and time reversal different. Starting from $q = 1, p = 0$ at $h = 0.50$, one gets $Q = 0.875, P = -0.50$, energy 0.5078125. A negative step returns to the initial values apart from roundoff. Passing this one reversal test says nothing about absolute phase accumulated over hundreds of periods.

The map preserves $q^2 + (1 - h^2/4)p^2$ exactly for the harmonic test. At $h = 0.5$ the coefficient of p^2 is 0.9375, so the preserved ellipses differ slightly from the circles of physical energy. Their reversible oscillation in physical energy is bounded for $|h| < 2$. The per-step phase is about 0.50536 at this step, giving a phase gain 0.536 radians after one hundred steps. As h is halved while physical integration time stays fixed, the overall phase error falls approximately by four. Measuring an energy oscillation, a reversal residual and a return time therefore probes three different properties of one apparently simple map.

Compare a symplectic map with the phase of a physical orbit

Change the step of the midpoint update. Distinguish preservation of phase-space structure from agreement of the measured oscillation frequency.

Open this experiment online

Try the calculation

Time step h (ω = 1) **0.5**

Number of forward steps **20**

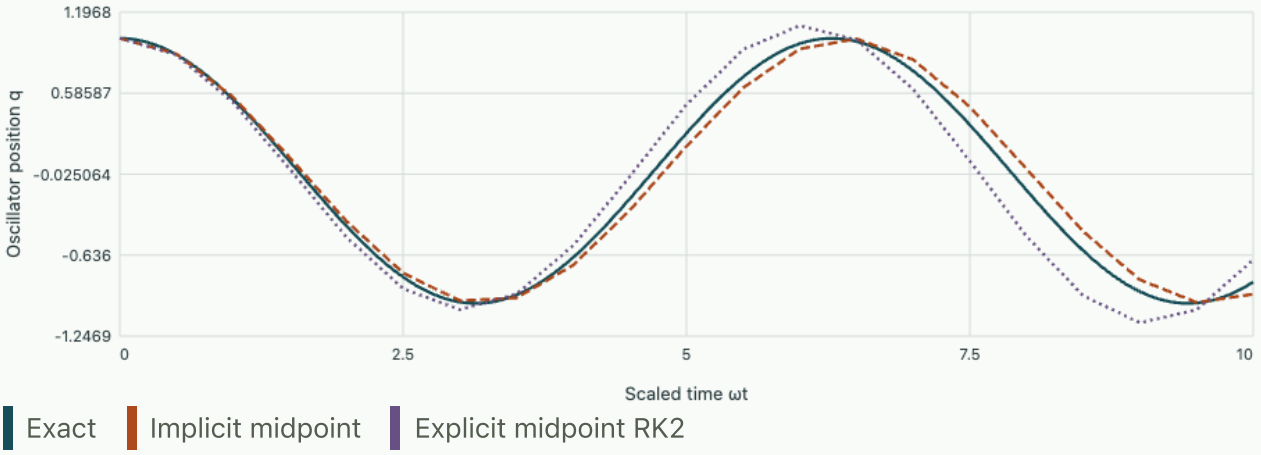

Implicit midpoint phase lag 0.2009 rad. Forward-backward distance from the start is 8.951e-16 for implicit midpoint and 0.3635 for explicit midpoint.

Relate the order of two pulses to their Poisson bracket

A canonical transformation close to identity can be built by applying two brief Hamiltonian operations in different orders. Take one free drift and one potential kick, each of short duration s. A drift then a kick gives

$$q' = q + sp/m,\ p' = p - sV'(q + sp/m).$$

A kick then a drift gives

$$p'' = p - sV'(q),\ q'' = q + s[p - sV'(q)]/m.$$

To second order their coordinate difference is $q' - q'' = s^2 V'(q)/m$; their momentum difference is $p' - p'' = -s^2 pV''(q)/m + O(s^3)$. The difference vector equals the Hamiltonian vector generated by $G = pV'(q)/m = \{V, T\}$, multiplied by s^2. The bracket sets the leading effect of reversing the operation order.

For the harmonic oscillator at $q = 1, p = 0, m = k = 1$ with $s = 0.10$, a drift then kick gives $(1, -0.10)$; kick then drift gives $(0.99, -0.10)$. The coordinate difference 0.01 equals $s^2 V'/m$, and the leading momentum difference is zero for this initial condition. At $q = 0, p = 1$, the complementary experiment gives a momentum difference of -0.01 and no coordinate difference. Running both initial states tests the two components of the bracket-generated perturbation. A single apparently correct coordinate update would not detect a sign swap in the other component.

An experimental implementation might use a short force pulse as a kick and free propagation between pulses. The pulse must be short enough that motion during the kick is negligible; otherwise its own kinetic drift enters the comparison at the same order as the desired bracket. Extrapolate the measured difference divided by s^2 to small s, and separately measure acquisition noise, which grows in relative importance under that division. Alternating the pulse order cancels many static calibration shifts but does not magically remove timing offsets correlated with the order. Treat the small bracket signal as a physical difference between two specified protocols.

A transformation preserves all coordinate–momentum brackets but a time integration on the transformed variables produces the wrong laboratory trajectory. Can the bracket check alone identify the error?

▼ **Work through the solution**

Canonical coordinates guarantee the form of Hamilton's equations. Their actual trajectories still require the correct transformed Hamiltonian, including explicit time dependence of the generating function, consistent initial momenta and a sufficiently accurate integrator. Transform an independently known initial state, compare the initial velocity and acceleration of a measurable coordinate, and follow both descriptions back to the same laboratory frame. A bracket test can establish that a change of variables is admissible without establishing that the correct energy function or physical input was attached to it.

Set compatible units before inspecting a symplectic residual

Suppose position is recorded in millimetres and momentum in kilogram metres per second. Scaling each numerical coordinate to unit variance is convenient for fitting a matrix, but independent scaling of each coordinate and momentum can change the bracket matrix from its textbook form. If $z' = Dz$ with diagonal D, then $J' = DJD^T$. For one pair this multiplies its bracket by the product of the position and momentum scale factors. In two pairs these factors can differ. A residual computed against the original J can flag a harmless unit change or, conversely, mask an error if scales happen to compensate.

Choose a characteristic length q_0, momentum p_0, and common action scale $q_0 p_0$ for each pair if the dimensionless chart is to have a common symplectic scale. Otherwise carry the transformed bracket explicitly through the test. With two oscillators of different physical units, a canonical nondimensionalisation may balance the dynamics better than using the same numerical length scale for both. Report the dimensional transformation along with any determinant or defect norm so another calculation can reconstruct which tangent vectors and measurement units were actually compared.

Tutorial on canonical tests

In two degrees of freedom try $Q_1 = q_1,\ Q_2 = q_2,\ P_1 = p_1 + \alpha q_2,\ P_2 = p_2$. Is this map canonical? What is the simplest modification that restores the condition?

▼ **Work through the solution**

The fundamental mixed momentum bracket is $\{P_1, P_2\} = \alpha$. Restore zero by also taking $P_2 = p_2 + \alpha q_1$, since then the extra term $\{p_1, \alpha q_1\} = -\alpha$ cancels. The added momentum vector is now the gradient of the scalar $\alpha q_1 q_2$, whose derivative matrix is symmetric. Both candidate maps preserve volume, reinforcing why volume alone cannot decide.

For the unit oscillator kick–drift map find a quadratic quantity it preserves exactly while its physical energy changes.

▼ **Work through the solution**

Direct substitution gives $Q^2 + P^2 - hQP = q^2 + p^2 - hqp$ for the kick–drift convention above. Multiplying by one half gives a positive modified quadratic invariant when $|h| < 2$. The first step at $h = 0.5$ gives $0.75^2 + (-0.50)^2 - 0.5(0.75)(-0.50) = 1.0$, equal to its initial value. At $h = 2$ the quadratic becomes degenerate and beyond it no longer bounds the motion.

A time-dependent momentum shift is generated by $F_2 = qP - a(t)q$. For a free physical particle find the transformed Hamiltonian and verify constant physical momentum.

▼ **Work through the solution**

The transformation gives

$$p = P - a,\ Q = q,$$
$$K = (P - a)^2/(2m) - \dot{a}\, Q.$$

Hamilton's equation gives $\dot{P} = +\dot{a}$, hence $\dot{p} = 0$. Omitting the explicit $\partial_t F_2$ term would predict constant P and a spurious acceleration of the original free particle. This test uses an observable whose physical behaviour is already fixed independently.

Compare generated canonical changes and numerical determinant tests.

David Tong develops canonical transformations and Poisson brackets in Hamiltonian dynamics.

Analytical mechanics from constraints to invariants · 9. Action, angle and the slowing clock at a separatrix

A phase portrait contains enough information to extract a period by differentiating an area. Use that fact to build a clock for finite-amplitude pendulum motion, determine precisely where slow-parameter invariance fails, and distinguish a librating trajectory from one that makes complete rotations.

Turn a closed phase-space loop into an action variable

For a one-degree-of-freedom Hamiltonian $H(q,p;\lambda)$ at fixed parameter λ, take a connected periodic orbit of energy E. Define its action by $J(E,\lambda)=(2\pi)^{-1}\oint p\,dq$, oriented along the actual motion. The units are energy times time. A smooth family of nested librating loops has $2\pi J$ equal to the enclosed canonical phase area. For circulation on a coordinate cylinder, such as an angle increasing through 2π, the integral still defines an action even though the loop winds around the cylinder. Its area interpretation and sign need a reference branch.

At fixed q,λ, differentiating $H(q,p(E,q))=E$ gives

$$\partial_E p = 1/H_p = 1/\dot{q}.$$

Differentiating the action integral yields $\partial_E J = T/(2\pi)$, because $dq/\dot{q}=dt$ around the orbit. At ordinary turning points $\dot{q}=0$, the derivative integrand has an integrable singularity while the two endpoints of the closed loop agree; one can justify the derivative using a local square-root coordinate. Inverting gives

$$\omega(J)=\partial_J E.$$

If θ is the angle conjugate to J, the transformed Hamiltonian is $E(J)$ and $\dot{\theta}=\omega(J)$ is constant. This canonical angle generally differs from the geometric angle reported by a camera.

For a unit-mass harmonic oscillator the energy curve $p^2+\omega_0^2q^2=2E$ is an ellipse. Its area is $2\pi E/\omega_0$, giving $J=E/\omega_0$ and a frequency independent of amplitude. One may take $q=\sqrt{2J/\omega_0}\sin\theta,\ p=\sqrt{2J\omega_0}\cos\theta$, whose bracket is one. The position turns nonuniformly in coordinate space even though the phase angle advances uniformly. Under a slow change in ω_0, constant J predicts $E\propto\omega_0$ and amplitude proportional to $1/\sqrt{\omega_0}$. Constant action does not mean constant mechanical energy while work is performed by a changing spring.

Integrate the finite-amplitude pendulum

Let $I=ml^2$, $\omega_0^2=g/l$, and measure q from downward vertical. The Hamiltonian $H=p^2/(2I)+I\omega_0^2(1-\cos q)$ has separatrix energy $E_s=2I\omega_0^2$. For a libration of turning angle $q_m<\pi$, define $k=\sin(q_m/2)=\sqrt{E/E_s}$. The positive momentum branch is $p=2I\omega_0\sqrt{k^2-\sin^2(q/2)}$. Set $\sin(q/2)=k\sin u$. Evaluating four quarter-arcs of the loop gives

$$J_{\mathrm{lib}} = \frac{8 I \omega_0}{\pi}\left[\mathsf{E}(k) - (1-k^2)\mathsf{K}(k)\right],$$

$$T_{\mathrm{lib}} = \frac{4}{\omega_0}\mathsf{K}(k).$$

Here $\mathsf{K}(k) = \int_0^{\pi/2} (1 - k^2 \sin^2 u)^{-1/2} du$ and $\mathsf{E}(k) = \int_0^{\pi/2} \sqrt{1 - k^2 \sin^2 u}\, du$. To verify the first formula after substitution, note that $k^2 \cos^2 u = (1 - k^2 \sin^2 u) - (1 - k^2)$. The transformed integral of $k^2 \cos^2 u / \sqrt{1 - k^2 \sin^2 u}$ splits exactly into the two quoted complete elliptic integrals. The period follows either by $dq/\dot{q}$ or by differentiating the action. That independent check is useful when numerical differentiation of noisy action estimates amplifies sampling errors.

At small k,

$$\mathsf{K} = (\pi/2)(1 + k^2/4 + \cdots),$$

$$T \approx (2\pi/\omega_0)(1 + q_m^2/16 + \cdots).$$

At $q_m = 60^\circ$, $k = 1/2$ and $\mathsf{K} \simeq 1.68575$, giving $T/T_{\mathrm{small}} = 1.0732$. A pendulum of length $1.00\,\mathrm{m}$ then has period about $2.153\,\mathrm{s}$, where the small-angle answer is $2.006\,\mathrm{s}$. Timing ten periods rather than one helps resolve the accumulated difference. Measuring the arc amplitude from a projected image requires a geometric correction if the swing plane is tilted relative to the camera.

Approach the saddle from either side

At the upright position $q = \pi$, the potential is maximal and the equilibrium is a hyperbolic saddle in phase space. Put $q = \pi + s$ with small s; the energy near the saddle is $H \simeq E_s + p^2/(2I) - I\omega_0^2 s^2/2$. For an orbit at $E_s - \Delta E$, the time spent in a fixed small neighbourhood includes an integral proportional to $\int ds / \sqrt{s^2 - 2\Delta E/(I\omega_0^2)}$. As ΔE decreases, this develops a logarithm. Equivalently $\mathsf{K}(k) \sim \ln[4/\sqrt{1-k^2}]$ as $k \to 1^-$. The separatrix encloses finite canonical area but its period is infinite. Hence $\partial_E J$ diverges although J itself remains finite.

On the positive rotation branch $E > E_s$, set $k_r = \sqrt{E_s/E} < 1$. A period is the time for q to increase through 2π, so there is only one positive branch of momentum in its action integral. Direct integration gives

$$J_{\mathrm{rot}} = (2/\pi)\sqrt{2IE}\,\mathsf{E}(k_r),$$

$$T_{\mathrm{rot}} = 4\sqrt{I/(2E)}\,\mathsf{K}(k_r).$$

At very high energy, the potential is a small modulation and these formulas approach free-rotor values $\sqrt{2IE}$ and $2\pi\sqrt{I/(2E)}$. At the separatrix the positive rotation action approaches $4I\omega_0/\pi$, half the limiting libration action $8I\omega_0/\pi$. The two actions count different closed paths on a cylinder. The factor two is a topological change in the cycle, not a discontinuous jump in the mechanical momentum at a point.

Test slow conservation against the actual orbit period

To treat slowly varying parameters, define instantaneous action–angle coordinates for each fixed λ. The generating function $W(q, J, \lambda)$ acquires explicit time dependence when $\lambda = \lambda(t)$, adding $\dot{\lambda}\,\partial_\lambda W$ to the transformed Hamiltonian. Its angle dependence produces an oscillating $\dot{J} = -\dot{\lambda}\,\partial_\theta \partial_\lambda W$. On a regular periodic orbit, the integral of an angle derivative over a cycle vanishes. If λ changes little during that cycle and there is no resonant complication, this cancellation explains why the action changes little on average. The requirement uses the actual orbit period at the chosen energy. Near a separatrix it cannot be justified merely by comparing a drive rate to the small-amplitude period.

Consider a parameter ramp lasting $20\,\mathrm{s}$ for the one-metre pendulum. Near the bottom this covers about ten periods. For $1 - E/E_s = 10^{-6}$, the asymptotic $\mathsf{K} \simeq \ln 4000 = 8.29$ gives a period of approximately $10.6\,\mathrm{s}$, so the same ramp spans less than two cycles. Even longer ramps fail the scale separation sufficiently close to the saddle. If a varying parameter changes the separatrix area until it meets the trajectory, continued use of a single analytic action branch is especially unreliable. A trajectory can pass into circulation or return to libration depending on its phase and the ramp history.

Compute an action without measuring momentum continuously

Suppose a camera tracks one-dimensional positions over one full cycle, and velocity estimates are noisy. For a known position-dependent potential and calibrated mass, an independent measurement of the turning energy allows phase-area integration without differentiating the camera trace. On a bound orbit $p_\pm(q) = \pm\sqrt{2m[E - V(q)]}$, so $J = \pi^{-1}\int_{q_-}^{q_+} \sqrt{2m[E - V(q)]}\,dq$. One needs a potential calibration, both turning positions and a common energy datum. An additive constant in the potential cancels when E is shifted by the same amount. An unrecognised dissipative force makes the inward and outward energy profiles different and invalidates the assumed single closed energy curve.

Take a particle in the potential $V(q) = a|q|$, $a > 0$, which can approximate opposed constant restoring forces away from a narrow central smoothing zone. Its turning displacements are $\pm E/a$. Integrate on the positive half and use symmetry to find

$$J = 4\sqrt{2m}E^{3/2}/(3\pi a).$$

Differentiating gives

$$T = 2\pi\,dJ/dE = 4\sqrt{2mE}/a.$$

The same period follows by constant acceleration: starting at rest at a positive turning point, the fall to the origin takes $\sqrt{2mE}/a$, one quarter period. Agreement across a nondifferentiable potential cusp is a useful check that the action calculation handles the turning boundaries rather than requiring sinusoidal motion.

For $m = 0.10\,\mathrm{kg}$, $a = 2.0\,\mathrm{N}$, and $E = 0.20\,\mathrm{J}$, the amplitude is $0.10\,\mathrm{m}$, action is $0.00849\,\mathrm{J\,s}$, and period is $0.400\,\mathrm{s}$. If the restoring strength a doubles slowly at fixed action, $E \propto a^{2/3}$ increases by $2^{2/3} = 1.59$, while the turning amplitude shrinks by $2^{-1/3} = 0.794$. A harmonic-oscillator action rule $J = E/\omega$ using

a single measured frequency would be incorrect here: the actual $E/\omega = ET/(2\pi)$ exceeds the action by a factor $3/2$. The equality found for a harmonic oscillator follows from its linear energy–action relation and need not generalise.

Separate the angle accumulated during a cycle from the action it encloses

In a slowly modulated oscillator an almost constant action can coexist with a measurable phase error. Consider $\ddot{q} + \omega(t)^2 q = 0$ with smooth positive ω. An approximate oscillation is $q = A(t)\cos\Phi(t)$. At leading order $\dot{\Phi} = \omega$. Cancelling the first-order sine term gives $2\dot{A}\omega + A\dot{\omega} = 0$, so $A\sqrt{\omega}$ is approximately constant. The amplitude law reproduces conservation of E/ω after averaging. The accumulated phase is $\int \omega(t)\,dt$, which can change by many radians during a slow parameter cycle even if the initial and final frequency and action agree.

For $\omega(t) = 10[1 + 0.10\sin(2\pi t/T_r)]\,\mathrm{s}^{-1}$ and $T_r = 20\,\mathrm{s}$, integration over one full ramp gives $200\,\mathrm{rad}$ of leading phase. The largest value of $|\dot{\omega}|/\omega^2$ is only a few 10^{-3}. To first order the final amplitude returns to its initial value, but the position at the end is set by a phase that is generally not an integer multiple of 2π. A calculation that expects to return to its initial point after the parameter cycle confuses action invariance with angle closure. A small constant frequency calibration error, integrated over a long ramp, can dominate the final phase error while producing little amplitude error.

A sudden frequency switch gives an instructive opposite limit with exact phase dependence. At fixed q, p, changing ω_1 instantly to ω_2 changes the action to $J_2 = p^2/(2m\omega_2) + m\omega_2 q^2/2$. Write the initial state at action J_1 using the harmonic angle. Then

$$J_2/J_1 = (\omega_1/\omega_2)\cos^2\theta + (\omega_2/\omega_1)\sin^2\theta.$$

For a frequency doubling, the ratio ranges from one half at a passage through the centre to two at a turning point. For a uniformly sampled ensemble the average ratio is 1.25, although the pre-switch and post-switch Hamiltonians are both perfectly integrable.

An experiment can therefore test slowness by preparing the same initial action at different phases and comparing the distribution of final actions. A broad phase-dependent distribution for a rapid switch narrows as the ramp becomes slow on a regular family of tori. Near a separatrix a slow external ramp can still yield a broad distribution because the orbital clock itself stalls. The size of the instantaneous energy, measured without phase and the final Hamiltonian, does not distinguish these mechanisms.

Resolve a separatrix in time without integrating arbitrarily close to the saddle

At exactly E_s, energy conservation gives $p = \pm 2I\omega_0\cos(q/2)$ on $-\pi < q < \pi$. Choose the increasing branch passing through $q = 0$ at $t = 0$. Separation of variables in $\dot{q} = 2\omega_0\cos(q/2)$ gives

$$\tan(\pi/4 + q/4) = e^{\omega_0 t}.$$

Therefore $q(t) = 4\arctan(e^{\omega_0 t}) - \pi$,

$$p(t) = 2I\omega_0 \operatorname{sech}(\omega_0 t).$$

This exact orbit approaches the upright saddle exponentially at both infinite endpoints. The two endpoints represent the same physical angle on the cylinder even though they differ by 2π on an unwrapped plot.

The separatrix momentum falls to one tenth of its maximum after $\omega_0 t = \operatorname{arcosh} 10 \approx 2.993$. At $\omega_0 = 3.13\,\mathrm{s^{-1}}$ that takes only $0.956\,\mathrm{s}$. Reaching one hundredth takes $\operatorname{arcosh} 100/\omega_0 \approx 1.69\,\mathrm{s}$. The logarithmic increase in time per retained significant digit explains why an apparently captured upright state can simply be a trajectory very close to the saddle. Measuring angular velocity as well as angular displacement makes the exponential approach easier to distinguish from a truly stationary upright solution.

The phase area enclosed by both separatrix branches can also be recovered directly. Integrating their difference gives

$$\int_{-\pi}^{\pi} 4I\omega_0 \cos(q/2)\,dq = 16I\omega_0.$$

Dividing by 2π yields the libration limit $8I\omega_0/\pi$ obtained using elliptic integrals. By contrast a trajectory winding once on the upper branch integrates only the upper momentum, giving half that value. Testing these two integrals on an unwrapped numerical phase trace can reveal a missing lower turning branch or a routine that silently wraps the angle before accumulating $p\,dq$.

Find a frequency directly from noisy orbital areas

Suppose a calibrated experiment measures the phase areas $A(E) = \oint p\,dq$ at several energies. With $J = A/(2\pi)$, the identity $dA/dE = T$ says that an area-versus-energy slope directly has units of time. Take three close energies $0.09, 0.10, 0.11\,\mathrm{J}$, with measured areas $0.180, 0.202, 0.225\,\mathrm{J\,s}$. A central difference gives $T \simeq (0.225 - 0.180)/0.020 = 2.25\,\mathrm{s}$ at the centre. If each area has an independent uncertainty $0.001\,\mathrm{J\,s}$, the propagated standard uncertainty of that difference is about $0.071\,\mathrm{s}$, before accounting for energy uncertainty and curvature of $A(E)$.

Decreasing the energy spacing would reduce smooth finite-difference bias but amplify the effect of those same area errors. A local fit over several energies can trade variance against the assumption of a smooth slope. Near a separatrix the actual slope varies rapidly, so a wide polynomial fit may smooth away precisely the period increase being sought. Compare with direct return times at selected energies, or fit the logarithmic form justified by the saddle expansion when the orbit is demonstrably in its asymptotic regime. A measured phase area can be highly accurate while an inferred frequency remains poorly constrained because it is a derivative.

A practical area estimate from ordered camera samples uses the polygon formula $\tfrac{1}{2}\sum_i (p_i + p_{i+1})(q_{i+1} - q_i)$, including the return to the initial point with a consistent sign. Very long time sampling can overrepresent the slow turn neighbourhood but need not corrupt a properly oriented

geometric line integral. It can make a uniform-clock finite difference of velocity near a turnaround noisy, however. If a dataset includes several cycles with dissipation, do not simply close the final state back to the beginning of the first cycle. Find individual return events, estimate the action per cycle and test whether its change is consistent with measured losses.

Construct the canonical angle on two sides of a turning point

For a bound one-dimensional potential take a reference crossing at the lower turning point and choose the increasing-q branch. A Hamilton–Jacobi generating integral is

$$W(q, J) = \int_{q_-}^{q} p(q', E(J))\, dq'.$$

Its angle is $\theta = \partial_J W = (dE/dJ) \int_{q_-}^{q} dq'/\dot{q}' = \omega t_{\mathrm{flight}}$ on that branch. At the upper turning point $\theta = \pi$ for a time-reversal-invariant kinetic-plus-potential Hamiltonian. On the return branch the same coordinate q must be assigned the complementary angle $2\pi - \theta_{\mathrm{outgoing}}(q)$, because its momentum has opposite sign. The coordinate alone is insufficient to reconstruct a unique phase.

For a harmonic oscillator beginning at its leftmost position a quarter-amplitude point is crossed at two different times. In coordinates $q = -A\cos\theta$ take $q = -A/2$. The increasing branch gives

$$\theta = \pi/3;$$

the returning branch gives $5\pi/3$. Their velocities have opposite signs. Using the principal arccosine for every time sample forces both branches onto the same interval and makes an apparently discontinuous phase that never completes a cycle. Measuring the sign of velocity or interpolating successive turning events restores the appropriate branch. Near a saddle, tiny velocities make this branch identification particularly sensitive to camera noise.

Once a reliable angle is available, the phase deviation from the uniform prediction $\theta(t_0) + \omega(t - t_0)$ becomes a useful diagnostic. A static potential with a wrongly calibrated shape can cause a phase error periodic in position even when its return time is fitted correctly. Dissipation usually changes the action as well, while a constant clock error causes a steadily accumulating phase drift. Compare the residual over several cycles at different amplitudes and plot it against reconstructed angle as well as laboratory time. These alternate plots test different physical explanations of the same timing mismatch.

Measure the area of a closed orbit

Inspect how deformation of a potential changes an energy contour. Compute its action before using it to infer an adiabatic frequency.

Open this experiment online

Try the calculation

Final to initial force ratio 2

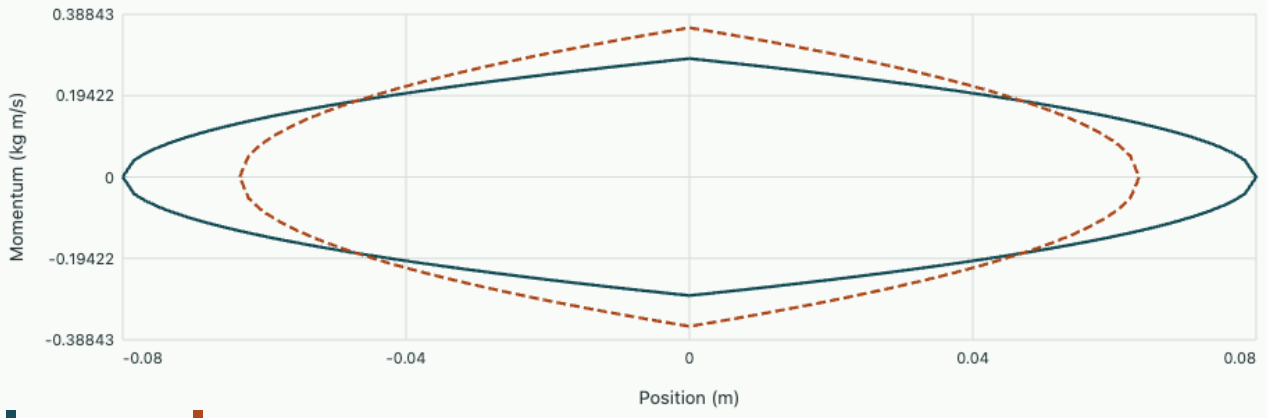

Final amplitude 0.0635 m, energy 0.254 J and period 0.3564 s.

Separate a true separatrix crossing from a change of angle convention

Imagine slowly reducing the pendulum's gravitational strength while a bob initially librates. The separatrix action $J_s = 8I\omega_0/\pi$ decreases with ω_0. Away from the crossing the orbit approximately maintains its own action, so its energy as a fraction of the instantaneous barrier rises. When the shrinking separatrix action reaches that of the orbit, no closed librating torus of that action remains. The system can enter one of the two circulation branches. Its action convention changes because the relevant closed curve on the cylinder now winds rather than traversing two momentum branches. An apparent numerical factor-of-two jump caused by this convention is distinct from the actual dynamics through the slow saddle neighbourhood.

For an initial libration action equal to 0.40 of the original separatrix action at fixed I, a parameter protocol reducing ω_0 to half its original value leaves J/J_s about 0.80, assuming adiabatic tracking remains valid. Reducing it to 0.30 of the initial value would formally give $J/J_s = 1.33$, impossible for a libration. The naive crossing estimate is $\omega_0 = 0.40\omega_{0,\mathrm{initial}}$, but the timing and selected rotation direction require integrating the actual trajectory near the saddle; the adiabatic argument loses uniform accuracy there. A local measure of p and unwrapped q supplies the physical distinction.

A real parameter protocol must specify how gravity strength changes. A pendulum length ramp changes both $I = ml^2$ and $\omega_0 = \sqrt{g/l}$, so its separatrix area scales as $I\omega_0 = m\sqrt{g}\,l^{3/2}$. Reducing length to 0.64 of its starting value reduces the separatrix action by $0.64^{3/2} = 0.512$, whereas replacing only ω_0 in a fixed-I model would predict the opposite trend. A literal change of length also brings radial kinetic energy and actuator work, as derived for the reelled pendulum. Specify the physical control path in parameter space before applying a numerical action law.

An unwrapped angle increases by 2π over a recorded interval but the phase portrait seems to contain a bounded loop. Can both observations be trusted simultaneously?

▼ **Work through the solution**

A true circulation winds around the cylindrical phase space, whereas a libration has zero net unwrapped displacement after a full return. A plot that wraps angles into a fixed interval and draws a line across its boundary can display an artificial closing segment. Conversely, measurement noise near $\pm\pi$ can make a naive unwrapping code insert a spurious 2π jump. Inspect signed momentum and the time-resolved crossing of the angle boundary, then reconstruct the loop in adjacent copies of the coordinate interval. Explicitly identifying the cycle on which the action was integrated resolves the apparent contradiction.

Infer work during an adiabatic change from a phase average

Differentiate the action integral at fixed energy with respect to the external parameter λ. The energy relation gives $\partial_\lambda p|_{E,q} = -H_\lambda/H_p$, so $J_\lambda|_E = -(2\pi)^{-1}\oint H_\lambda\,dt$. Combine this with $J_E = T/(2\pi)$ and differentiate at fixed J. The result is

$$\partial_\lambda E|_J = \langle \partial_\lambda H \rangle_{\mathrm{time}}.$$

A slowly changed parameter therefore does net reversible work at the orbit-averaged rate dictated by its conjugate generalised force. The average must weight time, not distance along the plotted phase curve.

For a harmonic spring with stiffness k, $H_k = q^2/2$ and $\langle q^2\rangle = A^2/2 = E/k$, giving $\partial_k E|_J = E/(2k)$. Integrating yields $E \propto \sqrt{k}$, consistent with $J = E/\omega$. A 4% slow stiffness increase raises energy by about 1.98% exactly under this law. Changing stiffness at a single turning point would instead add 4% to the energy for that sudden change. The difference quantifies why observing only identical start and end stiffnesses does not identify the work protocol.

Tutorial on interpreting an action experiment

A harmonic oscillator has energy $0.030\,\mathrm{J}$ and frequency $5.0\,\mathrm{Hz}$. Its stiffness is increased slowly until the frequency doubles. Determine action, final energy and relative amplitude.

▼ **Work through the solution**

The action is

$$0.030/(2\pi\cdot 5.0) = 9.55\times10^{-4}\,\mathrm{J\,s}.$$

Approximately constant action gives a final energy of $0.060\,\mathrm{J}$. With fixed mass and $E = m\omega^2A^2/2$, the final amplitude is $1/\sqrt{2}$ times its initial value. A sudden change performed at a particular phase would in general give a different final action.

A simulation estimates pendulum periods by differentiating sampled action values on a coarse uniform energy grid. Why is the last estimated period below the separatrix likely to be inaccurate even if the individual areas are well converged?

▼ **Work through the solution**

A finite difference averages $dJ/dE = T/(2\pi)$ over a finite energy interval. The derivative rises logarithmically near the saddle, so the average can underestimate its endpoint value markedly. Refine adaptively in the distance to E_s, use the elliptic quadrature or measure return times directly. The numerical integrator must also locate the long dwell near the unstable equilibrium without stepping across it artificially.

Two trajectories have energy $E_s + \delta$, one rotating clockwise and one anticlockwise. Can energy and the positive magnitude of rotation action distinguish them?

▼ **Work through the solution**

Both have the same speed at each angle and the same positive action magnitude and period. The sign of momentum or a signed orientation of the fundamental rotational cycle distinguishes the branches. Near the separatrix a numerical classifier looking only at energy and unsigned area can lose track of this information. Count the unwrapped angular change and inspect the sign of p to identify circulation direction.

Measure phase area and compare its change under a parameter ramp.

David Tong develops action–angle variables and adiabatic invariance.

Analytical mechanics from constraints to invariants · 10. Canonical perturbations, small denominators and resonant capture

A weak periodic force can produce a bounded ripple on most trajectories and a large change on a narrow band of initial conditions. Derive the averaging transformation away from resonance, construct the slow resonant dynamics where that transformation fails, and estimate the physically observable width and time scale of a resonance.

Separate the unperturbed clock from a weak correction

Take an integrable Hamiltonian $H(I,\theta,t)=H_0(I)+\epsilon H_1(I,\theta,t)$ in action–angle variables. With $\epsilon=0$, actions are constants and angles advance at $\boldsymbol{\omega}(I)=\partial_I H_0$. A perturbation with Fourier component $h_{\mathbf{n}}(I)\cos(\mathbf{n}\cdot\theta-\Omega t)$ drives action changes proportional to its sine. If the phase sweeps quickly through all angles, positive and negative contributions largely cancel. If $\mathbf{n}\cdot\boldsymbol{\omega}-\Omega$ is small, the perturbation acts with a coherent sign over a long time. We want a transformation that makes both statements quantitative.

Use a near-identity type-two generating function $F_2(\theta,J,t)=\theta\cdot J+\epsilon S_1(\theta,J,t)$. Old actions are $I=J+\epsilon\partial_\theta S_1$, and new angles are $\psi=\theta+\epsilon\partial_J S_1$. Expand $H_0(I)=H_0(J)+\epsilon\boldsymbol{\omega}(J)\cdot\partial_\theta S_1+O(\epsilon^2)$. At first order the new Hamiltonian is $K=H_0(J)+\epsilon[H_1+\partial_t S_1+\boldsymbol{\omega}\cdot\partial_\theta S_1]$. Replacing old by new angles inside that bracket produces only higher-order errors. To leave the averaged part $\langle H_1\rangle$, solve the homological equation

$$(\partial_t+\boldsymbol{\omega}\cdot\partial_\theta)S_1=-\big(H_1-\langle H_1\rangle\big).$$

For an oscillating cosine with detuning $\Delta=\mathbf{n}\cdot\boldsymbol{\omega}-\Omega$, choose $S_1=-h_{\mathbf{n}}\sin(\mathbf{n}\cdot\theta-\Omega t)/\Delta$. The transformation is useful while the resulting action displacement $\epsilon|\partial_\theta S_1|$ is small on the relevant action scale and the derivatives entering the angle transformation remain controlled. Small ϵ alone is insufficient if Δ is even smaller. A singular denominator says that this choice to remove the harmonic is unsuitable, not that the underlying mechanical force becomes infinite.

Obtain a nonlinear frequency shift from the angle average

A free oscillator with mass m, small-amplitude frequency ω_0, and quartic correction $\beta q^4/4$ has unperturbed coordinates $q=\sqrt{2I/(m\omega_0)}\sin\theta$. Substituting gives the correction $\beta I^2\sin^4\theta/(m^2\omega_0^2)$. Since $\langle\sin^4\theta\rangle=3/8$, the first-order averaged Hamiltonian is $K=\omega_0 J+3\beta J^2/(8m^2\omega_0^2)$. Its derivative gives

$$\omega=\omega_0+3\beta J/(4m^2\omega_0^2).$$

Expressing $J\simeq m\omega_0 A^2/2$ in terms of leading oscillation amplitude yields the frequency shift $3\beta A^2/(8m\omega_0)$. Oscillatory harmonics at $2\theta,4\theta$ change the waveform but do not contribute directly to this averaged first-order clock.

For $m = 0.20\,\mathrm{kg}$, $\omega_0 = 10.0\,\mathrm{s}^{-1}$, $\beta = 80\,\mathrm{N/m^3}$, and $A = 0.10\,\mathrm{m}$, the predicted shift is $0.150\,\mathrm{s}^{-1}$, about 1.5%. The nonlinear-to-linear force ratio at maximum displacement is $\beta A^2/(m\omega_0^2) = 0.040$, consistent with the expansion. At twice the amplitude the shift quadruples and the expansion parameter grows to 0.16. Measuring period over several amplitudes and plotting the frequency against A^2 tests both the slope and the onset of curvature from higher orders. A positive β stiffens the spring; a negative quartic term is only a local approximation unless higher powers restore global confinement.

Solve the slow motion in the resonant frame

Consider a rotor $H = I^2/(2\mathcal{I}) - \epsilon V\cos(\theta - \Omega t)$, where $\mathcal{I}$ is moment of inertia and $\epsilon V > 0$ has energy units. Choose $F_2 = (\theta - \Omega t)P$, so $P = I$,

$$\phi = \theta - \Omega t,$$

$$K = P^2/(2\mathcal{I}) - \Omega P - \epsilon V\cos\phi.$$

Completing the square gives $K = (P - P_*)^2/(2\mathcal{I}) - \epsilon V\cos\phi + \text{constant}$ with $P_* = \mathcal{I}\Omega$. This is an exact pendulum in the rotating frame. It retains the resonant cosine instead of attempting to average it away. Phase locking means libration of ϕ around zero; outside its separatrix the relative phase circulates.

The stable fixed point has $P = P_*, \phi = 0$; its small libration frequency is

$$\omega_{\mathrm{lib}} = \sqrt{\epsilon V/\mathcal{I}}.$$

The saddle at $\phi = \pi$ has energy $+\epsilon V$ relative to the same constant. At $\phi = 0$ that energy is reached for $|P - P_*| = 2\sqrt{\mathcal{I}\epsilon V}$, the resonance half-width in action. Its complete width is twice that number. For $\mathcal{I} = 0.050\,\mathrm{kg\,m^2}$, $\Omega = 8.0\,\mathrm{s}^{-1}$ and $\epsilon V = 0.0020\,\mathrm{J}$, the central action is $0.40\,\mathrm{kg\,m^2/s}$; the half-width is $0.020\,\mathrm{kg\,m^2/s}$ and small libration period $31.4\,\mathrm{s}$. The rotor makes many laboratory turns while its slow relative phase completes one libration.

An initial action inside the quoted half-width is necessary but not sufficient for trapping at every phase. At $\phi = \pi$, any nonzero $P - P_*$ is above the saddle energy. Compute the actual rotating-frame energy of the initial state and compare with the saddle. For $\phi = 0, P = 0.415$, the kinetic detuning energy is $0.00225\,\mathrm{J}$; subtracting $0.0020\,\mathrm{J}$ gives $0.00025\,\mathrm{J}$, below the saddle. With the same action at $\phi = \pi$ the value is $0.00425\,\mathrm{J}$, above the saddle. Selecting trajectories by mean frequency alone can therefore mix trapped and circulating populations.

Retain a resonant harmonic in a general integrable system

For one action with $H_0'(I_*) = \Omega$, use the rotating frame and expand $H_0(I) - \Omega I$ about I_*. The linear term vanishes, leaving $H_0''(I_*)(I - I_*)^2/2$. Retain the slowly varying resonant cosine and average the rapidly varying harmonics. When $H_0'' \neq 0$, this gives the same pendulum normal form with an effective inertia and possibly a reversed sign of the stable phase. The action half-width scales as $2\sqrt{\epsilon|V/H_0''|}$. Thus a weak perturbation can influence a band of width proportional to $\sqrt{\epsilon}$, parametrically larger than a typical nonresonant action ripple proportional to ϵ.

For an exactly harmonic oscillator $H_0 = \omega_0 I$ the curvature vanishes. One cannot replace H_0'' with zero in the width formula. An exactly tuned additive drive in a linear oscillator instead produces secular growth until damping, detuning, nonlinearity or a finite drive interval intervenes. In multiple actions, one first transforms to the resonant phase $\mathbf{n}\cdot\theta - \Omega t$ and complementary angles, preserving the canonical one-form. Other near-resonances can prevent isolation of a single pendulum. Apparent chaos inferred from a short irregular time trace alone needs additional tests, including resolved phase portraits, convergence under time refinement and identification of competing resonances.

Calculate a phase-locking threshold for a drive that sweeps in frequency

The exact rotating rotor also allows a tractable time-dependent drive frequency. Write the pattern angle as $\alpha(t)$, with $\Omega(t) = \dot{\alpha}$. In its frame $K = P^2/(2\mathcal{I}) - \Omega(t)P - \epsilon V\cos\phi$. Hamilton's equations give

$$\dot{\phi} = P/\mathcal{I} - \Omega(t),$$

$$\dot{P} = -\epsilon V \sin\phi.$$

Define the detuning momentum $p = P - \mathcal{I}\Omega(t)$. Even when $\dot{\phi} = 0$ at one instant, phase locking throughout a ramp requires $\dot{p} = 0$ and hence $\sin\phi_0 = -\mathcal{I}\dot{\Omega}/(\epsilon V)$. The restoring torque must be sufficient to accelerate the rotor along with the changing pattern.

For constant $\dot{\Omega}$ and $|\mathcal{I}\dot{\Omega}| < \epsilon V$, a stable locked phase with $\cos\phi_0 > 0$ exists. Perturbing the phase by η gives $\ddot{\eta} + (\epsilon V/\mathcal{I})\cos\phi_0\,\eta = 0$, so the libration softens as the required torque approaches its maximum. At threshold the stable and unstable stationary phases meet. Above it no fixed phase can provide the torque needed by the ramp. The mere existence of a stable locked solution still does not imply that an arbitrary initial phase and momentum will be captured in it. In a conservative system initial phase-space location and separatrix crossing are essential.

With the previous $\mathcal{I} = 0.050\,\mathrm{kg\,m^2}$ and $\epsilon V = 0.0020\,\mathrm{J}$, the largest trackable constant acceleration in this model is $0.040\,\mathrm{rad/s^2}$. At half that value the stable phase lags by $\pi/6$, and the small relative-phase frequency is

$$0.20\sqrt{\cos(\pi/6)} = 0.186\,\mathrm{s^{-1}}.$$

Increasing the drive frequency by $1.0\,\mathrm{rad/s}$ at this rate takes $50\,\mathrm{s}$, only about one and a half libration periods. Adiabatic capture estimates that additionally require many libration periods may therefore be unconvincing even though the elementary torque threshold is satisfied. A measured lag versus sweep rate assesses the static torque condition, while a full phase trajectory tests dynamic capture.

The same equations admit a tilted effective washboard potential in the accelerating frame, $U_{\mathrm{rel}} = -\epsilon V\cos\phi + \mathcal{I}\dot{\Omega}\,\phi$, as long as $\dot{\Omega}$ is constant. Its potential difference over a whole 2π turn is nonzero, so unwrap the relative phase before using its energy. Mapping every phase back to $[-\pi, \pi)$ hides this difference and produces artificial jumps in the inferred energy. In the original variables the

physical motor does work. There is no contradiction between a conserved local accelerating-frame energy for a constant ramp and the changing laboratory kinetic energy of a locked rotor.

Derive secular energy exchange in a pair of weakly coupled oscillators

Take two equal masses m with individual natural frequency ω_0 and potential coupling $k_c(q_1 - q_2)^2/2$. The normal coordinates $Q_\pm = (q_1 \pm q_2)/\sqrt{2}$ have frequencies $\omega_+ = \omega_0$,

$$\omega_- = \sqrt{\omega_0^2 + 2k_c/m}.$$

Release mass one at displacement A with both velocities and q_2 initially zero. Superposition gives

$$q_1 = A[\cos\omega_+ t + \cos\omega_- t]/2,$$
$$q_2 = A[\cos\omega_+ t - \cos\omega_- t]/2.$$

The slowly varying difference phase transfers oscillation amplitude between the masses over a time much longer than their rapid periods.

For $\omega_0 = 10\,\mathrm{s}^{-1}$ and $k_c/m = 1.0\,\mathrm{s}^{-2}$, the exact separation is

$$\sqrt{102} - 10 = 0.0995\,\mathrm{s}^{-1}.$$

The first near-complete exchange occurs at $t = \pi/|\omega_- - \omega_+| \approx 31.6\,\mathrm{s}$. Over a single fast period the displacements can look almost like uncoupled oscillations, despite large later energy redistribution. Perturbing two isolated oscillators while trying to average the coupling over both independent fast angles would discard a term depending on their slow difference phase. Retaining the resonant combination predicts the exchange; diagonalising the linear model supplies a reference solution for that approximation.

Detune the uncoupled springs so their natural frequencies have a separation large compared with $k_c/(m\omega_0)$. The coupled normal modes then align more closely with the original oscillators, and the energy exchange cannot reach its former depth. In a nonlinear problem the individual frequencies also depend on action, so the energy transfer can detune itself. To interpret an observed beating envelope, measure both normal frequencies and relative phases. An apparent loss of amplitude in oscillator one can be energy stored in oscillator two, distinguishable from damping through recovery at later times and a balance of the total Hamiltonian.

Estimate the accuracy of averaging over a finite observation time

For a nonresonant perturbation with initially slow action change, one can integrate the first-order drive along the unperturbed trajectory over the actual observation window instead of assuming an infinite-time average. For $H_1 = A\cos(\theta - \Omega t)$, $\dot{I} = A\sin(\Delta t + \phi_0)$ to leading order with $\Delta = \omega_0 - \Omega$. Thus $\Delta I(T) = A[\cos\phi_0 - \cos(\Delta T + \phi_0)]/\Delta$. For $\Delta \neq 0$ its absolute value remains at most $2|A/\Delta|$, and

its largest possible value over initial phase is $2|A\sin(\Delta T/2)/\Delta|$. For $\Delta \to 0$ the phase-dependent result tends to $AT\sin\phi_0$. The finite-time expression is regular right at resonance and shows exactly when a secular term emerges.

For $A = 0.001\,\mathrm{J}$, $T = 10\,\mathrm{s}$ and $\Delta = 0.20\,\mathrm{s}^{-1}$, the maximum-amplitude change in action over initial phase is $0.00841\,\mathrm{J\,s}$. At zero detuning the leading largest change is $0.0100\,\mathrm{J\,s}$, only modestly larger because this observation window resolves a frequency band of order $1/T$. For $\Delta = 2\pi/T$ the change after exactly T vanishes, although the action swung during the interval. A final-minus-initial measurement alone can mistake a completed nonresonant excursion for an entirely unperturbed trajectory. Recording at an additional end time tests that cancellation.

At leading order a force of finite duration produces this sine-over-detuning envelope even in a linear system. It is an observation-time bandwidth, distinct from the dynamical resonance width proportional to $\sqrt{\epsilon}$ in the nonlinear rotor. Repeat the experiment with doubled drive duration at fixed amplitude. Features that narrow inversely with the duration are evidence of finite-time spectral selection. A persistent bounded island in a stroboscopic phase portrait, with the predicted amplitude-dependent width and libration frequency, is evidence of the phase-locking dynamics. If drive amplitude is large enough to change the natural frequency appreciably over the interval, the unperturbed phase-integration formula ceases to describe the trajectory.

Construct a stroboscopic section with the right clock

For a time-periodic Hamiltonian sample (I, θ) every period of the external drive at a fixed drive phase. This creates a two-dimensional area-preserving map for one periodically forced degree of freedom. A phase-locked solution can become a fixed point of this map, and librating trajectories around it can form an island. Sampling at each crossing of a moving coordinate threshold instead can produce a different return map and a different phase weight. A return plot can look irregular simply because the drive phase was not held fixed at the samples.

Consider a rigid rotor commanded at $\Omega = 8\,\mathrm{s}^{-1}$. Its drive period is

$$2\pi/8 = 0.7854\,\mathrm{s}.$$

An acquisition system sampling nominally every $0.7900\,\mathrm{s}$ accumulates approximately $8(0.7900 - 0.7854) = 0.0368\,\mathrm{rad}$ of phase error per sample. After one hundred samples the sampling phase has moved about $3.68\,\mathrm{rad}$, enough to smear a narrow island across a substantial fraction of the plot. Interpolating trajectories to timestamps from a synchronised drive encoder controls that effect. Keep unwrapped relative phase as a separate channel to count actual slips.

A numerical area test on the stroboscopic map should use canonical action and angle or an equivalent canonical coordinate pair. A scatter plot of polar angle against angular velocity for a state-dependent inertia can distort area. Changes of pixel density, trajectory dwell time and resolution near the separatrix further affect visual appearance. To identify a resonance quantitatively, measure the action extent at the stable phase, the local libration period and the saddle crossing energy on independently prepared trajectories. Agreement among those three observations is less easily mimicked by a sampling artefact than the existence of a visually closed loop alone.

Recover a frequency shift by removing a secular term

Canonical averaging yields a frequency correction for the quartic oscillator. An independent derivation makes clear why a small difference in frequency can become a large trajectory error at long times. Write the equation as $\ddot{q} + \omega_0^2 q + (\beta/m) q^3 = 0$. Put $q = A x$, $\tau = \omega t$, $\lambda = \beta A^2/(m\omega_0^2)$ and seek $\omega = \omega_0(1 + c\lambda + \cdots)$,

$$x = x_0 + \lambda x_1 + \cdots .$$

Leading initial conditions $x(0) = 1, x'(0) = 0$ give

$$x_0 = \cos\tau .$$

At first order one finds

$$x_1'' + x_1 = 2c\cos\tau - \cos^3\tau .$$

Using $\cos^3\tau = (3\cos\tau + \cos 3\tau)/4$, the right-hand side contains a term $(2c - 3/4)\cos\tau$ resonant with the leading motion. Choosing $c = 3/8$ removes the forcing that would otherwise generate a term proportional to $\tau\sin\tau$. The frequency then agrees with the action-angle calculation. The remaining particular solution is $\cos 3\tau/32$. Including the homogeneous term required by $x_1(0) = x_1'(0) = 0$ gives

$$x_1 = (\cos 3\tau - \cos\tau)/32 .$$

This separates the leading frequency shift from an actual third-harmonic distortion of the orbit. Fitting only frequency and overlooking the small third harmonic cannot generally reproduce a precise waveform.

In the earlier example $\lambda = 0.040$, so the displacement amplitude at the third harmonic is $A\lambda/32 = 0.125\,\mathrm{mm}$ at $A = 0.10\,\mathrm{m}$. The frequency shift is about $0.15\,\mathrm{s}^{-1}$. After twenty seconds the uncorrected harmonic prediction is nearly three radians out of phase, far larger than the instantaneous third-harmonic displacement. A small-amplitude correction to the right-hand side can therefore cause an order-one error in the long-time phase. Measuring both the third harmonic and frequency gives two independent checks of the same inferred quartic stiffness. A drive electronics harmonic can mimic the former without producing the amplitude-dependent free-oscillation frequency.

Inspect growth on a parametrically driven orbit

Move the drive away from resonance and examine stroboscopic growth. Determine whether changing phase, amplitude or forcing frequency is responsible.

Open this experiment online

Try the calculation

Fractional stiffness modulation	0.08
Damping γ (1/s)	0.1
Drive frequency Ω (rad/s)	20

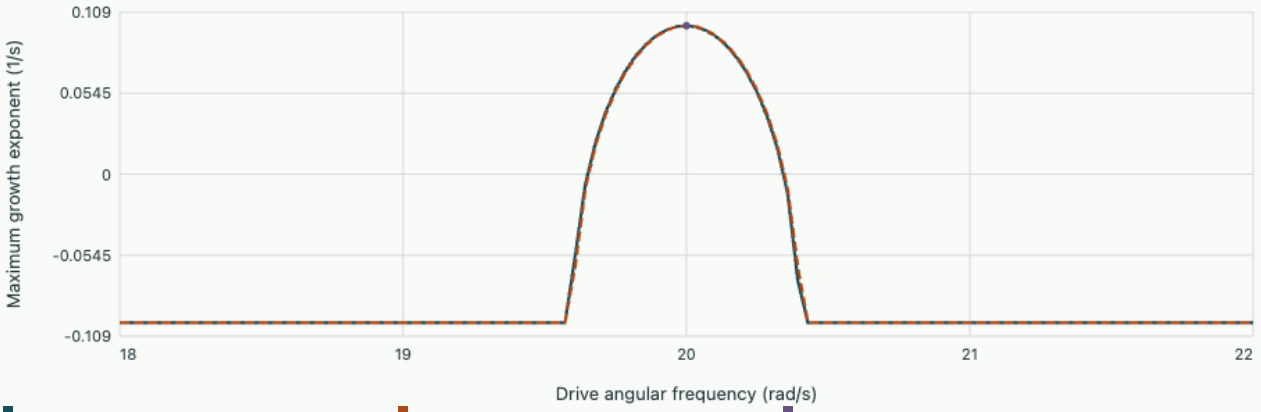

One-period numerical map Weak-modulation average Selected exponent

At Ω = 20 rad/s, numerical exponent 0.09997 s⁻¹ and averaged exponent 0.1 s⁻¹. Amplitude doubling time 6.934 s.

Test overlap of nearby resonances without declaring chaos from one curve

Take a rotor driven by two weak periodic patterns with distinct angular speeds Ω_1, Ω_2. For an isolated pattern j, the earlier calculation gives a resonant centre $P_j = \mathcal{I}\Omega_j$ and half-width $\Delta P_j = 2\sqrt{\mathcal{I}\epsilon V_j}$. Comparing the sum of estimated half-widths with the separation $|P_2 - P_1|$ is a practical indication of when the isolated-island approximation may fail. It does not by itself prove every trajectory between the resonances is chaotic. The relative phases, other harmonics and the actual time dependence determine the global structure.

For the same inertia $0.050\,\mathrm{kg\,m^2}$, choose $\Omega_1 = 8.0\,\mathrm{s^{-1}}$, $\Omega_2 = 8.6\,\mathrm{s^{-1}}$, and forcing energies 0.0020 and $0.00050\,\mathrm{J}$. The centres differ by $0.030\,\mathrm{kg\,m^2/s}$; the individual half-widths are 0.020 and $0.010\,\mathrm{kg\,m^2/s}$. Their nominal intervals just touch. Halving both forcing energies shrinks both widths by $1/\sqrt{2}$, leaving a gap. Doubling both makes the estimated intervals overlap. The speed difference corresponds to a beat period $2\pi/0.6 = 10.47\,\mathrm{s}$, another clock that must be resolved when recording nearby motion.

Transforming into the first rotating frame makes the first perturbation stationary and leaves the second with time dependence proportional to $\cos[\phi - (\Omega_2 - \Omega_1)t]$. A stroboscopic map sampled at the beat period is therefore more informative than a map with unsynchronised lab sampling. Prepare nearby initial conditions, compare their separation over multiple beat periods, and repeat with a refined symplectic time step and a modestly varied observation interval. Short-term stretching near an ordinary hyperbolic fixed point is possible even in a fully integrable pendulum. Evidence for widespread chaotic transport requires more than the growth of one separation during one saddle passage.

A student finds an apparent threshold by plotting whether the momentum ever crosses the midpoint between the two resonant centres. What additional evidence distinguishes irregular transport from a single large regular libration?

▼ **Work through the solution**

A regular libration may cross that midpoint repeatedly inside one island, especially near its separatrix. Plot return pairs at a fixed beat phase, check for closed invariant curves or broader area filling, and track unwrapped relative phase to see whether it slips irregularly between the two patterns. Vary initial conditions and compare the statistical trend with the isolated-width estimate. Confirm that energy balance in the driven system includes explicit work by both patterns; a drift of the autonomous single-pattern energy is expected once the second drive is present.

Use phase reversal to isolate the resonant action transfer

For an initially weak sinusoidal drive, prepare two otherwise identical trajectories with initial relative phases differing by π. Their leading changes of action during a short resonant pulse have opposite signs, since $\dot{I}$ is proportional to $\sin\phi_0$. Half the difference isolates that phase-sensitive term, whereas half the sum can reveal phase-independent heating or higher-order effects. With drive coefficient $A = 0.001\,\mathrm{J}$, duration $2.0\,\mathrm{s}$ and initial phases $\pm\pi/2$, short-pulse first-order predictions differ by $0.0040\,\mathrm{J\,s}$. The test requires that detuning and nonlinear phase drift over the pulse remain small.

Perform the comparison at several durations. A linear growth of the early phase-sensitive difference is compatible with coherent transfer. Subsequent saturation, reversal or a slow oscillation can reflect the resonant pendulum dynamics once the action shift changes the phase. Friction can also saturate a response, but it produces mechanical energy loss and typically modifies the two phase preparations in different ways from conservative trapping. Measuring work from the applied torque and the full phase history adds the independent information needed to separate those explanations. A final amplitude alone gives neither the sign of the action transfer nor its phase dependence.

Tutorial on weak forcing

Far from resonance let a one-mode perturbation be $A\cos(\theta - \Omega t)$ with $A = 0.001\,\mathrm{J}$ and detuning $0.50\,\mathrm{s^{-1}}$. What first-order ripple scale should appear in the old action?

▼ **Work through the solution**

The generating function has amplitude $A/|\Delta| = 0.002\,\mathrm{J\,s}$. For harmonic number one its angle derivative has the same amplitude, so the old action oscillates about the averaged action on that scale. At detuning $0.01\,\mathrm{s^{-1}}$ the nominal ripple would be fifty times larger. Check its size against the action scale and the change of detuning across the ripple before trusting that continuation.

In the rotor example the forcing energy is multiplied by four. What happens to the resonant action, action width and small-amplitude libration period?

▼ **Work through the solution**

The central action is set by $H_0' = \Omega$ and stays $0.40\,\mathrm{kg\,m^2/s}$. The half-width doubles to $0.040\,\mathrm{kg\,m^2/s}$. The libration frequency doubles, so the period halves to $15.7\,\mathrm{s}$. These predictions apply to the exact sinusoidal rotor model; other harmonics of a physical drive may also change as its amplitude increases.

A slowly swept drive seems to carry a phase-locked rotor beyond its original resonance band. Is this inconsistent with the static separatrix estimate?

▼ **Work through the solution**

A varying $\Omega(t)$ moves the resonance centre $\mathcal{I}\Omega(t)$. In coordinates measured from that moving centre the equation for detuning momentum has an additional torque-like term $-\mathcal{I}\dot{\Omega}$. Locking can persist if the available restoring torque can track the ramp and the initial motion stays inside the evolving island. The static width describes a fixed-frequency section. Comparing a captured trajectory to its initial centre after the sweep tests the wrong phase portrait.

Compare a resonance driven by a varying stiffness with a rotating additive potential.

David Tong's Hamiltonian course develops canonical variables and adiabatic invariants.

Analytical mechanics from constraints to invariants · 11. Action density, stress waves and the boundary that reflects them

A chain of coupled masses becomes an elastic field when the wavelength is long compared with the spacing. Derive the field equation and its boundary traction from the same variation, follow energy and stress across a junction, and decide whether a measured pulse is limited by material waves or by numerical dispersion.

Pass from a discrete rod to an action density

Let equal masses of spacing a move longitudinally by $u_j(t)$, with nearest-neighbour spring constant k_s and mass m_s per site. Their Lagrangian is $\sum_j [m_s \dot{u}_j^2/2 - k_s(u_{j+1}-u_j)^2/2]$. For variations smooth on the spacing, $(u_{j+1}-u_j)/a \to u_x$ and $\sum_j a\, f_j \to \int f(x)\,dx$. Hold the line density $\rho A = m_s/a$ and axial rigidity $EA = k_s a$ fixed. The continuum Lagrangian density per unit reference length is

$$\mathcal{L} = \rho A\, u_t^2/2 - EA\, u_x^2/2,$$

with A area, ρ volume density and E Young modulus. Both terms have units of joules per metre. This is a slender-rod model with small strain, primarily uniaxial stress and wavelengths long compared with the cross-sectional dimensions.

Vary the field in the action over $[0,L]\times[t_1,t_2]$. Integration of $\rho A\, u_t \delta u_t$ by parts in time, with fixed endpoint fields, produces $-\rho A\, u_{tt}\delta u$. Integration of $-EA u_x \delta u_x$ by parts in space produces $+\partial_x(EA u_x)\delta u$ and a remaining term $-[EA u_x \delta u]_0^L$. Thus the interior equation is $\rho A u_{tt} = \partial_x(EA u_x)$, and the end force conjugate to displacement is axial force $N = EA u_x$. Adding external work $F_L(t)\delta u(L)$ at the right face yields

$$N(L) = F_L.$$

A prescribed displacement instead imposes $\delta u(L)=0$, leaving its reaction as an output. Keeping this boundary term prevents prescribing displacement and independent traction simultaneously at the same end of a second-order rod.

Determine the energy flux and characteristic impedance

Assume time-independent coefficients. Multiply the field equation by u_t and rearrange to obtain

$$\partial_t[\rho A u_t^2/2 + EA u_x^2/2] + \partial_x[-EA u_x u_t] = 0.$$

The energy flux is $-N u_t$, with positive sign denoting energy moving towards increasing x. The minus sign follows the convention of positive tensile N: positive mechanical power entering through a right face is $N u_t$, which is inward with respect to the rod on its left. This identity controls energy transport across both smooth material changes and sharp joints.

For a homogeneous right-moving wave $u = F(x - ct)$, $c = \sqrt{E/\rho}$, particle velocity $v = u_t = -cF'$ and axial force $N = EAF' = -Zv$, where $Z = \rho A c = EA/c$. A left-moving wave has $N = +Zv$. The impedance is force divided by particle velocity and has units $\mathrm{kg/s}$. If one instead uses stress, impedance is ρc per unit area. Doubling the area of the same material keeps wave speed unchanged but doubles the force–velocity impedance. A transit-time measurement and a reflection measurement therefore provide independent material or geometry information.

For a rod with $E = 70\,\mathrm{GPa}$, $\rho = 2700\,\mathrm{kg/m^3}$ and $A = 1.0 \times 10^{-4}\,\mathrm{m^2}$, $c \approx 5092\,\mathrm{m/s}$ and $Z \approx 1375\,\mathrm{kg/s}$. A right-going compressive pulse with particle speed $0.020\,\mathrm{m/s}$ carries axial force $-27.5\,\mathrm{N}$, compressive stress $0.275\,\mathrm{MPa}$, and instantaneous power $Zv^2 = 0.550\,\mathrm{W}$ across a section. A rectangular approximation lasting $100\,\mu\mathrm{s}$ carries about $55\,\mu\mathrm{J}$ and occupies $0.509\,\mathrm{m}$. The pulse speed is kilometres per second; the material particles move only millimetres per second. Treating these as the same velocity would spoil force, impulse and energy estimates.

Match a bonded interface and distinguish amplitude from power

At a perfect massless bond displacement and axial force are continuous. For an incident right-going velocity amplitude v_i in rod 1, let v_r be reflected left-going velocity and v_t transmitted right-going velocity. Velocity continuity gives

$$v_i + v_r = v_t.$$

Force continuity gives

$$-Z_1 v_i + Z_1 v_r = -Z_2 v_t.$$

Thus

$$r_v = \frac{Z_1 - Z_2}{Z_1 + Z_2},$$

$$t_v = \frac{2Z_1}{Z_1 + Z_2},$$

$$\mathcal{R} = r_v^2,$$

$$\mathcal{T} = \frac{Z_2}{Z_1} t_v^2 = \frac{4Z_1 Z_2}{(Z_1 + Z_2)^2}.$$

The power fractions add to one for real positive impedances. The reflected force coefficient has opposite sign to the reflected velocity coefficient because the wave direction reverses. At a free end $Z_2 \to 0$, reflected velocity equals incident velocity, so end velocity doubles while total force vanishes. At a rigid end $Z_2 \to \infty$, velocity reverses and force doubles. The sign a strain gauge reports can therefore differ from that of a velocity-sensitive optical measurement at the same reflection.

A step from the worked rod into one of the same material with twice the cross-sectional area gives $Z_2 = 2Z_1$, $r_v = -1/3$, $t_v = 2/3$, and power fractions $1/9$ and $8/9$. A reduced transmitted velocity amplitude does not imply that most energy is reflected. If the interface includes a concentrated mass M_b

, force jumps instead obey $N_2 - N_1 = M_b \dot{v}_b$ with signs determined by forces exerted on that mass from either side. At high frequency the reaction of that mass can mimic a much stiffer termination. Frequency-dependent reflection is then an expected boundary effect, rather than evidence that the bulk modulus varies with frequency.

Connect continuum modes to their lattice predecessor

For a periodic chain the exact discrete equation is

$$m_s \ddot{u}_j = k_s (u_{j+1} - 2u_j + u_{j-1}).$$

Substitute $u_j = U e^{i(kja - \omega t)}$ to obtain

$$\omega = 2\sqrt{k_s/m_s}\,|\sin(ka/2)|.$$

In the first positive Brillouin zone, $\omega/(ck) = \sin(ka/2)/(ka/2)$ and group velocity $d\omega/dk = c\cos(ka/2)$, where $c = a\sqrt{k_s/m_s}$. The continuum rod retains only the leading low-ka term. A wave with eight sites per wavelength has phase speed about $0.9745c$ and group speed $0.9239c$. A narrowband packet's peak can arrive later than the continuum prediction even when a single crest is timed fairly accurately.

A finite-difference code approximating the continuum rod can produce the same spatial dispersion with its mesh spacing in place of a physical lattice spacing. Distinguish them experimentally or numerically by changing the computational mesh while holding the physical structure fixed. Lattice effects persist as the numerical grid is refined; artificial spatial dispersion diminishes. A separate time-step study is needed if a time integrator also disperses the wave. Comparing both peak arrival and phase at two frequencies tests more of the dynamics than fitting a single transit time.

Derive transverse beam waves from curvature energy

A slender beam bending laterally is governed by a different elastic energy from the axial rod. Let $w(x,t)$ denote small transverse deflection of its neutral axis. Under the Euler–Bernoulli assumption that cross sections remain plane and normal to that axis, the axial strain a distance z from the neutral axis is approximately $-z w_{xx}$. Integrating the local elastic energy $E\epsilon_{xx}^2/2$ across the section gives $EI_A w_{xx}^2/2$ per unit length, where $I_A = \int z^2\,dA$ is a geometrical second moment of area, with units m^4. It is distinct from a mass moment of inertia. The kinetic contribution uses line density ρA as before.

Varying $\mathcal{L} = \rho A w_t^2/2 - EI_A w_{xx}^2/2$ requires integrating twice by parts in space. With constant coefficients the interior variation gives

$$\rho A w_{tt} + EI_A w_{xxxx} = 0.$$

The boundary terms are $-[EI_A w_{xx}\delta w_x] + [(EI_A w_{xx})_x \delta w]$. Thus slope variations pair with bending moments and displacement variations with shear forces, with signs set by the chosen face orientation. A

clamped end prescribes both deflection and slope; a free end sets moment and shear to zero. A simply supported end prescribes deflection and zero bending moment. Using only one boundary condition per end, as for the axial rod, leaves the fourth-order beam problem underdetermined.

A sinusoid $e^{i(kx-\omega t)}$ gives

$$\omega = \sqrt{EI_A/(\rho A)}\, k^2.$$

Phase speed grows proportionally to wavenumber and group speed is twice phase speed in this model. A narrow transverse pulse in a long beam consequently spreads even in a perfectly homogeneous non-dissipative continuum. By contrast the axial rod was nondispersive in its long-wavelength continuum approximation. At high enough frequency the simple bending model omits rotary inertia, shear deformation and eventually three-dimensional elastic behaviour. Extrapolating its unbounded speed to arbitrary k would use the slender, low-frequency approximation far beyond its derivation.

For a simply supported beam with length L, the sine modes satisfy both end conditions and give

$$\omega_n = (n\pi/L)^2 \sqrt{EI_A/(\rho A)}.$$

For a rectangular section of width w_b and thickness d in the bending direction, $I_A = w_b d^3/12$ and $A = w_b d$. Doubling thickness doubles all the natural angular frequencies at fixed L, E, ρ, whereas doubling width alone leaves the ideal frequencies unchanged. The stiffness increases and so does the inertia. A beam with $L = 0.50\,\mathrm{m}$, $d = 5.0\,\mathrm{mm}$ and the earlier aluminium properties has $\sqrt{EI_A/(\rho A)} \approx 7.35\,\mathrm{m^2/s}$, giving fundamental $46.2\,\mathrm{Hz}$. The second bending mode is near four times that frequency, a clear difference from the approximately harmonic axial mode sequence.

Match a force pulse to a support spring and dashpot

A right termination exerts force on the rod through a dashpot with mechanical impedance Z_L. For a real positive dashpot impedance the reflected velocity fraction is $r = (Z - Z_L)/(Z + Z_L)$. Taking $Z_L = Z$ gives zero reflection at the termination even though energy leaves a finite rod: the dashpot dissipates the arriving power. With $Z_L = 3Z$ one obtains a reflected velocity of $-1/2$ of the incident value, a reflected energy fraction one quarter and absorbed power fraction three quarters. A free or rigid end also reflects energy, but it absorbs no net power in the ideal limit. A measured weak reflection alone is therefore not proof of weak damping inside the rod.

For a pure end spring of stiffness k_L attached to a rigid support, the velocity impedance is $Z_L = k_L/(i\omega)$ under $e^{i\omega t}$. It is imaginary, so the reflection coefficient has unit magnitude at every frequency and a frequency-dependent phase. At low frequency the spring impedance is large and the end looks nearly fixed. At high frequency its impedance is small and the end looks nearly free within the lumped approximation. An impulsive signal contains many frequencies and can return with a changed waveform even without any transmitted or dissipated energy. A support combining a resistor-like dashpot and a spring gives both amplitude loss and phase variation.

A measurement with strain gauges at two positions can separate forward and backward waves if their path delays are resolved. In a narrow frequency band the two records are linear combinations of advancing and returning phase factors. If the gauge spacing corresponds to an integer number of half wavelengths, these combinations become linearly dependent and the separation is ill-conditioned. Change the spacing, use a broadband pulse, or combine a velocity measurement with a strain measurement at one station so that the two characteristic directions enter with opposite signs. The relation $v = (v_+ + v_-)$, $N = Z(-v_+ + v_-)$ then gives a direct local decomposition.

Derive sound propagation from mass and momentum conservation

The displacement-action argument has a fluid analogue. Take an initially uniform fluid of density ρ_0 and pressure p_0, moving little from equilibrium in one spatial dimension. Write small perturbations ρ', p', v. Linearised mass conservation is

$$\partial_t \rho' + \rho_0 \partial_x v = 0.$$

Momentum balance for a short fluid parcel is $\rho_0 \partial_t v = -\partial_x p'$. If compression over an acoustic cycle is approximately isentropic, $p' = c_s^2 \rho'$ with $c_s^2 = (\partial p/\partial \rho)_s$. Differentiate the first equation in time, eliminate the velocity derivative with momentum balance, and obtain $\partial_t^2 p' = c_s^2 \partial_x^2 p'$.

The thermodynamic derivative matters because pressure can respond differently when compression is slow enough for heat exchange. For a perfect gas with ratio of specific heats γ, isentropic perturbations give

$$c_s^2 = \gamma p_0 / \rho_0.$$

Taking an isothermal derivative would give p_0/ρ_0 instead. For $p_0 = 101\,\mathrm{kPa}$, $\rho_0 = 1.20\,\mathrm{kg/m^3}$, and $\gamma = 1.40$, the isentropic speed is about $343\,\mathrm{m/s}$, while the isothermal calculation gives $290\,\mathrm{m/s}$. A measured transit time can discriminate between these constitutive conditions. Wall heat exchange in a very narrow tube can alter which approximation is appropriate over a chosen frequency band.

For a right-moving sound wave $p' = \rho_0 c_s v$, with the pressure positive in compression. This differs in sign from the tensile-positive axial force used for the rod, so match physical force conventions before borrowing formulas across the two examples. The acoustic power per area is $p' v$. For sinusoidal pressure with rms amplitude $1.0\,\mathrm{Pa}$ in the stated gas, the mean intensity is

$$p_{\mathrm{rms}}^2 / (\rho_0 c_s) = 2.43 \times 10^{-3}\,\mathrm{W/m^2}.$$

A peak amplitude of $1.0\,\mathrm{Pa}$ would yield half this number. Writing rms or peak explicitly prevents a routine factor-of-two error when comparing a microphone measurement with an energy flux.

Determine whether a measured transit reveals a modulus or a

geometry

Suppose two axially loaded slender rods have measured wave speeds agreeing within their uncertainties. That alone determines only the ratio E/ρ under the slender-rod assumptions. Measuring force–velocity impedance $Z = \rho A c$ and cross section as well gives $\rho = Z/(Ac)$ and $E = Zc/A$. With $Z = 1375\,\mathrm{kg/s}$, $c = 5092\,\mathrm{m/s}$ and $A = 1.0 \times 10^{-4}\,\mathrm{m^2}$, the inversion gives

$$\rho = 2700\,\mathrm{kg/m^3},$$

$$E = 70.0\,\mathrm{GPa}.$$

If area were overestimated by five percent, both inferred quantities would be underestimated by almost five percent while their ratio remained correct.

Now examine a thick elastic solid under a narrow compressional disturbance with wavelengths short compared with its transverse dimensions. Lateral deformation can be constrained by surrounding material. In an isotropic three-dimensional continuum the longitudinal plane-wave modulus is $\lambda + 2\mu_s$, where λ, μ_s are Lamé coefficients, rather than the uniaxial-stress Young modulus of a slender rod. The shear-wave speed satisfies $c_T^2 = \mu_s/\rho$ and longitudinal speed $c_L^2 = (\lambda + 2\mu_s)/\rho$. Measuring both, together with density, can recover the two independent elastic moduli. Using only one longitudinal speed to infer Young modulus without specifying the deformation geometry can give a physically incorrect value.

For $\rho = 2500\,\mathrm{kg/m^3}$, $c_L = 5000\,\mathrm{m/s}$ and $c_T = 3000\,\mathrm{m/s}$, these relations give

$$\mu_s = 22.5\,\mathrm{GPa},$$

$$\lambda = 17.5\,\mathrm{GPa}.$$

The implied Young modulus $E = \mu_s(3\lambda + 2\mu_s)/(\lambda + \mu_s) = 54.8\,\mathrm{GPa}$, while $\rho c_L^2 = 62.5\,\mathrm{GPa}$. Both numbers represent material stiffness, but they enter different mechanical boundary conditions. A long thin specimen of the same material should have an axial speed closer to $\sqrt{E/\rho} = 4680\,\mathrm{m/s}$. Comparing the bulk and rod experiments tests the constitutive and geometrical assumptions behind the measured speed.

Derive orthogonality when a rod changes material along its length

For a rod with positive varying density $\rho(x)$, area $A(x)$ and modulus $E(x)$, a separated free oscillation $u(x,t) = \phi(x)\cos \omega t$ satisfies

$$-[EA\phi']' = \omega^2 \rho A \phi.$$

Suppose two modes ϕ_n, ϕ_m satisfy the same homogeneous fixed or free boundary conditions and the correct continuity of displacement and axial force across every perfectly bonded interface. Multiply the first equation by ϕ_m, the second by ϕ_n, subtract and integrate. Interior terms produced by integration by parts cancel pairwise, including the interface flux terms, and the endpoint terms vanish. Thus

$$(\omega_n^2 - \omega_m^2) \int \rho A \phi_n \phi_m \, dx = 0.$$

Mode shapes with distinct frequencies are orthogonal under the mass-weighted inner product, not generally under a simple average of displacements measured at uniformly spaced stations. An initial velocity distribution $v_0(x)$ projects onto mode n with coefficient $\int \rho A v_0 \phi_n \, dx / \int \rho A \phi_n^2 \, dx$. In a rod with a heavy section, the same imposed velocity there stores more energy and carries more modal weight. An experiment interpreting raw camera amplitudes without line-density weighting can misassign energy among modes. Normalising each measured mode shape to unit maximum does not fix the mass weighting needed for energies.

Multiplying one eigenvalue equation by its own shape gives

$$\omega_n^2 = \int EA(\phi_n')^2 dx / \int \rho A \phi_n^2 dx.$$

For an admissible trial function satisfying prescribed displacement conditions, the same quotient bounds the fundamental squared frequency from above when rigid translations are excluded. Consider a uniform fixed–free rod and trial $\phi = x/L$. The numerator is EA/L and denominator $\rho A L/3$, giving $\omega_{\mathrm{trial}} = \sqrt{3}\, c/L$. The exact fundamental is $\pi c/(2L)$, so this one-parameter shape overestimates frequency by about 10.3%. It need not satisfy the free-end traction condition itself because that is a natural condition of the variational minimiser; it does need to satisfy the essential fixed-end displacement.

For a free–free rod the constant displacement mode has zero frequency. Using an arbitrary positive trial function without removing its mass-weighted mean can drive a quotient towards zero by adding a large constant. To estimate the first deforming mode impose orthogonality to the rigid translation, $\int \rho A \phi \, dx = 0$. This has an immediate mechanical interpretation: the deformation mode should not translate the centre of mass of an isolated rod. The null mode and its mass-weighted constraint reappear in numerical eigenproblems built from discretised stiffness and mass matrices.

Find where a discrete elastic chain ceases to look continuous

Shorten the wavelength relative to the lattice spacing. Compare the phase and group velocities with those inferred from a continuum action.

Open this experiment online

Try the calculation

Sites per wavelength 10

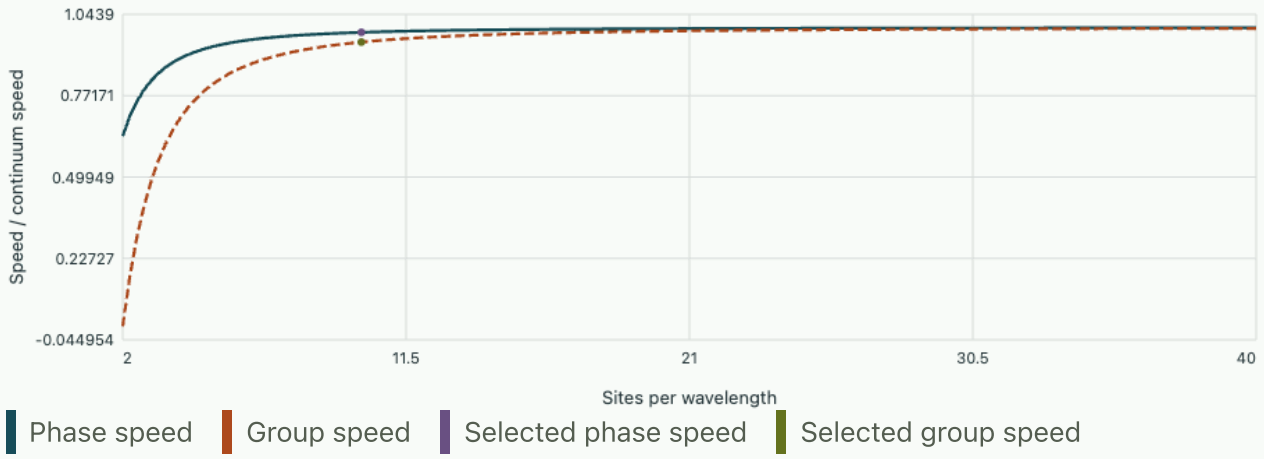

Frequency and phase speed are 98.36% of the continuum prediction. Group speed is 95.11%.

Track work and impulse in a one-dimensional pulse experiment

A finite displacement pulse provides a useful warning about integrating strain and velocity records. A right-going strain pulse of one sign can carry net momentum $\int \rho A v \, dx$. Because $v = -c u_x$, its integrated material momentum is $-\rho A c[u(+\infty) - u(-\infty)]$ at a fixed time. A localised displacement bump that returns to the same displacement on both sides has zero net ordinary material momentum, even though its energy is positive and travels to the right. Its strain and particle-velocity records contain positive and negative parts. A unipolar velocity pulse leaves behind a displacement step, produced by a source that has supplied net impulse.

For a right-moving rectangular velocity pulse of amplitude $0.020\,\mathrm{m/s}$, duration $100\,\mu\mathrm{s}$ in the worked rod, the local displacement jump measured in time is $2.0\,\mu\mathrm{m}$. Its impulse magnitude across a section is $Zv\Delta t = 2.75 \times 10^{-3}\,\mathrm{N\,s}$, while its transmitted energy is

$$Zv^2\Delta t = 55.0\,\mu\mathrm{J}.$$

A second equal pulse of opposite velocity sign launched later cancels the net displacement and material momentum but doubles the transmitted energy. Thus integrating a signed velocity signal and integrating its square distinguish different properties of the same experimental record.

A displacement sensor has a small linear drift during a burst. Which inferred observables are particularly sensitive?

▼ **Work through the solution**

Differentiating adds a constant offset to particle velocity. Integrating that apparent velocity over a long window produces a growing spurious displacement jump and momentum estimate. Squaring it adds both

a cross term with the physical velocity and a positive baseline energy. Measure a pre-pulse baseline, choose an integration interval covering the physical pulse, and test that the result is stable when the window is moderately extended. An independent strain gauge gives another characteristic combination; comparison with $N = -Zv$ can expose drift or an overlapping reflection.

Can a finite-element rod model with a plausible first eigenfrequency still fail an impulse test?

▼ Work through the solution

The first frequency mostly probes a long-wavelength weighted stiffness-to-mass ratio. A brief pulse contains higher modes and is sensitive to temporal resolution, dispersion, boundary tractions and the way discrete source work enters. Verify modal frequencies at several wavelengths, check the pulse's positive energy and signed impulse separately, and compare the measured incoming and reflected characteristic fluxes. A single standing-wave eigenvalue cannot validate all of those physically independent balances.

Recover a jump condition at an interface with a point mass

For a concentrated mass M_b joining two rods include $M_b u_t(x_b)^2/2$ as a separate contribution to the Lagrangian. Its time variation contributes $-M_b u_{tt}\delta u$ at the joint. The left and right rod boundary terms contribute respectively $-N_1\delta u$ and $+N_2\delta u$. Requiring stationarity for an independently varying shared displacement gives exactly $N_2 - N_1 = M_b u_{tt}$. This derivation identifies both the sign and the constitutive assumption of a perfectly bonded, nonslipping joint.

For identical rods and a sinusoidal drive at angular frequency ω, the reflected velocity coefficient becomes $r = -i\omega M_b/(2Z + i\omega M_b)$ under the stated phasor convention. At $\omega M_b = 2Z$ it reflects half the power and transmits half. The mass itself absorbs no cycle-averaged energy, though it stores kinetic energy during a cycle. For $Z = 100\,\mathrm{kg/s}$ and $M_b = 0.10\,\mathrm{kg}$, the equal-power frequency is about $318\,\mathrm{Hz}$. A real joint that loses appreciable power at that frequency needs a damping or radiation term in addition to its measured mass.

Tutorial on stress waves

A gauge $0.80\,\mathrm{m}$ from a free end records the echo of a sharp disturbance in the worked rod. What echo delay and strain sign should it expect?

▼ Work through the solution

The extra path from gauge to end and back is $1.60\,\mathrm{m}$, giving $1.60/5092 = 0.314\,\mathrm{ms}$. A free end has zero net axial force, so the reflected force and strain have opposite signs to the incident ones. The velocity reflection keeps its sign. Finite pulse width and any change of material between gauge and end can obscure that simple result.

A bonded step has measured reflected velocity coefficient -0.20 and no detectable dissipation. Infer its impedance ratio and transmitted energy fraction.

▼ **Work through the solution**

Rearranging $r_v = (1 - r)/(1 + r)$ gives

$$r = Z_2/Z_1 = (1 - r_v)/(1 + r_v) = 1.50.$$

The energy reflection is 0.04 and transmission 0.96. The velocity transmission is 0.80, whose square alone is only 0.64. Multiplying by the transmitted-to-incident impedance ratio recovers the correct energy fraction.

A rod model with a prescribed displacement at its right end reports nonzero work there, even though the variational boundary term vanished in deriving its equation. Is there a contradiction?

▼ **Work through the solution**

Vanishing of $N\delta u$ follows because the allowed virtual displacement at a prescribed boundary is zero. Actual boundary velocity can be nonzero when the prescribed displacement varies in time. The actuator supplies power Nu_t at the right boundary. Compare the time-integrated input with the change of stored energy plus any losses or outgoing energy rather than identifying an admissible variation with actual displacement.

Compare a finite chain with its long-wavelength continuum.

Fließbach includes string vibrations, beam bending and sound in his continuum mechanics treatment.

Analytical mechanics from constraints to invariants · 12. Relativistic collisions, centre-of-momentum energy and thresholds

Two particles with the same total laboratory energy can have very different energy available for changing their internal state. Determine the energy and motion of the centre-of-momentum system, reconstruct two-body elastic scattering, and follow how a detector threshold transforms between frames.

Form the conserved total four-momentum

For a particle with rest mass m, energy E and momentum $\mathbf{p}$, write $p^\mu = (E/c, \mathbf{p})$ with metric signature $+---$. The on-shell condition $E^2 - c^2 p^2 = m^2 c^4$ holds for each freely propagating particle. In an isolated collision sum the incoming four-momenta and equate them to the outgoing sum. A frame-independent measure of the total is $s = (E_1 + E_2)^2 - c^2 |\mathbf{p}_1 + \mathbf{p}_2|^2$, defined here with units of energy squared. Some books assign momentum-squared units to s instead; stating this convention fixes all factors of c. The centre-of-momentum energy is $\sqrt{s}$.

A boost along the total momentum brings it to zero if the total four-vector is timelike. Its velocity is $\mathbf{V}_{\mathrm{cm}} = c^2(\mathbf{p}_1 + \mathbf{p}_2)/(E_1 + E_2)$. Individual particles can approach the speed of light while this frame is slow or even stationary in the laboratory when their momenta cancel. A pair of perfectly parallel massless rays gives a null total and has no rest frame. For massive particles the positive total rest energy generally ensures a timelike total. Knowing $\sqrt{s}$ determines the internal energy available, while $\mathbf{V}_{\mathrm{cm}}$ determines how the final directions and energies are seen by a laboratory camera.

Expand the square using the two on-shell conditions to obtain

$$s = m_1^2 c^4 + m_2^2 c^4 + 2(E_1 E_2 - c^2 \mathbf{p}_1 \cdot \mathbf{p}_2).$$

At fixed energies the dot product shows why head-on motion gives more centre-of-momentum energy than parallel motion. This relation also applies when one participant is a photon by setting its rest mass to zero. A familiar Newtonian analogy separates centre-of-mass translational kinetic energy from relative kinetic energy. In relativity the exact separation is carried by the invariant mass of the total four-vector and the boost of that total.

Compare a fixed target with two opposing beams

Let both incoming particles have rest energy $mc^2 = \mathcal{M}$. With one initially stationary and the other carrying kinetic energy K, the invariant is $s = 4\mathcal{M}^2 + 2\mathcal{M}K$. By contrast, two identical beams carrying kinetic energy K_b each and meeting with opposite momenta give

$$\sqrt{s} = 2(\mathcal{M} + K_b).$$

If a specified final channel has minimum sum of rest energies $\mathcal{W}$, the massive products at threshold have zero relative momentum in their common centre-of-momentum frame. The fixed-target threshold is $K_{\mathrm{th}} = (\mathcal{W}^2 - 4\mathcal{M}^2)/(2\mathcal{M})$ when positive. A symmetric collider needs $K_b = (\mathcal{W} - 2\mathcal{M})/2$ in each beam. The channel must also satisfy other conservation laws; these equations give kinematic conditions.

For an abstract excitation channel with $\mathcal{M} = 1.00\,\mathrm{GeV}$ and $\mathcal{W} = 3.00\,\mathrm{GeV}$, the fixed-target projectile needs $K = 2.50\,\mathrm{GeV}$, whereas each symmetric beam needs $0.50\,\mathrm{GeV}$. At the fixed-target threshold the total lab energy is $4.50\,\mathrm{GeV}$ and the total momentum times c is

$$\sqrt{3.50^2 - 1.00^2} = 3.354\,\mathrm{GeV}.$$

Hence $V_{\mathrm{cm}}/c = 0.7454$ and $\gamma_{\mathrm{cm}} = 1.50$. The final system has centre-of-momentum energy $3.00\,\mathrm{GeV}$ but still carries substantial bulk motion in the laboratory. Equating an energy deficit directly to projectile kinetic energy would ignore its conserved momentum.

Solve any two-body final state in its momentum frame

Let the two final particles have rest energies $\mathcal{M}_3, \mathcal{M}_4$. In the centre-of-momentum frame their spatial momenta have equal magnitudes p_* and opposite directions. Energy conservation gives

$$E_3^* + E_4^* = \sqrt{s}.$$

Subtract their squared mass-shell relations to obtain

$$(E_3^*)^2 - (E_4^*)^2 = \mathcal{M}_3^2 - \mathcal{M}_4^2.$$

Factoring this difference gives

$$E_3^* = \frac{s + \mathcal{M}_3^2 - \mathcal{M}_4^2}{2\sqrt{s}},$$

$$cp_* = \frac{\sqrt{[s - (\mathcal{M}_3 + \mathcal{M}_4)^2][s - (\mathcal{M}_3 - \mathcal{M}_4)^2]}}{2\sqrt{s}}.$$

The square root exposes the threshold and is symmetric under interchanging the products. When the masses are equal, each receives exactly $\sqrt{s}/2$. When they differ, equal momenta do not mean equal energies or velocities. At threshold the momentum vanishes, so an angular distribution there becomes a delicate concept; a boost can send both products in the same lab direction even when they move apart appreciably above threshold.

For $\sqrt{s} = 5.0\,\mathrm{GeV}$, $\mathcal{M}_3 = 2.0\,\mathrm{GeV}$ and $\mathcal{M}_4 = 1.0\,\mathrm{GeV}$, the energies are 2.80 and $2.20\,\mathrm{GeV}$. Each gives

$$cp_* = \sqrt{2.8^2 - 2.0^2} = \sqrt{2.2^2 - 1.0^2} = 1.960\,\mathrm{GeV}.$$

Their speed ratios cp_*/E^* are 0.700 and 0.891. Summing these two speeds would exceed c as a numerical closing rate in that frame, but the speed of either particle measured from the other's rest frame follows relativistic velocity addition and remains below c.

Transform a centre-of-momentum angular pattern to a detector

Choose the laboratory boost along z with parameters β, γ. A product emitted at polar angle θ_* has $p_{z,*} = p_* \cos\theta_*$,

$$p_{\perp,*} = p_* \sin\theta_*.$$

A Lorentz boost to the laboratory gives $E = \gamma(E^* + \beta c p_* \cos\theta_*)$,

$$c p_z = \gamma(c p_* \cos\theta_* + \beta E^*),$$

$$p_\perp = p_{\perp,*}.$$

Use a quadrant-aware angle from the resulting longitudinal and transverse components. A tangent formula alone loses the distinction between a particle moving backward and one moving nearly forward when its denominator changes sign.

For particle 3 in the preceding example take $\beta = 0.60, \gamma = 1.25$ and emission at 90° in the centre-of-momentum frame. The laboratory energy is $3.50\,\mathrm{GeV}$, axial momentum times c is $2.10\,\mathrm{GeV}$, and transverse momentum times c remains $1.960\,\mathrm{GeV}$. The polar angle is 43.0°. A detector that accepts only angles above 60° would miss this event despite its centre-of-momentum emission being transverse. To convert an angular density, transform the solid-angle Jacobian or count the preimage of each finite acceptance bin; matching angles by name between frames is insufficient.

If the detector instead accepts a product only above lab energy $E_{\min}$, the inequality becomes $\cos\theta_* \geq [E_{\min}/\gamma - E^*]/(\beta c p_*)$ for positive β, p_*. With $E_{\min} = 4.0\,\mathrm{GeV}$ this gives $\cos\theta_* \geq 0.340$. For an isotropic distribution in its own momentum frame that detector accepts fraction $(1 - 0.340)/2 \simeq 0.330$, assuming full azimuth and no other losses. At $\beta = 0$ energy selection becomes independent of angle, so the divided expression must be replaced by its original inequality.

Follow an elastic collision of equal masses all the way to the laboratory

In a Newtonian elastic collision of equal masses with one initially at rest, the two nonzero outgoing velocities are perpendicular. At relativistic energies that rule changes even when the collision remains exactly elastic. For equal final masses in the centre-of-momentum frame the two outgoing energies and momentum magnitudes are equal. In the laboratory where target 2 was initially at rest, the boost speed of the centre equals the speed of each particle in the momentum frame: boosting initially stationary particle 2 into that frame supplies the equality. Write this common dimensionless speed as β, and let particle 1 scatter through angle θ_* to the positive boost axis. Particle 2 leaves with opposite momentum.

With $p_* c = \beta E^*$, the laboratory longitudinal components are $p_{1z} = \gamma p_*(1 + \cos\theta_*)$ and $p_{2z} = \gamma p_*(1 - \cos\theta_*)$, and their transverse components are opposite with magnitude $p_* \sin\theta_*$. The two lab polar angles therefore obey $\tan\theta_1 = \tan(\theta_*/2)/\gamma$ and $\tan\theta_2 = \cot(\theta_*/2)/\gamma$. Multiplying gives

$$\tan\theta_1 \tan\theta_2 = 1/\gamma^2.$$

At low speed $\gamma \to 1$, so $\theta_1 + \theta_2 \to 90^\circ$. For finite boost the opening angle becomes smaller. Endpoint cases where one outgoing particle is stationary leave its direction undefined and must be handled separately.

Take rest energy $\mathcal{M}$ and projectile kinetic energy $K = 2\mathcal{M}$ against an identical stationary target. The invariant energy is $\sqrt{8}\mathcal{M}$ and the laboratory total energy is $4\mathcal{M}$, giving $\gamma_{\mathrm{cm}} = \sqrt{2}$. For a transverse centre-of-momentum collision, both products have laboratory angle $\arctan(1/\sqrt{2}) = 35.26^\circ$ on opposite sides of the beam, so the opening is 70.53°. Both laboratory energies are $2\mathcal{M}$; their kinetic energies are each $\mathcal{M}$, sharing the incident kinetic energy equally. Angular data and energy partition together offer an overdetermined test of elastic equal-mass kinematics.

For a general θ_*, the lab kinetic-energy fractions are $[1 + \cos\theta_*]/2$ and $[1 - \cos\theta_*]/2$ of the incoming kinetic energy in this equal-mass geometry. This follows by inserting $E^* = \gamma_{\mathrm{cm}}\mathcal{M}$ in the boost and using $K = 2\mathcal{M}(\gamma_{\mathrm{cm}}^2 - 1)$. Equal masses do not imply equal final energies in the laboratory; that occurs for the transverse centre-of-momentum geometry. A detector threshold of $0.25K$ on both products selects $|\cos\theta_*| \le 0.50$. For an isotropic momentum-frame distribution that condition accepts half the events irrespective of the azimuth, provided the lab apparatus covers both directions.

Compare two methods of estimating missing invariant mass

Suppose a known laboratory total has energy $5.0\,\mathrm{GeV}$ and axial momentum times c of $3.0\,\mathrm{GeV}$. One registered product has energy $2.0\,\mathrm{GeV}$, longitudinal momentum times c of $1.0\,\mathrm{GeV}$, and transverse momentum times c of $0.60\,\mathrm{GeV}$. Subtracting vectors gives missing energy $3.0\,\mathrm{GeV}$, axial momentum times c of $2.0\,\mathrm{GeV}$, and transverse momentum times c of $-0.60\,\mathrm{GeV}$. Its invariant mass energy is

$$\sqrt{9 - 4 - 0.36} = 2.154\,\mathrm{GeV}.$$

Dropping the transverse measurement would give $2.236\,\mathrm{GeV}$, an error of about 3.8%. Subtracting reported kinetic energies instead of total energies would introduce an uncontrolled rest-energy offset.

The same result can be reconstructed in the initial centre-of-momentum frame. The total invariant energy is $4.0\,\mathrm{GeV}$, so the laboratory boost is

$$\beta = 0.60, \gamma = 1.25.$$

Transforming the observed product back gives $E^* = 1.25(2.0 - 0.60 \times 1.0) = 1.75\,\mathrm{GeV}$ and $cp_z^* = 1.25(1.0 - 0.60 \times 2.0) = -0.25\,\mathrm{GeV}$, while its transverse component stays $0.60\,\mathrm{GeV}$. Missing energy is $2.25\,\mathrm{GeV}$, and missing squared momentum times c^2 is $0.25^2 + 0.60^2$. The invariant is again $4.64\,\mathrm{GeV}^2$. Repeating the computation in two frames checks signs and coordinate components without adding independent experimental information.

To propagate uncertainty use the squared quantity before taking its square root. With $c = 1$ for numerical units, perturbations satisfy

$$\delta M_{\mathrm{miss}}^2 = 2E_{\mathrm{miss}}\delta E_{\mathrm{miss}} - 2\mathbf{p}_{\mathrm{miss}} \cdot \delta\mathbf{p}_{\mathrm{miss}}.$$

If the energy and momentum of one detected particle come from the same calibrated tracking measurement they may be strongly correlated. Treating those uncertainties as independent can seriously misestimate the spread, especially near a missing-mass threshold where M^2 is close to zero. Retain the full covariance and report a distribution in mass squared near that boundary. Mapping negative noisy values to zero before averaging biases the result upward and erases information about detector resolution.

Recover a recoil energy from photon scattering

Consider an incoming photon of energy E colliding with a free particle of rest energy $\mathcal{M}$ initially at rest. The outgoing photon has energy E' and turns through angle θ in the original laboratory. Four-momentum conservation gives the final target energy $\mathcal{M} + E - E'$ and its squared momentum times c^2 is $E^2 + E'^2 - 2EE'\cos\theta$. Imposing the final target mass-shell condition and cancelling equal squares yields

$$\mathcal{M}(E - E') = EE'(1 - \cos\theta).$$

Therefore

$$E' = \frac{E}{1 + (E/\mathcal{M})(1 - \cos\theta)}.$$

The scattered energy equals the incident energy for perfect forward scattering, whereas backscattering transfers most energy at fixed incident E. Rearrangement gives

$$1/E' - 1/E = (1 - \cos\theta)/\mathcal{M}.$$

Multiplying by hc gives the usual wavelength shift with scale $h/(mc)$. The argument uses only four-momentum conservation and the initial target mass to determine kinematics. It does not give the probability of any scattering angle, which requires an interaction model. Bound target motion or initially moving scatterers change the measured line shape even when the elementary free-particle kinematics is understood.

Take $E = \mathcal{M}/2$. At $\theta = 90^\circ$ the outgoing photon energy is $\mathcal{M}/3$; at $\theta = \pi$ it is $\mathcal{M}/4$. In the right-angle event the target kinetic energy is

$$E - E' = \mathcal{M}/6.$$

Its final momentum magnitude times c can be computed from its energy as $\sqrt{(7\mathcal{M}/6)^2 - \mathcal{M}^2} = \sqrt{13}\mathcal{M}/6$, or from the photon momentum triangle as $\sqrt{(\mathcal{M}/2)^2 + (\mathcal{M}/3)^2}$. These two values agree. A detector that measures only target kinetic energy can infer the photon angle if the initial photon energy was known and the free stationary target assumptions hold.

The maximum possible target kinetic energy is $2E^2/(\mathcal{M} + 2E)$. For $E \ll \mathcal{M}$ this is approximately $2E^2/\mathcal{M}$, much smaller than the incident energy. At $E \gg \mathcal{M}$ the recoiling target can receive most of the photon energy. Scanning incident energy therefore changes both the absolute and fractional accessible

recoil range. If an observed event falls beyond that kinematic edge, changing only the angular cross section cannot explain it; examine energy calibration, initial target motion, coincidence assignment or overlapping events.

Identify what two unknown detector scales can be calibrated together

A two-body decay at rest into two photons yields equal energies and an opening angle of 180°. In any frame its invariant parent rest energy is

$$Mc^2 = \sqrt{2E_1E_2(1-\cos\alpha)}.$$

This formula remains valid when the parent moves and the detected photon energies differ. A common multiplicative energy calibration factor multiplies the reconstructed mass by that factor. An angular bias also changes the inferred mass, with fractional derivative $\frac{1}{2}\sin\alpha/(1-\cos\alpha) = \frac{1}{2}\cot(\alpha/2)$. Nearly collinear photon pairs are therefore particularly sensitive to angular uncertainties, even when their individual energy measurements are accurate.

For $E_1 = 2.0\,\mathrm{GeV}$, $E_2 = 1.0\,\mathrm{GeV}$, $\alpha = 60^\circ$, the reconstructed rest energy is $\sqrt{2}\,\mathrm{GeV}$, although the lab energy sum is $3.0\,\mathrm{GeV}$. A one-degree positive error in the opening angle changes the inferred mass by approximately $0.5\cot 30^\circ(\pi/180) = 1.51\%$. Measuring events with a range of opening angles can distinguish an angular offset from a common energy-scale factor, since the latter has no such angular amplification. A calibration performed only on back-to-back pairs is weakly sensitive to opening-angle errors to first order.

Invariant reconstruction is especially valuable when different observers disagree on which laboratory particle appears fast or forward. Agreement requires the entire event be expressed in one frame, with coincident incoming and outgoing measurements and a consistent sign convention for momentum. A Lorentz transformation cannot repair a mispaired event. Estimate statistical backgrounds and detector resolution independently before interpreting a narrow or displaced mass feature. The invariant provides a kinematic check; it gains physical meaning from the measurement model used to construct it.

Reconstruct a two-body decay with a nonzero boost

A parent with known rest energy W decays into one massive daughter of rest energy m_dc^2 and one photon. In the parent rest frame the common momentum magnitude follows from the two-body formula, so photon energy is

$$E_\gamma^* = [W^2 - (m_dc^2)^2]/(2W).$$

For a moving parent, the lab photon energy spans a range depending on the emission angle:

$$E_\gamma = \gamma E_\gamma^*(1+\beta\cos\theta_*).$$

The end energies $E_{\max}, E_{\min}$ for emission forward and backward have product $(E_\gamma^*)^2$ and ratio $(1+\beta)/(1-\beta)$. Thus a measured energy band can give both the rest-frame line energy and the parent speed if its full angular range is observed and all parents share a common boost.

Take $W = 3.0\,\mathrm{GeV}$,

$$m_d c^2 = 1.0\,\mathrm{GeV}.$$

The rest-frame photon energy is $4/3\,\mathrm{GeV}$. With $\beta = 0.60, \gamma = 1.25$, the accessible lab endpoints are 2.667 and $0.667\,\mathrm{GeV}$. Their geometric mean recovers $1.333\,\mathrm{GeV}$, and $(E_{\max} - E_{\min})/(E_{\max} + E_{\min}) = 0.600$ recovers the boost. The total energy released as rest energy difference is $2.0\,\mathrm{GeV}$, larger than the photon energy in the rest frame because the massive daughter must recoil. Assigning all the rest-energy difference to radiation ignores that conserved momentum even before any laboratory transformation.

If the parent decays isotropically in its rest frame, $\cos\theta_*$ is uniformly distributed. The linear photon-energy relation then gives a flat lab energy density between the endpoints when every direction is detected with equal efficiency and the parent boost is fixed. A laboratory detector covering only a forward cone selects part of the interval and can produce an apparently shifted line or a nonuniform spectrum. A spread of parent speeds superposes intervals with different endpoints. Before interpreting spectral width as an intrinsic lifetime or a spread in masses, separate angular acceptance, boost distribution and instrumental resolution.

The lab photon angle obeys $\cos\theta_{\mathrm{lab}} = (\cos\theta_* + \beta)/(1 + \beta\cos\theta_*)$. At transverse rest-frame emission $\cos\theta_* = 0$, the lab photon points at about 53.1° for the stated boost. Its energy is $1.667\,\mathrm{GeV}$. The corresponding massive daughter has a different aberration relation because its rest-frame speed is below c. A photon angle formula should not be reused for a massive track. Transform its actual four-vector to draw the two lab directions and compare them with the expected missing momentum of the unobserved partner.

Compare elapsed times along different trajectories

Study proper time and laboratory coordinate time for the same motion. Identify the invariant clock interval before comparing a measurement between frames.

Open this experiment online

Try the calculation

Speed / speed of light **0.8**

Gate separation (light-μs) **12**

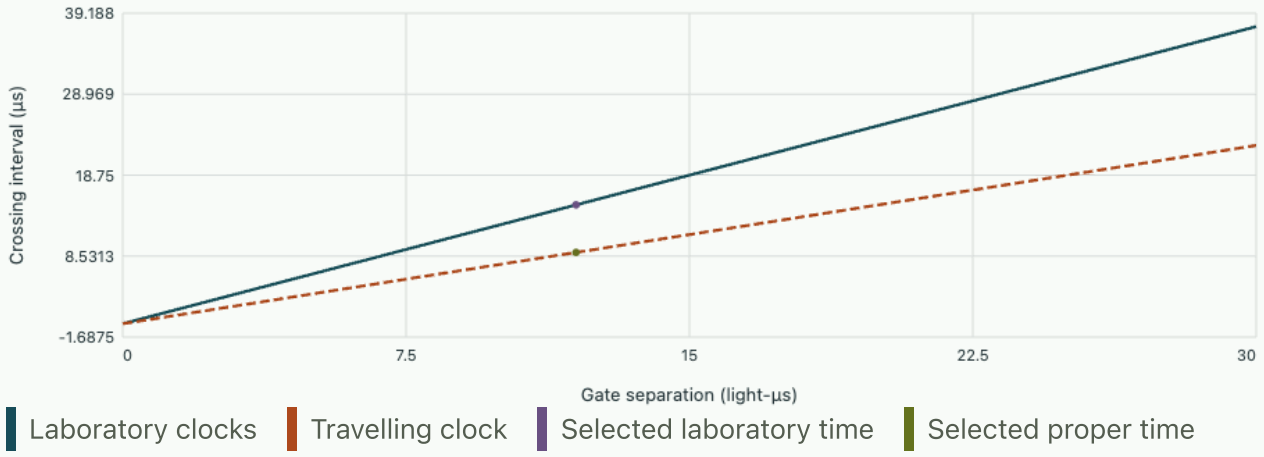

The laboratory records 15 μs. The travelling clock records 9 μs.

Audit a relativistic event using dimensionless rapidity

For one-dimensional motion define rapidity y by $E = mc^2 \cosh y,\ cp = mc^2 \sinh y$. Then $v/c = \tanh y$ and collinear boosts add or subtract rapidities. The invariant for two collinear massive particles becomes

$$s = \mathcal{M}_1^2 + \mathcal{M}_2^2 + 2\mathcal{M}_1\mathcal{M}_2 \cosh(y_1 - y_2).$$

The available energy depends on their relative rapidity, not on their common boost. At very high same-direction energies, constructing $E_{\text{total}}^2 - (cp_{\text{total}})^2$ can lose floating-point precision through subtraction. Expressing the input with known rest energies and relative rapidity can be numerically better conditioned.

For two equal masses at rapidities 3.0 and 2.0,

$$\sqrt{s} = 2\mathcal{M}\cosh(0.5) = 2.2553\mathcal{M}.$$

A common boost adding ten to both leaves this value unchanged even though each lab energy grows by orders of magnitude. Their centre-of-momentum rapidity is 2.5 in the initial frame because equal masses at rapidities ± 0.5 have opposite momenta. A particle starting at rapidity three appears to move only at $\tanh(0.5) = 0.462c$ in that frame. This separates a very large laboratory kinetic energy from a modest relative collision energy.

A computation obtains slightly negative s for two very energetic nearly parallel massive tracks, even though both individual four-vectors were formed from positive masses. What calculation can distinguish rounding from a physical inconsistency?

▼ **Work through the solution**

Recalculate using independently measured directions and rest masses. For a track of known momentum magnitude, evaluate $E - cp = \mathcal{M}^2/(E + cp)$ so that a small positive difference is recovered without subtracting nearly equal large numbers. In a collinear test use the rapidity expression; at nonzero angle separate the positive angular term $c^2 p_1 p_2 (1 - \cos\alpha)$, with $1 - \cos\alpha = 2\sin^2(\alpha/2)$. Compare with higher precision and propagated measurement covariance. For ideal future-directed massive four-vectors their total cannot be spacelike, so a stable negative value would indicate inconsistent measured inputs or a reconstruction error rather than a new kinematic channel.

Choose a laboratory energy convention for published event tables

An event table may label one column beam energy while another experiment quotes beam kinetic energy for the same particle. The distinction is a full rest energy. For a stationary equal-mass target, inserting total projectile energy E_{proj} gives

$$s = 2\mathcal{M}^2 + 2\mathcal{M}E_{\mathrm{proj}};$$

inserting kinetic energy K requires

$$s = 4\mathcal{M}^2 + 2\mathcal{M}K.$$

At a quoted numerical beam value $2\mathcal{M}$ the two interpretations yield centre-of-momentum energies $\sqrt{6}\,\mathcal{M}$ and $\sqrt{8}\,\mathcal{M}$, distinct enough to change whether a final channel is kinematically open.

Before comparing two angular or energy spectra, record which particle was initially at rest, the energy convention, whether angles refer to the momentum frame or laboratory, and which particles passed the selection. Each changes an equation already derived above. A sample with a laboratory energy cut can acquire a forward asymmetry even if the underlying centre-of-momentum scattering is perfectly isotropic. Mapping every selected event back to the momentum frame without also correcting the angle-dependent acceptance will preserve that selection bias. The conserved invariant determines the accessible final kinematics; the detector determines which part of that set becomes visible.

Tutorial on collision measurements

At fixed-target energy $K = 0.020\mathcal{M}$, compare the available kinetic energy above the two incoming rest energies in the momentum frame with the Newtonian reduced-mass prediction.

▼ **Work through the solution**

Expansion gives

$$\sqrt{s} = 2\mathcal{M}\sqrt{1 + K/(2\mathcal{M})} \simeq 2\mathcal{M} + K/2 - K^2/(16\mathcal{M}).$$

The leading available energy is half the lab projectile kinetic energy, as for two equal Newtonian masses with one at rest. The correction here is $0.000025\mathcal{M}$, about one quarter percent of the leading available kinetic energy. An energy expansion must subtract the rest-energy offset before calculating a relative error.

Two photons of equal energy E_γ intersect at angle α. Derive the total centre-of-momentum energy, including the parallel and antiparallel limits.

▼ **Work through the solution**

The mass-shell terms vanish and the spatial momenta have magnitude E_γ/c. Thus

$$s = 2E_\gamma^2(1-\cos\alpha) = 4E_\gamma^2\sin^2(\alpha/2).$$

Parallel rays have a null total and zero invariant energy, although laboratory energy is $2E_\gamma$. Opposing rays have zero net momentum and centre-of-momentum energy $2E_\gamma$. A relative closing rate is not the invariant energy.

An unknown neutral product escapes an otherwise recorded two-body event. Which four-vector combination should a detector reconstruct, and what does a negative inferred mass squared suggest?

▼ **Work through the solution**

Subtract the measured final four-momenta from the known incoming total and square the missing four-vector with the stated metric. A single missing physical massive product gives its positive rest mass squared after the appropriate powers of c; a massless one gives zero. A significantly negative result indicates an inconsistent reconstruction, an unaccounted incoming momentum, event mismatch or measurement bias. Multiple escaping products generally yield their combined invariant mass and cannot be identified uniquely from that scalar alone.

Compare velocity and momentum transformations across reference frames.

Fließbach's mechanics text includes a full final treatment of special relativity.

Analytical mechanics from constraints to invariants · 13. Which path is shortest across the surface of a cone?

A point can move along a conical surface while its azimuth and height both change. Unroll the geometry and predict the shortest path between two marked points. The measurable minimum radius distinguishes the geodesic from a line drawn along a horizontal circle.

Turn the constraint into a distance measurement

Let r denote the slant distance from the apex and α the angle between the cone's side and its central axis. A point at r lies on a horizontal circle of radius $r \sin\alpha$. Small radial and azimuthal displacements on the surface meet at right angles. Their squared distance adds to $ds^2 = dr^2 + r^2 \sin^2\alpha \, d\phi^2$. The change of variable $\psi = \phi \sin\alpha$ turns this into the polar metric of a plane. Cutting the cone along a generator and flattening it produces a sector of opening angle $2\pi \sin\alpha$.

Without a tangential force a particle follows a straight line in the unrolled sector. Its coordinates need not evolve linearly in the original azimuth. For two positions at equal slant distance R separated by physical azimuth $\Delta\phi$ of magnitude at most π, the shortest branch uses a straight chord spanning $\Delta\psi = \sin\alpha \, \Delta\phi$. Bisecting the isosceles triangle gives

$$L = 2R \sin(|\Delta\psi|/2),$$

$$r_{\min} = R \cos(\Delta\psi/2).$$

The other copies of the endpoint correspond to winding around the cone on different branches. The chord formula uses a branch reached without passing through the apex. When the physical endpoints are diametrically opposite, clockwise and anticlockwise branches have equal shortest length. A laboratory string stretched across the interior would use the three-dimensional chord, which need not stay on the surface.

Detect the departure from the horizontal ring

For a cone of half-angle 30 degrees, two marks 120 degrees apart at slant distance 5 cm appear only 60 degrees apart in the plane. Their shortest surface path is 5.00 cm long and passes through radius 4.33 cm. Staying on the horizontal ring would require $R\Delta\psi = 5.24$ cm. The straight three-dimensional chord between the same marks is only 4.33 cm long but cuts through the cone. Comparing those three lengths distinguishes a free-space displacement from two distinct constrained motions.

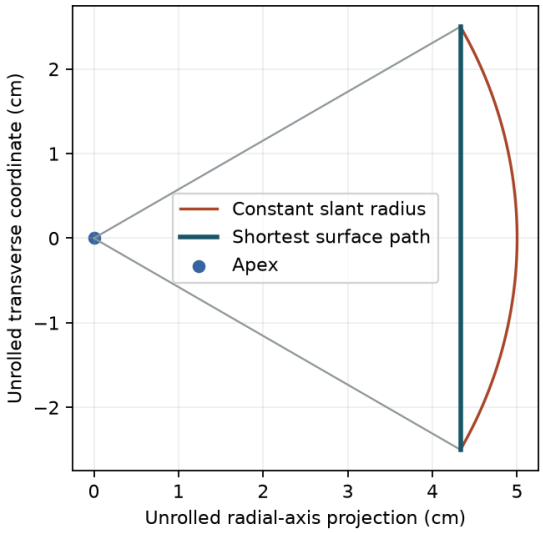

The endpoints share a radius while the middle of the geodesic lies closer to the apex. Both axes measure lengths intrinsic to the surface.

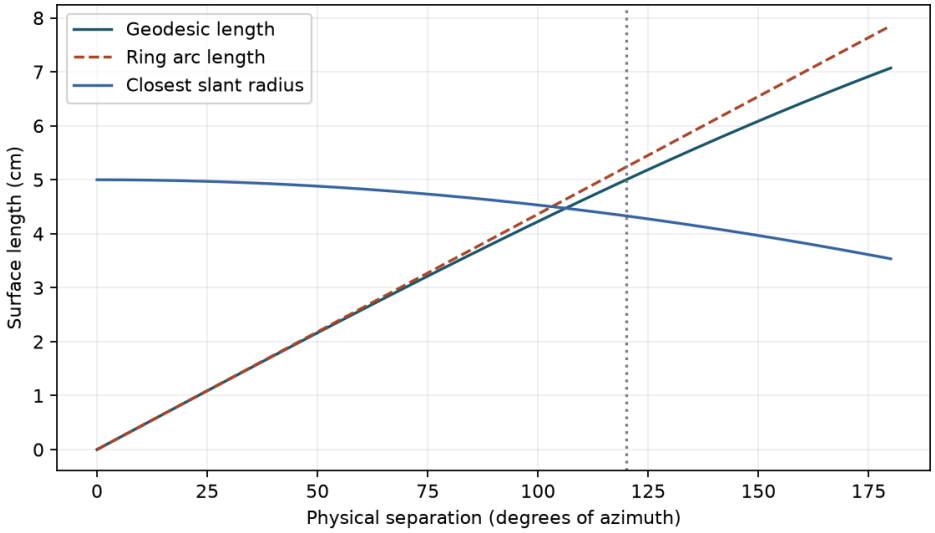

Changing only the endpoint separation alters the sag towards the apex. At small separation the geodesic length approaches the circular arc.

Exercise · infer the slope

Two marks at slant distance 10 cm and azimuth separation 120 degrees have a geodesic of length 10 cm. What is the cone half-angle?

▼ Work through the solution

The measured chord gives

$$\sin(\Delta\psi/2) = 10/(2 \cdot 10) = 1/2.$$

The shortest branch has $\Delta\psi = 60^\circ$, hence $\sin\alpha = 60/120 = 1/2$ and $\alpha = 30^\circ$. Use the same angular units in the ratio.

Exercise · compare with a weakly curved path

Find the relative excess of ring length over geodesic for a small unrolled separation δ. Why does a very small patch look flat?

▼ **Work through the solution**

Expanding $2\sin(\delta/2) = \delta - \delta^3/24 + \cdots$ gives

$$(R\delta - L)/(R\delta) = \delta^2/24 + O(\delta^4).$$

Both paths have the same tangent at leading order. The cone away from its apex is intrinsically developable; the small difference here measures the curvature of the chosen ring inside that developed plane.

Try it · Cone

Change the inputs and compare the recalculated curves with the preceding derivation and baseline figure. The axes give the units; the numerical readout states the model assumptions and any limiting cases. Reset the inputs to return to the reference setting.

Open this live calculation

Try the calculation

Cone half-angle (degrees)	30
Endpoint azimuth separation (degrees)	120
Slant radius (cm)	5

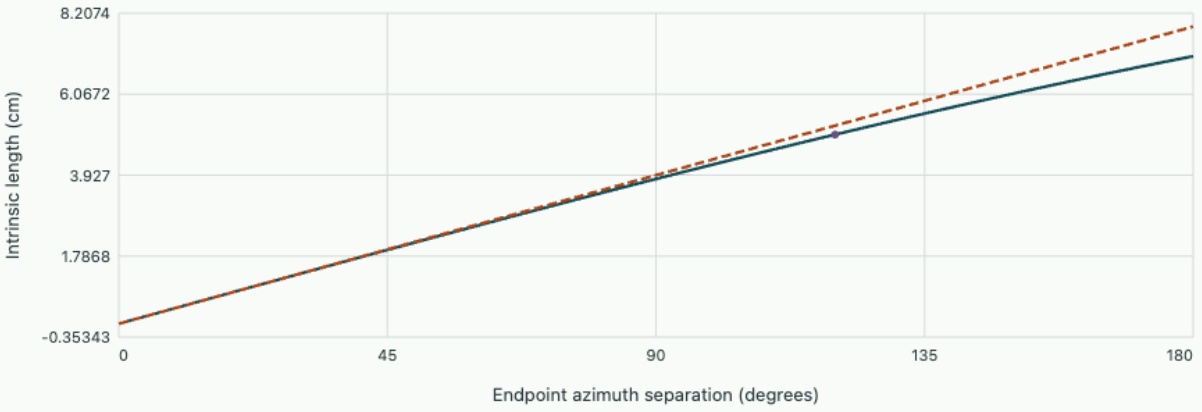

Closest slant radius 4.3301 cm. Cut and unroll the cone to obtain the straight chord; the planar distance is the intrinsic surface distance.

Download the corresponding editable notebook. The browser recalculates the reduced equations directly; the notebook exposes the full calculation and its checks.

Open editable notebook Download .ipynb

Analytical mechanics from constraints to invariants · 14. Motion in a medium and momentum carried across a boundary

Two beads can approach exactly the same terminal speed with recognisably different histories. A sand cart can slow down while the total horizontal momentum of sand and cart stays fixed. Both observations begin by specifying which material the equation of motion follows.

Infer the force law from a falling bead

Choose downward displacement as positive. A submerged bead of volume V, density ρ_b and mass m displaces fluid of density ρ_f. In a fluid initially at rest the static pressure gradient supplies buoyancy $\rho_f V g$. Combine the two constant forces into $m g_e = (\rho_b - \rho_f) V g$. Assume a heavy bead, negligible wall effects and sufficiently slow changes to neglect added mass and viscous memory. A drag law must reverse sign when the velocity changes sign.

$$m\dot{v} = m g_e - b v,$$

$$m\dot{v} = m g_e - c|v|v.$$

In the first model b has units kg/s, in the second c has units kg/m. Equating drag to the effective weight gives $v_\infty = m g_e / b$ or $v_\infty = \sqrt{m g_e / c}$. Near zero speed both models give initial acceleration g_e. Equal initial slope and equal terminal speed therefore leave the force law undetermined.

Solve both initial-value problems

Choose the characteristic time $\tau = v_\infty / g_e$ and write $u = v / v_\infty$, $s = t / \tau$. Starting from rest the positive-speed branches obey $du/ds = 1 - u$ and $du/ds = 1 - u^2$. Separation and integration from zero give $-\ln(1 - u) = s$ and $\operatorname{artanh} u = s$. A second integration supplies displacements that a camera can measure directly.

$$u_{\mathrm{lin}} = 1 - e^{-s},$$

$$z_{\mathrm{lin}} = v_\infty \tau (s - 1 + e^{-s}).$$

$$u_{\mathrm{quad}} = \tanh s,$$

$$z_{\mathrm{quad}} = v_\infty \tau \ln(\cosh s).$$

To start a data analysis, fit the early displacement to $g_e t^2 / 2$ and determine the late speed independently. After this scaling, each curve is a prediction with no free fitting amplitude. With $g_e = 9.81$ m/s² and $v_\infty = 3.0$ m/s the time scale is 0.306 s. The competing predictions already differ by about 0.39 m/s at 0.30 s.

Recall · Which drag law has a mechanical basis here?

For a rigid sphere of radius a moving slowly in a Newtonian fluid the creeping-flow result is $b = 6\pi\eta a$. Check $\mathrm{Re} = 2a\rho_f|v|/\eta$ throughout the run. When inertia matters a pressure-drag model uses $c = \rho_f C_D A/2$ with frontal area A. Treating C_D as constant requires a range in which it varies slowly.

OneSimulation experiment · Two trajectories with the same terminal speed

Try the force laws in your browser

Adjust the common terminal speed, effective gravity and RK4 step. The curves are recomputed from the two equations of motion above. Keep the physical parameters fixed while reducing the step to distinguish integration error from a different drag law. Then compare the time needed to reach 90% of the terminal speed.

This browser calculation implements RK4 directly. The notebook below runs the same initial-value problem with OneSimulation; set its `terminal`, `g` and `step` to the displayed values to reproduce the comparison. The constant-coefficient drag assumptions still apply.

Open this experiment online

Try the calculation

Terminal speed (m/s)	3
Effective gravity (m/s²)	9.81
RK4 time step (s)	0.01

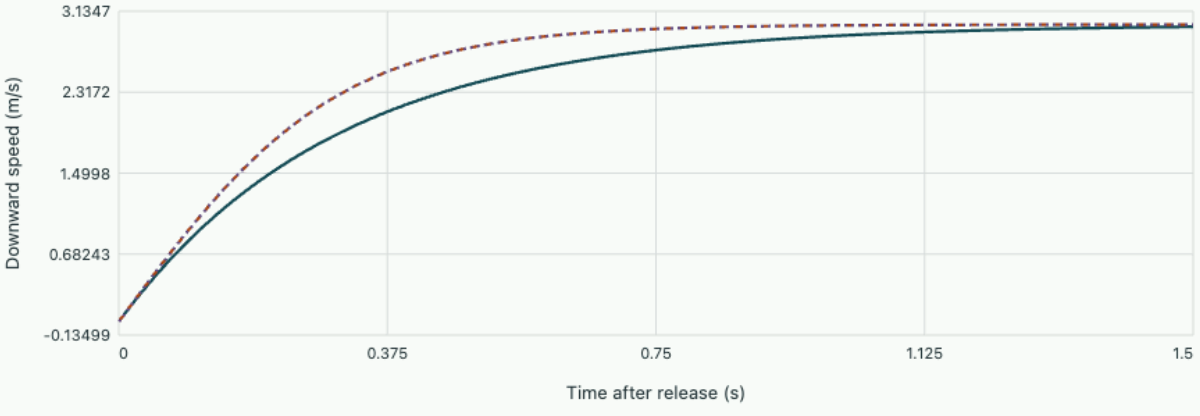

Characteristic time = 0.30581 s. Maximum quadratic-drag integration error = 5.18e-8 m/s. At 0.30 s the exact speeds are 1.87519 and 2.2605 m/s. Actual step = 0.01 s.

Reproduce with OneSimulation

Change the terminal speed and the time step. Compare the entire computed trace with the exact quadratic result, then identify where the two force models separate most visibly.

Run the downloaded notebook with OneSimulation, NumPy and Matplotlib installed. The output below was recorded with the displayed calculation.

```
"""Drop a bead from rest in two media with equal terminal speeds."""
import numpy as np
import matplotlib.pyplot as plt
from onesim.numerics.time import ClassicalRungeKutta4TimeIntegrator

g, terminal = 9.81, 3.0  # effective downward acceleration and terminal speed
step = 0.01
time = np.arange(151) * step
method = ClassicalRungeKutta4TimeIntegrator()

def rates(speed, t):
    linear, quadratic = speed
    return (g * (1 - linear / terminal),
            g * (1 - quadratic * abs(quadratic) / terminal**2))

speeds = [(0.0, 0.0)]
for t in time[:-1]:
    speeds.append(method.advance(speeds[-1], rates, step, time=t))
linear, quadratic = np.array(speeds).T
exact = terminal * np.tanh(g * time / terminal)
print(f"At 0.30 s: linear {linear[30]:.4f} m/s, quadratic {quadratic[30]:.4f} m/s")
print(f"Largest RK4 discrepancy for quadratic drag: {max(abs(exact-quadratic)):.2e} m/s")
plt.plot(time, linear, label="Linear drag")
plt.plot(time, quadratic, label="Quadratic drag")
plt.axhline(terminal, linestyle=":", color="grey", label="Terminal speed")
plt.xlabel("Time after release (s)")
plt.ylabel("Downward speed (m/s)")
plt.legend()
plt.tight_layout()
plt.savefig("physics-drag-laws.png", dpi=160)
```

Computed output

```
At 0.30 s: linear 1.8752 m/s, quadratic 2.2605 m/s
Largest RK4 discrepancy for quadratic drag: 5.18e-08 m/s
```

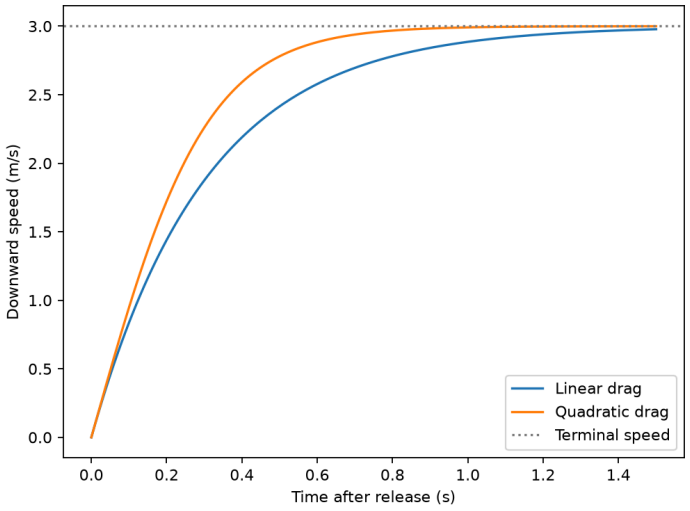

Two trajectories with the same terminal speed.

Download editable notebook · Download Python script

Derive the equation for a changing collection of matter

Let a horizontal cart of instantaneous mass M and speed v collect grains at rate $\dot{M} > 0$. Just before collection a small parcel dM has horizontal laboratory velocity w. Over dt the momentum of cart plus parcel changes by the external impulse. The incoming parcel is included on the initial side so that the comparison follows the same matter.

$$Mv + w\,dM + F_{\text{ext}}\,dt = (M + dM)(v + dv).$$

Drop the product $dM\,dv$, divide by time and keep the finite acceleration. The relative speed determines how strongly the intake changes the cart velocity.

$$M\dot{v} = F_{\text{ext}} + (w - v)\dot{M},$$

$$\frac{d(Mv)}{dt} = F_{\text{ext}} + w\dot{M}.$$

Take a 20 kg cart rolling at 3 m/s on a level frictionless track. Grains falling vertically carry zero horizontal momentum. After collecting 10 kg, the common speed is 2 m/s. The horizontal kinetic energy falls from 90 J to 60 J. The collisions can dissipate energy even though the horizontal external impulse vanishes. The vertical momentum and gravitational energy belong to a separate balance.

Recall · Moving boundaries and signs

The formula uses laboratory-frame w immediately outside the cart and signed mass rate into the cart. For outflow use the velocity of matter as it leaves. A leaking cart with material departing at the cart's horizontal speed has no resulting horizontal acceleration.

Tutorial on identifying a mechanical system

1 · When do the two beads reach 90% of the terminal speed?

▼ **Work through the solution**

The dimensionless times are $\ln 10 = 2.303$ and $\operatorname{artanh}(0.9) = 1.472$. At the stated parameters these are 0.704 s and 0.450 s. An early-velocity measurement distinguishes the laws more efficiently than another terminal-speed estimate.

---

2 · Infer an intake speed from a measured acceleration

▼ **Work through the solution**

A 12 kg cart moving at 1.5 m/s gains 0.40 kg/s and accelerates at 0.020 m/s² along a level frictionless track. From $w = v + M\dot{v}/\dot{M}$ the grains enter at 2.10 m/s. Using $F = d(Mv)/dt$ without an inlet flux would falsely infer an external force.

---

3 · Test a radius scaling before fitting a drag coefficient

▼ **Work through the solution**

For spheres of the same density, effective weight scales as a^3. Stokes drag then predicts $v_\infty \propto a^2$. At fixed C_D, quadratic drag gives $v_\infty \propto a^{1/2}$. Doubling radius gives speed ratios 4 and $\sqrt{2}$. Check Reynolds numbers, wall clearances and bead density before inferring a force law.

For further study see Taylor, Classical Mechanics, chapters 1–4 on force laws, dissipative motion and momentum transport.

Analytical mechanics from constraints to invariants · 15. From a repeating trajectory to a chaotic attractor

A damped pendulum under a periodic drive can settle into the same orbit on each run yet visit a different point on successive drive periods. A return map supplies the right clock for distinguishing a new period from a slowly decaying transient.

Build a map from a continuous mechanical experiment

Consider a pendulum with dimensionless time in units of its small-angle period divided by 2π. Let q be the positive damping rate, A the drive amplitude and ω the drive frequency.

$$\dot{\theta} = p,$$

$$\dot{p} = -qp - \sin\theta + A\cos(\omega t).$$

Prepare all observations at drive phase zero and evolve for $T = 2\pi/\omega$. The stroboscopic map takes (θ_n, p_n) to (θ_{n+1}, p_{n+1}). Complete rotations can be plotted modulo 2π while the unwrapped angle tracks transport. An attracting period-one orbit appears as one point after transients. A period-two orbit alternates between two points and returns after $2T$.

For a small patch in the state plane the instantaneous fractional area growth is the divergence $\partial_\theta p + \partial_p \dot{p} = -q$. Integration over a period gives a Jacobian determinant e^{-qT}. Phase-area contraction allows an attractor. A periodically driven Hamiltonian system at $q = 0$ instead has a unit determinant.

> **Recall · Why use a section at fixed drive phase?**
>
> Two trajectories with identical angle and speed can accelerate differently at different phases of an external drive. Sampling once per drive period compares equal external conditions. Recording at a nearby period can turn a perfectly regular response into an apparent cloud of points.

Calculate a period doubling in a solvable map

Near a flip bifurcation with only one slow direction, a one-dimensional map helps explain stability changes. The logistic map $f(x) = rx(1-x)$ on $0 \le x \le 1$ for $0 < r \le 4$ is an illustrative return law. Its r is not a calibrated pendulum torque. An interior fixed point is $x_* = 1 - 1/r$. For a small displacement $\delta_{n+1} \simeq f'(x_*)\delta_n$, giving a multiplier $2 - r$. Its magnitude crosses one at $r = 3$ with negative sign.

To find the new orbit, solve $f(f(x)) - x = 0$ and remove the two fixed-point factors x and $x - x_*$. The remaining quadratic has roots

$$x_\pm = \frac{r + 1 \pm \sqrt{(r-3)(r+1)}}{2r}.$$

Its two-step multiplier is $f'(x_+)f'(x_-) = -r^2 + 2r + 4$. At $r = 3.2$ it is 0.16 and deviations fall by that factor every two observations. At $r = 1 + \sqrt{6}$ it reaches -1, so that orbit loses stability. Additional

doublings create intervals of higher-period motion. Periodic windows interrupt the chaotic parameter range.

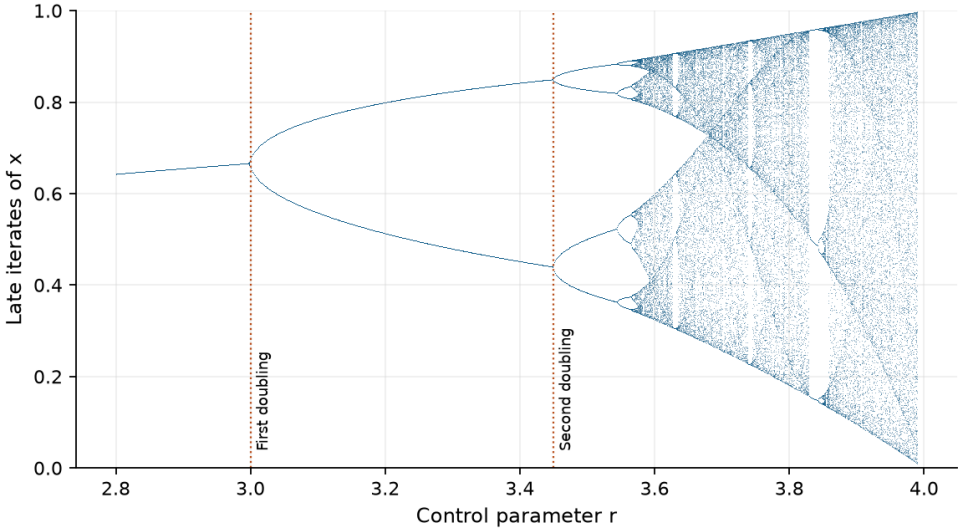

Each column records 120 late iterates at one setting after discarding 850 returns. First one branch splits, then each of its daughters splits. Narrow periodic windows remain visible among broader bands.

Try it · Logistic

Change the inputs and compare the recalculated curves with the preceding derivation and baseline figure. The axes give the units; the numerical readout states the model assumptions and any limiting cases. Reset the inputs to return to the reference setting.

Open this live calculation

Try the calculation

Return-map parameter r **3.6**

Initial state **0.2**

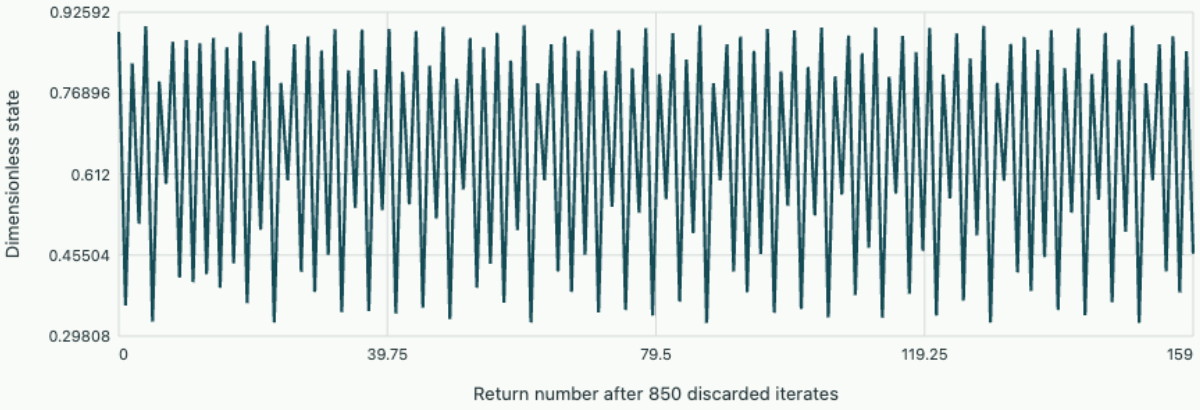

Late return sequence

Finite-window Lyapunov estimate 0.13665 per return. Positive values suggest sensitive dependence; repeat with nearby initial states and longer notebooks before identifying an attractor.

Estimate a growth rate while keeping the observations bounded

A separation eventually saturates at the attractor size. To estimate growth over many periods, multiply the local tangent factors and take a logarithm before averaging. Along a sampled orbit the largest exponent of the scalar map is

$$\lambda_N = \frac{1}{N}\sum_{j=0}^{N-1} \ln\left|r(1-2x_j)\right|.$$

For $r = 4$ the substitution $x = \sin^2\phi$ maps an iteration to angle doubling modulo the symmetries of the sine. Typical invariant-measure trajectories have $\lambda = \ln 2$ per iteration. Exceptional exact initial

conditions, including a critical point that maps onto zero, do not estimate that typical value. Finite precision eventually creates repetitions. Report the sampling window and discard transient returns.

For a mechanical test, integrate two nearby pendulum trajectories, sample at T, rescale the difference back to its small original norm and accumulate its log growth. Repeat with smaller time step and different starting points in the same basin. A positive long-time exponent and recurrent bounded motion are distinct pieces of evidence. Slow beats and noisy sensors can broaden a spectrum without deterministic chaos.

Tutorial on return maps

1 · Predict the number of observed return points

▼ **Work through the solution**

For $r = 3.2$, the roots of the two-cycle are about 0.5130 and 0.7995. Check directly that the first maps near 0.7995. Two sensor samples cannot distinguish a two-cycle from a transient. Repeated pairs should approach these values with the calculated two-step multiplier.

---

2 · Separate dissipation from instability

▼ **Work through the solution**

For $qT = 0.4$ the area factor is 0.6703. If one real multiplier of a period-one orbit is -1.2, its partner is $0.6703/(-1.2) = -0.559$. The orbit expands along one direction despite contracting area in total.

---

3 · Design a finite-time comparison

▼ **Work through the solution**

An apparent doubling every three drive periods corresponds to $\ln 2/3 = 0.231$ per return. Repeat the estimate with several initial separations above roundoff and below the nonlinear scale, increase the observation window and verify persistence when the numerical step is halved.

For further study see Taylor, Classical Mechanics, chapters 11–12 on nonlinear oscillations, the driven pendulum and chaos.

Analytical mechanics from constraints to invariants · 16. From differential acceleration to three-dimensional strain and stress

An accelerometer in a falling laboratory can read zero while a pair of falling test masses moves apart. A crystal can support different longitudinal and transverse speeds in the same direction. Both measurements require the spatial variation of a vector field, represented by a tensor.

Derive the relative acceleration in a falling frame

Let a laboratory origin fall freely at position $\mathbf{R}$ in the field $\mathbf{g}(\mathbf{R}) = -GM\mathbf{R}/R^3$ of a spherical source. Over a small separation $\boldsymbol{\xi}$ choose parallel nonrotating axes. Subtract the origin's acceleration and expand to first order:

$$\ddot{\xi}_i = g_i(\mathbf{R} + \boldsymbol{\xi}) - g_i(\mathbf{R}) \simeq T_{ij}\xi_j,$$

$$T_{ij} = \frac{GM}{R^3}(3n_i n_j - \delta_{ij}),$$

$$\mathbf{n} = \mathbf{R}/R.$$

The radial eigenvalue is $2GM/R^3$. Both transverse eigenvalues are $-GM/R^3$. Outside the source the sum vanishes as required by $\nabla \cdot \mathbf{g} = 0$. Over a short time the fractional change of an initially stationary separation along an eigenvector is $T_i t^2/2$. Near Earth's surface $g/R \simeq 1.54 \times 10^{-6}$ s⁻². Free masses initially separated by 2 m radially acquire a relative acceleration near 6.2 μm/s².

Recall · Which frame cancels gravity?

The origin's uniform acceleration cancels at all test masses when forming the difference. A rotating frame contributes centrifugal and Coriolis terms as well. For a small free-fall experiment state how axes are maintained and which relative velocities were initially present.

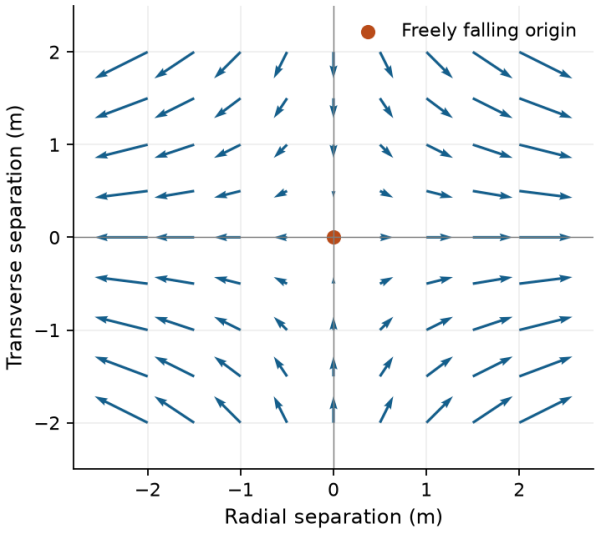

Relative acceleration in the freely falling laboratory. Two neighbours separated radially pull apart, while a transverse pair draws together. The common acceleration of the origin has been subtracted.

Try it · Tidal

Change the inputs and compare the recalculated curves with the preceding derivation and baseline figure. The axes give the units; the numerical readout states the model assumptions and any limiting cases. Reset the inputs to return to the reference setting.

Open this live calculation

Try the calculation

Central mass / Earth mass 1

Laboratory radius / Earth radius 1

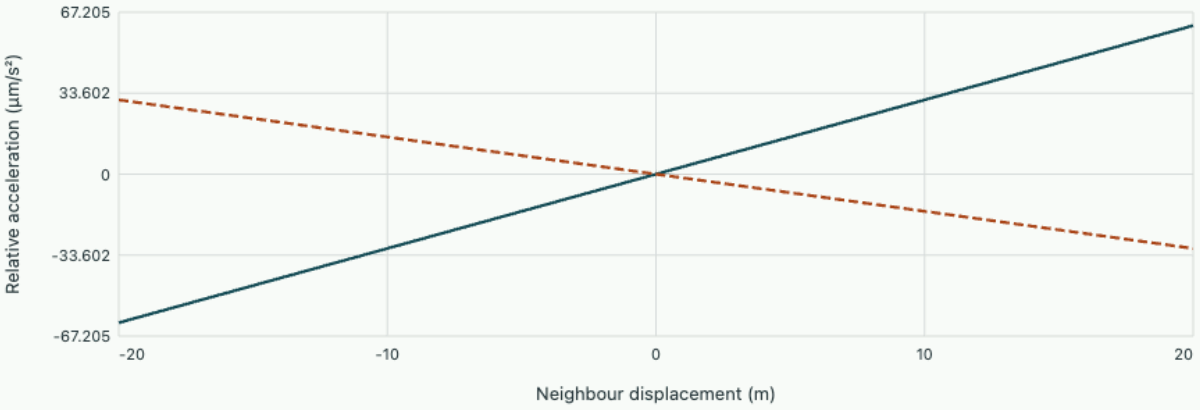

Tidal eigenvalues (2,−1,−1) × 1.541e-6 s⁻²; their sum is zero outside the source. Displacements must remain small compared with the laboratory radius.

Compare nearby material points before and after a displacement

Label a reference point by $\mathbf{X}$ and let its displacement be $\mathbf{u}(\mathbf{X})$. An initial segment $d\mathbf{X}$ becomes $(I + \nabla \mathbf{u}) d\mathbf{X}$. Expand its squared length, retaining the first-order terms. The antisymmetric part drops out of the quadratic form for length change.

$$d\ell'^2 - d\ell^2 = 2\, dX_i\, \varepsilon_{ij}\, dX_j,$$

$$\varepsilon_{ij} = \tfrac{1}{2}(\partial_i u_j + \partial_j u_i).$$

The trace gives fractional volume change. A rigid translation has zero displacement gradient. An infinitesimal rotation has an antisymmetric gradient, so it has zero linear strain as well. For simple shear $u_x = \gamma y$ the component $\varepsilon_{xy} = \gamma/2$ explains the factor of two between tensor and engineering shear strain.

Build Hooke's law from symmetries and an energy

On a cut normal to $\mathbf{n}$, force per area is the traction $t_i = \sigma_{ij} n_j$. Balancing moments in a continuum without intrinsic body couples gives symmetric Cauchy stress. In an initially unstressed isotropic linear solid a quadratic elastic energy can depend only on the two independent rotationally invariant quadratic forms of the strain.

$$W = \tfrac{1}{2}\lambda (\operatorname{tr}\varepsilon)^2 + \mu\, \varepsilon_{ij}\varepsilon_{ij},$$

$$\sigma_{ij} = \partial W / \partial \varepsilon_{ij} = \lambda \operatorname{tr}\varepsilon\, \delta_{ij} + 2\mu \varepsilon_{ij}.$$

Under uniform dilation $\varepsilon = \eta I$ the bulk modulus is $K = \lambda + 2\mu/3$. Pure shear isolates μ. Stability requires $K > 0$ and $\mu > 0$. The general anisotropic relation $\sigma_{ij} = C_{ijkl}\varepsilon_{kl}$ need not reduce to two constants. Crystal symmetry decides which entries can be determined by rotating a sound measurement.

Recover both moduli from two arrival times

Balance of linear momentum gives $\rho \ddot{u}_i = \partial_j \sigma_{ij}$ in a homogeneous body with no body force. A plane longitudinal displacement has nonzero divergence. A transverse displacement has zero divergence. Substitution gives their phase speeds:

$$c_L^2 = (K + 4\mu/3)/\rho,$$

$$c_T^2 = \mu/\rho.$$

For a solid of density 2500 kg/m³ with $c_L = 5000$ m/s and $c_T = 3000$ m/s the two moduli are $\mu = 22.5$ GPa and $K = 32.5$ GPa. One longitudinal speed would determine only their combination. Short wavelengths comparable with the lattice spacing, or waves in a thin guide, require dispersion or geometric corrections before using these bulk equations.

Tutorial on differential measurements

1 · Recover a missing tidal eigenvalue

▼ Work through the solution

Two transverse values measured outside a spherical source are each -1.5×10^{-6} s⁻². Zero trace implies a radial value $+3.0 \times 10^{-6}$ s⁻². A positive radial gradient means the higher test mass falls slightly less quickly.

---

2 · A diagonal cut through a sheared specimen

▼ Work through the solution

Let only $\sigma_{xy} = \sigma_{yx} = 4$ MPa be nonzero. With $\mathbf{n} = (1, 1, 0)/\sqrt{2}$, traction is $4\mathbf{n}$ MPa. The same stress state that is pure shear on coordinate planes becomes a purely normal traction on this cut.

---

3 · Test isotropic elasticity using an additional wave

▼ **Work through the solution**

If c_T differs systematically for two orthogonal transverse polarisations at the same direction and frequency, a homogeneous isotropic bulk model predicts the wrong degeneracy. Check the sample dimensions and alignment first, then measure crystal orientation before assigning a distinct shear modulus.

For further study see Taylor, Classical Mechanics, chapters 9 and 16 on noninertial observers and elastic continua.